

**Klonierung und funktionelle Analyse der Zellerkennungsmoleküle
Tenascin-R, Tenascin-C und P0 in Entwicklung und Regeneration
im Zebrafisch *Danio rerio* (Hamilton 1822)**

**Dissertation
zur Erlangung des Grades
Doktor der Naturwissenschaften
Dr. rer. nat.**

**vorgelegt
von Dipl.-Biol. Jörn Schweitzer
aus
Celle**

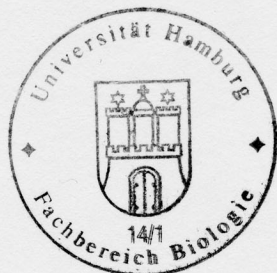
**Hamburg
2003**

Genehmigt vom
Fachbereich Biologie der
Universität Hamburg
auf Antrag von Frau Professor Dr. M. SCHACHNER

Weitere Gutachter der Dissertation:
Herr Professor Dr. L. RENWRANTZ

Tag der Disputation: 31. Januar 2003

Hamburg, den 17. Januar 2003



Udo Wienand

Professor Dr. U. Wienand
Dekan

1. INTRODUCTION	1
1.1 NEURAL CELL ADHESION MOLECULES	1
1.2 MYELIN PROTEIN ZERO	1
1.3 THE TENASCIN FAMILY	2
1.4 THE ZEBRAFISH (<i>DANIO RERIO</i>)	5
1.5 OUTGROWTH OF MOTOR AXONS IN THE DEVELOPING ZEBRAFISH	6
1.6 REGENERATION IN THE CENTRAL NERVOUS SYSTEM OF THE ZEBRAFISH	7
1.7 AIM OF THIS WORK	9
2. MATERIALS	10
2.1. ENZYMES AND REACTION KITS	10
2.2 REAGENTS, DISPOSABLES, ETC	11
2.3 INSTRUMENTS	11
2.4 OLIGONUCLEOTIDES	12
2.5 MORPHOLINOS	12
2.6 ANTIBODIES	13
2.7 BACTERIAL STRAINS	13
2.8 BACTERIAL MEDIA	14
2.9 VECTORS	14
2.10 ZEBRAFISH	15
2.11 BUFFERS AND STOCK SOLUTIONS	15
3. EXPERIMENTAL PROCEDURES	18
3.1 VARIOUS MOLECULAR BIOLOGICAL METHODS	18
3.1.1 Photometric quantification of nucleic acids	18
3.1.2 DNA agarose gel electrophoresis	18
3.1.3 Restriction of DNA	19
3.1.4 Sequencing of DNA	19
3.1.5 Maintenance of bacterial strains	19
3.1.6 Precipitation of DNA	20
3.1.7 Production of competent bacteria	20

3.2 CLONING IN PLASMID VECTORS	21
3.2.1 Preparation / enzymatic manipulation of insert DNA	21
3.2.2 Enzymatic manipulation of vector DNA prior to cloning	22
3.2.3 Ligation of plasmid vector and insert DNA	22
3.2.4 TA cloning	23
3.2.5 (Re-) Transformation of DNA into bacteria	23
3.3 PURIFICATION OF NUCLEIC ACIDS	23
3.3.1 Plasmid DNA purification from bacterial cultures	23
3.3.2 PCR/DNA fragment purification	25
3.3.3 DNA fragment extraction from agarose gels	25
3.3.4 Total RNA isolation from zebrafish brain tissue	25
3.3.5 Purification of mRNA	26
3.4 NUCLEIC ACID AMPLIFICATION	26
3.4.1 Generating RNA by In-vitro transcription	27
3.5 CDNA CLONING	28
3.5.1 First strand synthesis, RT-PCR	28
3.5.2 Rapid amplification of cDNA ends	29
3.5.3 Cloning of cDNAs for myelin protein zero, tenascin-r and tenascin-c	29
3.6 PURIFICATION AND LABELING OF NUCLEIC ACID PROBES	32
3.7 ANALYSIS OF NUCLEIC ACIDS BY HYBRIDIZATION	32
3.7.1 Northern blot analysis	32
3.7.2 RNA in situ hybridization (ISH) on cryosections	33
3.7.3 Whole mount RNA in situ hybridization	35
3.7.4 Screening of a zebrafish cDNA library	36
3.8 IMMUNOHISTOCHEMISTRY	36
3.8.1 Indirect immunofluorescence on sections	36
3.8.2 Whole mount immunohistochemistry	37
3.8.3 Tracing of optic axons	37
3.9 ZEBRAFISH SURGERY	38
3.9.1 Optic nerve crush and enucleation	38
3.9.2 Spinal cord transection	38

3.10 PERTUBATION OF GENE EXPRESSION BY INJECTION OF MRNAs, PROTEINS OR MORPHOLINOS INTO FRESHLY FERTILIZED ZEBRAFISH EGGS	38
3.11 QUANTITATIVE ANALYSIS	42
3.11.1 Quantitative analysis of trunk ventral motor growth	42
3.11.2 Quantification of cells expressing P0 mRNA	42
3.11.3 Quantification of neurite outgrowth	42
3.12 ORGANOTYPIC RETINAL CELL CULTURE	43
3.12.1 Preparation of in vitro substrate	43
3.12.2 Retinal explant culture	44
3.13 WESTERN BLOT ANALYSIS	44
4. RESULTS	45
4.1 EXPRESSION OF PROTEIN ZERO IS INCREASED IN LESIONED AXON PATHWAYS IN THE CENTRAL NERVOUS SYSTEM OF ADULT ZEBRAFISH	45
4.1.1 Molecular cloning of protein zero (P0) cDNA in zebrafish	45
4.1.2 Expression of zebrafish P0 mRNA during development in the hindbrain and spinal cord is associated with myelination	47
4.1.3 P0 mRNA is expressed during development of the optic system and in other areas of the CNS	49
4.1.4. P0 mRNA is expressed in the PNS	50
4.1.5 P0 mRNA is upregulated in the lesioned optic pathway	52
4.1.6 Expression of P0 mRNA is increased in the lesioned spinal cord	57
4.2 EVIDENCE FOR A ROLE OF TN-R AS A REPELLENT GUIDANCE MOLECULE FOR REGENERATING OPTIC AXONS IN ADULT FISH	59
4.2.1 Zebrafish possess a TN-R gene	59
4.2.2 TN-R mRNA and protein are present in the brain of adult zebrafish	61
4.2.3 Newly generated optic axons in the adult encounter TN-R as a homogeneous substrate in the retina	62
4.2.4 TN-R expression is low in the normal and lesioned optic nerve and tract in adult fish	64
4.2.5 Optic axons encounter TN-R in a border-like situation in the brain	66
4.2.6 TN-R is present during development of the optic projection	70
4.2.7 Axonal reactions to TN-R in vitro depend on the way the molecule is presented	71

4.3 TENASCIN-C IS INVOLVED IN OUTGROWTH OF MOTOR AXONS IN THE TRUNK OF ZEBRAFISH _____	74
4.3.1 <i>Molecular cloning of a full-length tenascin-C cDNA in zebrafish</i> _____	74
4.3.2 <i>TN-C immunoreactivity is localized in the pathway of outgrowing motor axons in the trunk during development of the zebrafish</i> _____	76
4.3.3 <i>Overexpression of the EGF-like domains of TN-C resulted in abnormal outgrowth of ventral motor axons</i> _____	78
4.3.4 <i>Injection of a recombinant TNCEGF fragment also leads to aberrant motor axon outgrowth</i> _____	81
4.3.5 <i>The overexpression of TNCEGFmyc mRNA or injection of the EGF-L fragment does not affect trunk structures, muscle pioneers and other axon trajectories.</i> _____	84
4.3.6 <i>TN-C is required for motor axon pathfinding in the developing zebrafish</i> _____	86
4.3.7 <i>TN-C immunoreactivity is absent from the horizontal myoseptum of unplugged mutants</i> _____	89
4.3.8 <i>TN-C mRNA is expressed by adaxial cells during outgrowth of ventral motor axons in the trunk</i> _____	91
5. DISCUSSION _____	93
5.1 EXPRESSION OF PROTEIN ZERO IS INCREASED IN LESIONED AXON PATHWAYS IN THE CENTRAL NERVOUS SYSTEM OF ADULT ZEBRAFISH _____	93
5.1.2 <i>Identification of a homolog of P0 in zebrafish.</i> _____	93
5.1.3 <i>P0 mRNA is probably expressed by oligodendrocytes during CNS development.</i> _____	94
5.1.4 <i>P0 mRNA is expressed in the PNS of zebrafish</i> _____	95
5.1.5 <i>Zebrafish P0 may have functions in axon regeneration</i> _____	95
5.1.6 <i>The initial upregulation, but not the late peak of P0 mRNA expression after an optic nerve lesion is independent of the presence of regenerating axons</i> _____	96
5.1.7 <i>The peak of P0 mRNA expression after optic nerve lesion correlates with remyelination</i> _____	97
5.1.8 <i>There are similarities and differences in the regulation of glial recognition molecules between the lesioned optic nerve and spinal cord</i> _____	98
5.1.9 <i>Early expression of P0 mRNA in rhombomeres is not related to myelination</i> _____	98
5.2 EVIDENCE FOR A ROLE OF TENASCIN-R AS A REPELLENT GUIDANCE MOLECULE FOR REGENERATING OPTIC AXONS IN ADULT FISH _____	100
5.2.1 <i>Tenascin-R is expressed in the CNS of adult fish</i> _____	100
5.2.2 <i>The axonal reactions to tenascin-R in fish depend on the way the molecule is encountered</i> _____	101

5.2.3 <i>The distribution of tenascin-R in the optic pathway in the brain suggests a boundary function of the molecule for regenerating axons</i>	101
5.2.4 <i>Tenascin-R may have a dual function for newly growing optic axons</i>	102
5.3 TENASCIN-C IS INVOLVED IN OUTGROWTH OF MOTOR AXONS IN THE TRUNK OF ZEBRAFISH	104
5.3.1 <i>Identification of a TN-C homolog in zebrafish</i>	104
5.3.2 <i>TN-C immunoreactivity is concentrated at the level of the horizontal myoseptum in the pathway of outgrowing motor axons.</i>	105
5.3.3 <i>Perturbations of TN-C specifically affect motor nerves.</i>	106
5.3.4 <i>TN-C is involved in growth and pathfinding of ventral motor nerves</i>	107
5.3.5 <i>The distribution of TN-C immunoreactivity is altered in unplugged but not stumpy mutants</i>	109
5.3.6 <i>What is the function of TN-C during outgrowth of ventral motor axons?</i>	110
6. LITERATURE	113
7. ZUSAMMENFASSUNG	132
7. SUMMARY	135
8. APPENDIX	137
8.1 ABBREVIATIONS	137
8.2 MORPHOLINO SEQUENCES	139
8.3 FULL LENGTH CDNA SEQUENCES OF MYELIN PROTEIN ZERO, TENASCIN-R AND TENASCIN-C	139
8.4 VECTOR MAPS	144
8.5 PUBLICATIONS AND POSTER PRESENTATIONS	145
CURRICULUM VITAE	146
DANKSAGUNG	147

1. Introduction

1.1 Neural cell adhesion molecules

Neurons, the basic information processing units of the nervous system, are characterized by a complex polar morphology that is essential for their function. To attain their precise morphology, neurons extend cytoplasmatic processes (axons and dendrites), which establish synaptic connections in a highly regulated way (Tessier-Lavigne and Goodman, 1996). Every step of neuronal development is genetically governed by endogenous determinants, as well as by environmental signals including diffusible signals or contacts with neighboring cells or the extracellular matrix (ECM). Cell-cell and cell-matrix interactions are particularly critical for the orderly development of the nervous system. Many of these are mediated by neural recognition/cell adhesion molecules (CAMs) and by ECM components (Fields and Itoh, 1996; Tessier-Lavigne and Goodman, 1996). (modified after M. Evers, Dissertation, Universität Bochum)

1.2 Myelin protein zero

Myelin protein zero (P0) is a member of the Ig superfamily of recognition molecules (Brümmendorf and Rathjen, 1993). P0 is constitutively expressed in glial cells in the fish CNS and PNS (Stratmann and Jeserich, 1995; Yoshida and Colman, 1996), while in mammals its expression is restricted to Schwann cells in the PNS (reviewed in Martini and Schachner, 1997; Sommer and Suter, 1998; Spiryda, 1998). P0 contains a single Ig-like domain and accounts for over half the total protein in compact PNS myelin in amniotes (Lemke and Axel, 1985). The molecule mediates the compaction of myelin sheaths in the mammalian PNS by homophilic binding mechanisms (D'Urso et al., 1990; Filbin et al., 1990; Schneider-Schaulies et al., 1990; Shapiro et al., 1996). Mice homozygous for a null mutation in the P0 gene show severely hypomyelinated nerves during development (Giese et al., 1992). The molecule may not only play a role in myelination, but also in regeneration of axons, since it promotes neurite outgrowth *in vitro* (Schneider-Schaulies et al., 1990) and promotes regeneration of axons, when P0 expressing cells are transplanted into the adult mammalian CNS (Yazaki et al., 1994). After a lesion of the PNS in amniotes, P0 is initially downregulated by myelinating

Schwann cells. A subsequent upregulation depends on the presence of regrowing axons (Gillen et al., 1995; Gupta et al., 1988; Gupta et al., 1993; LeBlanc and Poduslo, 1990; Mitchell et al., 1990), but not necessarily on direct contact of axonal and glial cell membranes (Bolin and Shooter, 1993). Expression of P0 mRNA has recently been analyzed during early development of zebrafish (Brösamle and Halpern, 2002). In this work, expression of P0 mRNA in the zebrafish is detected at 2 days postfertilization (dpf), first in the ventral hindbrain, close to the midline. During the next 8 days, expression spreads rostrally to the midbrain and optic nerve, and caudally to the spinal cord. Unlike its closest homologue, trout IP1, zebrafish P0 transcripts were found to be restricted to the CNS in this study. Ultrastructurally, the expression of P0 correlated well with myelination. Myelinated axons were first detected at 4 dpf in the ventral hindbrain, where they were loosely wrapped by processes of glia cells. By 7 dpf, bundles of heavily myelinated axons were observed in the same region.

1.3 The tenascin family

Members of the tenascin family belong to the extracellular matrix (ECM) which is a complex network of macromolecules. Tenascins are large multimeric proteins and contain common structural modules. Each member has an amino-terminal cysteine-rich domain, followed by arrays of epidermal growth factor-like (EGF) domains and fibronectin type III-like (FN III) domains. At the carboxy-terminus, a single fibrinogen-like (FBG) domain is located. In contrast to the other family members, TN-X and TN-Y contain serine and proline rich parts, which are inserted in the array of FN III domains. So far, six members of the tenascin family have been described, named tenascin-C (TN-C) (Chiquet and Fambrough, 1984; Erickson and Bourdon, 1989; Erickson and Inglesias, 1984; Grumet et al., 1985; Kruse et al., 1985); tenascin-R (TN-R) (Nörenberg et al., 1992; Pesheva et al., 1989; Rathjen et al., 1991), tenascin-W (TN-W) (Weber et al., 1998) tenascin-X (TN-X) (Bristow et al., 1993), tenascin-Y (TN-Y) (Hagios et al., 1996; Tucker et al., 1999) and the recently cloned tenascin-N (TN-N) (J. Neidhardt, Dissertation, Universität Hannover). An overview of the tenascin family members and their multimeric structure is given in Fig.1.

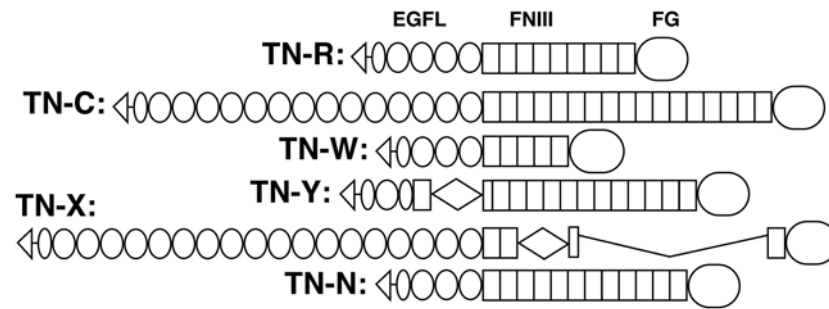


Fig.1. Tenascin family members and their structural motifs.

Tenascin family members consists of a cysteine-rich domain at their 5' end (triangle), followed by EGF-like repeats (ovals), FN III repeats (rectangles) and a fibrinogen knob (large circle). A rhombus designates a serine-proline rich domain. Tenascin-X consists of at least 33 FN III repeats (modified after Jones and Jones, 2000). Tenascin-N in the mouse is a recent addition to the tenascin family (J. Neidhardt, Dissertation, Universität Hannover).

TN-C, the most well known member of the tenascin family, is mainly expressed by immature and reactive astrocytes. (Bartsch, 1996; Crossin et al., 1986; Kawano et al., 1995). In the developing murine CNS, expression of TN-C has been consistently observed in regions of active axonal growth. For instance, retinal ganglion cell axons elongate in a TN-C-rich environment (Bartsch, 1996). In the chick visual system, TN-C is associated with the cell surface of glial fibers and growing axons (Bartsch et al., 1995), suggesting that TN-C may not only support axonal growth but in addition may guide axons to their appropriate targets in vivo. In the PNS, TN-C immunoreactivity is detectable in developing peripheral nerves, whereas the protein is restricted to the perineurium and to nodes of Ranvier in adult nerves (Bartsch, 1996; Martini, 1994). Expression of TN-C has been reported to be upregulated in a variety of lesion paradigms. For instance, stab wounds induce an upregulation of TN-C by Golgi epithelial cells in the cerebellar cortex (Bartsch, 1996) or the re-expression of the protein by reactive astrocytes in the cerebral cortex. In both paradigms, elevated levels of TN-C mRNA and protein are restricted to the immediate vicinity of the lesion sites. In the early developing zebrafish *Danio rerio*, TN-C mRNA is expressed in specific domains of the brain (Tongiorgi et al., 1995b). In the trunk, TN-C mRNA is expressed by somites, neural crest cells, roof plate, notochord, hypochord and tail fin bud. TN-C immunoreactivity in the trunk is present in the migratory pathway of neural crest cells during their period of migration and also in the intersomitic furrows (Tongiorgi, 1999). TN-C immunoreactivity is further confined to the posterior half of each body segment at very early developmental stages (Bernhardt et al., 1998). In the retina of a 3 day-old juvenile zebrafish, TN-C mRNA can be detected in the

ganglion cell layer, the inner nuclear layer and the outer nuclear layer. Expression levels of TN-C mRNA at later developmental stages are decreased. For example, there is no detectable expression of TN-C mRNA in the adult retina which remains unchanged after a lesion of the optic nerve (Bernhardt et al., 1996). TN-C has been demonstrated in numerous *in vitro* studies to be adhesive or anti-adhesive (Dorries et al., 1996; Faissner and Kruse, 1990; Grumet et al., 1985; Kruse et al., 1985; Tan et al., 1987), to support or restrict cell migration of certain cell types (Chuong et al., 1987; Husmann et al., 1992; Tan et al., 1987) and to promote or inhibit neurite outgrowth (Bartsch, 1996; Dorries et al., 1996; Faissner and Kruse, 1990; Lochter and Schachner, 1993a; Lochter et al., 1991). TN-C deficient mice (Saga et al., 1992) revealed functions for TN-C in the formation, maturation, and stabilization of the neuromuscular junction (Cifuentes-Diaz et al., 2002; Cifuentes-Diaz et al., 1998).

TN-R is expressed predominantly in the CNS by oligodendrocytes with highest expression during the period of active myelination (Bartsch et al., 1993; Fuss et al., 1993). TN-R is detectable at contact sites between unmyelinated axons, at the interface between axons and myelinating processes of oligodendrocytes and in myelin sheaths (Bartsch et al., 1993). TN-R is also expressed by subpopulations of neurons in the retina, hippocampus and spinal cord and highly accumulates at the nodes of Ranvier in the adult (Bartsch et al., 1993; Ffrench-Constant et al., 1986). TN-R is also a component of the perineuronal nets surrounding neuronal cell bodies of inhibitory interneurons (Weber et al., 1999). After a crush of the optic nerve in mice, the strong expression of TN-R mRNA in the optic nerve is slightly increased and severed axons do not regenerate. In contrast, TN-R immunoreactivity disappears from the lesioned optic nerve of salamanders, which is concomitant with the regeneration of optic axons (Becker et al., 1999; Becker et al., 2000b). These observations suggest that TN-R might be involved in interactions between oligodendrocytes and neurons during myelin formation and axonal regeneration (Schachner et al., 1994). TN-R influences axon growth in a complex manner, depending decisively on the way in which it is presented to growing axons and on the neuronal cell type analyzed (reviewed in Schachner et al., 1994). For example, the growth of dorsal root ganglion neurites is promoted on a homogeneous substrate of TN-R, while a substrate border repels these neurites *in vitro* (Taylor et al., 1993). Growth of neurites of other cell types is inhibited (Pesheva et al., 1993; Taylor et al., 1993) or promoted on a homogeneous substrate (Lochter and Schachner, 1993a; Lochter et al., 1994; Nörenberg et al., 1995). The morphological analysis of the optic nerves of TN-R deficient mice on the ultrastructural level revealed no difference in myelination and structure of nodes of Ranvier (Weber et al., 1999).

TN-W has been only identified in the zebrafish so far (Weber et al., 1998) and its mRNA is expressed during ontogenetic development in embryos and juvenile animals. TN-W is present in the lateral plate mesoderm and in the presumptive sclerotome. Migrating cells of sclerotomal and neural crest origin also show high levels of expression. Furthermore, non-neuronal cells in the dorsal root ganglia express detectable levels of TN-W. The expression partially overlaps with that of TN-C mRNA, suggesting an involvement of both molecules in neural crest and sclerotome migration and in the formation of the skeleton.

As the largest member of the tenascin family, TN-X is predominantly expressed in connective tissue, in heart and skeletal muscle, tumor tissues, skin and in the vicinity of blood vessels (Hasegawa et al., 1997; Ikuta et al., 2000; Lethias et al., 2001; Sakai et al., 1996). TN-X has been associated to a disease, called the Ehler-Danlos syndrome (Burch et al., 1997).

TN-Y was identified in the chicken and is expressed by different types of muscles, but also in lung, kidney, skin and in the nervous system. In the CNS it shows a partially overlapping, but also complementary expression pattern with TN-C (Fluck et al., 2000; Hagios et al., 1999; Tucker et al., 1999)

The newest member of the tenascin family, TN-N, is mainly expressed in kidney and spleen. Low level expression, however, has also been detected in the murine CNS (J. Neidhardt, Dissertation, Universität Hannover).

In comparison to TN-C, TN-R and TN-X only little is known about TN-Y, TN-W and TN-N, and their *in-vivo* function still remains to be elucidated.

1.4 The zebrafish (*Danio rerio*)

The zebrafish (*Danio rerio*) belongs to the family of Cyprinidae in the order of Cypriniformes and the category of Osteichthyes. Zebrafish are tropical sweet water fish and can be found in India, Pakistan, Nepal and South-Asia.

For several reasons, the zebrafish has become a model system in biology to study genetics and development. Zebrafish embryos develop outside of the mother making them accessible to perturbation by injecting reagents directly into the egg. Furthermore, the embryos are transparent, allowing the direct observation of developing tissues and organs in the living embryo. The early development of the zebrafish is very fast and the nervous system is patterned at 16 hours post fertilization (hpf). Single neurons can be easily identified, therefore making the zebrafish an excellent tool to study neurobiological processes like axon guidance (Baier et al., 1996). At 24 hpf, nearly all organs of the zebrafish are formed. The juvenile

zebrafish hatch at 3 days after fertilization and reach sexual maturation at an age of 3 to 4 months. The zebrafish is easy to breed and produces high numbers of descendants (up to 300 eggs in a week) over the whole year. The size of the zebrafish genome is approximately 1.7×10^9 bp and is distributed over 25 chromosomes. A first unfinished version of the complete sequenced genome was available in 2002 the complete finished sequence is projected to be available in 2005. Large parts of the zebrafish genome underwent duplications during telost evolution (Taylor et al., 2001). About 30 % of the genes in the zebrafish are present in duplicates compared to their homologues in other vertebrates (Van de Peer et al., 2002). An example are the genes for L1.1 and L1.2 (Tongiorgi et al., 1995a) in zebrafish which are the homologues of the mouse L1 gene.

1.5 Outgrowth of motor axons in the developing zebrafish

Due to its relative simplicity, the stereotypic motor axon outgrowth in the trunk of embryonic zebrafish is an attractive system to study mechanisms of axon guidance (Westerfield and Eisen, 1988). The motor nerves in the segmentally arranged trunk are pioneered by the axons of the so-called rostral (RoP), medial (MiP) and primary motor neurons (CaP) in each hemisegment. The CaP axon is the first to exit the spinal cord in a midsegmental position from where it grows ventrally between the notochord and somite. The other primary axons join the CaP axon in the midsegmental pathway, but only up to the horizontal myoseptum, where the MiP axon retracts from the common pathway to pioneer the dorsal motor nerve and the RoP axon diverges laterally. The CaP axon is the only one to continue ventral growth beyond the horizontal myoseptum to establish the ventral motor nerve. Primary axons are later followed by secondary axons, which grow along the same pathways (Eisen et al., 1986; Ott et al., 2001; Pike et al., 1992; Westerfield et al., 1986).

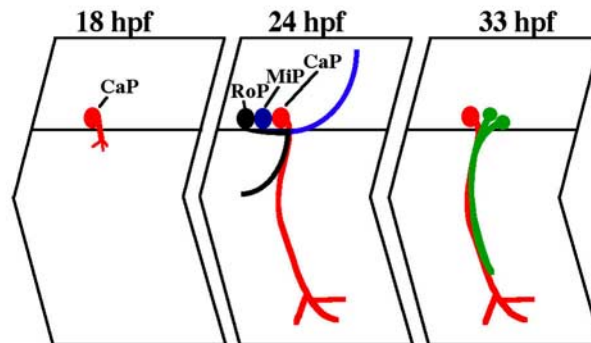


Fig.2. The CaP axon defines the midsegmental ventral motor axon pathway. Schematic representations of trunk muscle segments are shown. Axon outgrowth by the CaP axon (red) is initiated at approximately 17-19 hpf. At 24 hpf it has extended into the ventral somite. Other primary motor axons grow towards the dorsal (MiP axon; blue) or lateral musculature (RoP axon; black). These neurons are present also at 18 and 33 hpf, but for clarity are only depicted for 24 hpf. At 33 hpf, secondary motor axons (green) have entered the ventral motor axon pathway and are fasciculated with the CaP axon.

1.6 Regeneration in the central nervous system of the zebrafish

The central nervous system (CNS) of fish is growing throughout its lifetime, it retains the capacity to regrow severed axons and restore functionally appropriate connections with target areas into adulthood (Gaze, 1970). In this capacity, the fish CNS differs from the adult mammalian CNS, which generally does not support axon regeneration, but resembles the adult mammalian peripheral nervous system (PNS) in which axon regeneration occurs. Success and failure of axon regeneration apparently depends on intrinsic factors of the neurons as well as on the extrinsic glial cell environment (reviewed in Fawcett and Geller, 1998).

The non-permissive properties of reactive astrocytes and oligodendrocytes in lesioned axon pathways are in part responsible for the failure of axon regeneration in the mammalian CNS (for review, see Fawcett and Asher, 1999; Schnell and Schwab, 1993). Similar to mammals, the major glial cell types in fish CNS are astrocytes and oligodendrocytes (Maggs and Scholes, 1990; Wolburg and Bouzehouane, 1986). The response of these cells to fiber tract lesions in the fish CNS has been studied extensively in the visual pathway (reviewed in

Bernhardt, 1999; Stuermer et al., 1992). There is evidence that a non-permissive glial scar with its growth-inhibitory proteoglycans, which prevents regrowth of lesioned CNS axons in mammals (Bradbury et al., 2002; Davies et al., 1997), may not form after a lesion of the fish optic nerve (Becker and Becker, 2002; Hirsch et al., 1995). In addition, fish CNS myelin and oligodendrocytes may contain no or low amounts of neurite outgrowth inhibitors (Sivron et al., 1994; Wanner et al., 1995) that interfere with axon growth in the CNS of mammals (Bregman et al., 1995; Chen et al., 2000; GrandPre et al., 2000).

Glial cells in the lesioned CNS of mammals also lack growth-promoting molecules that are upregulated after a lesion of the regenerating PNS (reviewed in Fu and Gordon, 1997; Martini, 1994). In the regenerating CNS of fish, glial expression of growth-promoting molecules increased after a lesion. For example, the expression of members of the immunoglobulin (Ig) superfamily of recognition molecules, such as L1-related molecules and the neural cell adhesion molecule (NCAM) is increased in glial cells after optic nerve lesion (Ankerhold et al., 1998; Bernhardt et al., 1996). Molecules of the Ig superfamily are membrane proteins involved in homo- and heterophilic adhesion, as well as in signal transduction (for review see Crossin and Krushel, 2000; Schachner et al., 1990; Walsh and Doherty, 1997). L1-related molecules and NCAM promote neurite outgrowth (see for instance Appel et al., 1995; Frei et al., 1992; Haspel et al., 2000; Saffell et al., 1995) and may thus support axon regeneration in fish (reviewed in Bernhardt, 1999; Stuermer et al., 1992). However, in mammals these molecules are not detectably upregulated by glial cells after a lesion (Becker et al., 2001a). In agreement with the differences in the expression of growth-promoting and inhibiting molecules between fish and mammalian glial cells, oligodendrocyte-like cells of goldfish support regeneration of optic axons *in vitro*, while mammalian oligodendrocytes inhibit it (Ankerhold et al., 1998; Bastmeyer et al., 1991).

1.7 Aim of this work

Members of the Ig-like superfamily have been shown to be upregulated during regeneration of axons in the CNS of adult fish and therefore might contribute to successful axonal regeneration. The aim of the first part one of this work was to find additional molecular aspects of successful axonal regeneration in the environment of lesioned axons in the CNS of fish. Therefore the cDNA for myelin protein zero, another member of the Ig-like superfamily was cloned and the expression of its mRNA during development and regeneration of the adult CNS of the zebrafish was described.

In the past decade, six members of the tenascin family have been identified and characterized. TN-R and TN-C are expressed in the central nervous system and show diverse functions on outgrowing neurites and migrating neural cells. In contrast to this striking *in vitro* functions, gene deficient mice of TN-C or TN-R have rather disappointing phenotypes in the central nervous system. To gather more data on the *in vitro* and *in vivo* functions of these molecules, TN-C and TN-R were analysed in more detail in the zebrafish.

In the second part of the study, the TN-R homologue of the zebrafish was cloned and expression patterns of its mRNA and the corresponding protein described during development and regeneration of retina ganglion cell axons in the adult CNS.

The expression of TN-C in the developing zebrafish was described in earlier studies but nothing is known about the *in vivo* functions of this molecule in the zebrafish. In the third part of the study a potential role of TN-C as a guidance factor for motor axons in the trunk of the developing zebrafish was analyzed *in vivo*.

2. Materials

2.1. Enzymes and reaction kits

DNA polymerases

Advantage TM -2	BD Biosciences Clontech	Heidelberg, D
Advantage TM -HF2		
Advantage TM -GC2		
HotStar Taq	Qiagen	Hilden, D
Klenow enzyme	Roche	Mannheim, D
<i>PfuTurbo</i> [®]	Stratagene	Amsterdam, NL
<i>PfuTurbo</i> [®] Hotstart		
Taq DNA Polymerase	Invitrogen	Karlsruhe, D

Restriction endonucleases

Various	AGS Hybaid	Heidelberg, D
Various	MBI Fermentas	St. Leon-Rot, D
Various	NEB	Frankfurt a. M., D

(DNA-dependent) RNA polymerases

T3/T7/SP6 pol.	Roche	Mannheim, D
Megascript TM kit	Ambion	Cambridge, UK
mMessage mMachine TM kit SP6		

Reverse transcriptases (RT), (RNA-dependent) DNA polymerases

Omniscript TM RT	Qiagen	Hilden, D
Sensiscript ^{TN} RT		
Superscript ^{TM RT}	Invitrogen	Karlsruhe, D

Miscellaneous

DNase I	Roche	Mannheim, D
Shrimps alkaline phosphatase (SAP)		
T4 DNA Ligase		
Rapid Ligation TM kit		

Megaprime™ System	APB	Freiburg, D
Probequant G50-columns		
pGEM-T vector system	Promega	Mannheim, D
rRNasin		
First choice™ RLM-RACE kit	Ambion	Cambridge, UK
Topo TA cloning	Invitrogen	Karlsruhe, D
5' RACE kit		

2.2 Reagents, disposables, etc

If not itemized in this paragraph, origin of enzymes and reaction kits is referenced in the corresponding sections. All chemicals were obtained from the following companies in *pro analysis* quality: Amersham Pharmacia Biotech (APB, Freiburg), Bio-Rad (Munich, D), Invitrogen (Karlsruhe, D), Carl Roth (Karlsruhe, D), Merck (Darmstadt, D), Serva (Heidelberg, D) and Sigma-Aldrich (Deisenhofen, D). Molecular cloning reagents were obtained from Ambion (Cambridge, UK), APB (Freiburg, D), BD Biosciences Clontech (Heidelberg, D), Promega (Mannheim, D), Qiagen (Hilden, D) and Statagene (Amsterdam, NL). DNA and RNA purification kits were purchased from APB (Freiburg, Germany) and Qiagen (Hilden, D). Nucleic acid molecular weight markers were purchased from Roche and NEB (Frankfurt a. M., D).

2.3 Instruments

Equipments not listed in the table below were of common laboratory standard. Particular devices are referenced throughout the respective protocols.

Centrifuges

Sorvall	Kendro, Hanau, D	RC50 <i>plus</i> with SLA3000, SLA 1500, SA600 and HB-6 rotors
Eppendorf	Hamburg, D	Microcentrifuge 5415D Bench-top centrifuges 5417R and 5403
Jouan, Inc	Winchester, VA, USA	Bench-top centrifuge CR422

Liquid scintillation counting

Wallac	Freiburg, D	Liquid scintillation counter 1409
--------	-------------	-----------------------------------

Miscellaneous

APB	Freiburg, D	UV crosslinker
Fujifilm	Raytest, Straubenhardt, D	Phosphimager BAS-1000
Herolab	Wiesloh, D	E.A.S.Y. UV-light documentation
Leica	Bensheim, D	Cryostat CM3050
Zeiss	Goettingen, D	Axiophot
		Laser scanning microscope Zeiss LSM510

Power supplies

Bio-Rad	Munich, D	Power Pac series
---------	-----------	------------------

Spectrophotometer

APB	Freiburg, D	Ultrospec 3000/DPV-411 printer
-----	-------------	--------------------------------

Thermal cyclers

Eppendorf	Hamburg, D	Mastercycler <i>gradient</i>
MJ Research	Waltham, MA, USA	PTC-200 DNA Engine™ <i>classic</i>

2.4 Oligonucleotides

Oligonucleotides/primers were synthesized by MWG biotech AG (Ebersberg, D) or Metabion (Planegg, Martinsried, D).

2.5 Morpholinos

Morpholine-based antisense oligonucleotides were synthesized by Gene Tools LLC (Philomath, OR, USA). Morpholino sequences are listed in the appendix.

2.6 Antibodies

The polyclonal antibodies Sus-ten (Bartsch et al., 1995) and anti TN-C (Tongiorgi, 1999) to TN-C, monoclonal antibodies 596, 597 (Pesheva et al., 1989) and polyclonal antibodies termed EGF-L and FN-2 (Xiao et al., 1998) to TN-R and monoclonal antibodies O1 and O4, which label myelin (Sommer and Schachner, 1981) have been described. Monoclonal antibodies G-A-5 to glial fibrillary acidic protein, CS-56 to chondroitin sulfate proteoglycans and B-5-1-2 to acetylated tubulin were purchased from Sigma-Aldrich (Deisenhofen, D). Monoclonal antibody Linc to label retinal axons was originally developed by (Steen et al., 1989) and obtained from the developmental studies hybridoma bank (DSHB). Monoclonal antibody 9E10, recognizing the myc-epitope was purchased from Covance (Princeton, USA). Monoclonal antibody 4C4, recognizing microglia/macrophages was a kind gift from Drs A. Dowding and J. Scholes. Monoclonal antibody F59 recognizing adaxial cells in the zebrafish (Devoto et al., 1996) was a kind gift from Dr. Stockdale.

Secondary antibodies

For indirect immunofluorescence, CyTM 2-, 3- and 5- conjugated antibodies (diluted 1:200) and horseradish peroxidase-conjugated antibodies (diluted 1-200) to rabbit, rat or mouse were used, respectively (all from Dianova, Hamburg, D)

2.7 Bacterial strains

<i>E. Coli</i> DH5 α	Invitrogen
<i>E. Coli</i> Top 10	Invitrogen
<i>E. Coli</i> NR 3704 (dam ⁻)	Institut Prof. Schachner

2.8 Bacterial media

All media were autoclaved prior to use.

Luria broth (LB per liter)	10	g	NaCl
	10	g	tryptone or peptone
	5	g	yeast extract
	→ pH 7.0 with 5 N NaOH (optional)		
LB agar (per liter)	10	g	NaCl
	10	g	tryptone or peptone
	5	g	yeast extract
	20	g	agar
→ pH 7.0 with 5 N NaOH (optional)			

The following antibiotics were added when needed (1000 fold stock solutions): 100 mg/l ampicillin (LB-amp), 25 mg/l kanamycin (LB-kan).

2.9 Vectors

pBluescript [®] II SK/KS	Stratagene	Cloning vector
pCR [®] 2.1 Topo	Invitrogen	Topo cloning host vector
pCR [®] II Topo	Invitrogen	Topo cloning host vector
pCR [®] II Blunt Topo	Invitrogen	Topo cloning host vector
pGEM [®] -T easy	Promega	TA cloning vector
pCS2MT	Rupp et al., 1994	Cloning vector to generate mRNA overexpression constructs

2.10 Zebrafish

Adult (body length > 2 cm, age > 4 months) and developing zebrafish, *Danio rerio*, were taken from our breeding colony or bought at a fish breeder and raised according to standard protocols (Westerfield, 1989). Prior to surgery, adult fish were kept in groups of 10 animals at a 14 hour light and 10 hour dark cycle and a temperature of 27°C. After surgery, fish were kept individually in two liter tanks. Fish were fed dried fish food and live brine shrimp. All animal experiments were approved by the University and State of Hamburg animal care committees and conformed to NIH guidelines.

2.11 Buffers and stock solutions

Buffers and stock solutions are listed below. All more method-specific solutions are specified in the accompanying sections.

Blocking buffer (whole mount immunohistochemistry)

	1	% (v/v)	DMSO
	1	% (v/v)	normal goat serum
	1	% (w/v)	BSA
	0.7	% (v/v)	Triton-X 100
DAB-stock solution	1	% (w/v)	Diaminobenzidine
Danieau solution	58	mM	NaCl
	0.7	mM	KCl
	0.4	mM	MgSO ₄
	0.6	mM	Ca(NO ₃) ₂
	5	mM	HEPES
		pH 7.6	
DIG blocking stock	10	g	Blocking reagent (Roche)
	100	ml	DIG buffer 1
DIG buffer 1 (2 X)	0.2	M	maleic acid

	0.3	M	NaCl → pH 7.5 (solid NaOH)
DEPC-H ₂ O	0.1	% (w/v)	diethylpyrocarbonate → autoclave after stirring overnight
DNA-sample buffer (5x) (DNA-gels)	20 0,025	% (w/v) % (w/v)	glycerol in TAE buffer orange G
dNTP-stock solutions (PCR)	25	mM	each dATP, dCTP, dGTP, dTTP
EDTA stock solution	0.5	M	EDTA → pH 8.0
Ethidiumbromide- staining solution (DNA-gels)	10	µg/ml	ethidiumbromide in 1xTAE
Formaldehyde gel running buffer	0.1 40	M mM	MOPS pH7.0 sodium acetate
RNA-gel (5X)	5	mM	EDTA
Formaldehyde gel loading buffer	50 1	% (v/v) mM	glycerol EDTA
RNA-gel 5x	0.25 0.25	% (w/v) % (w/v)	bromphenol blue cylene cyanol
4 % Paraformaldehyde	4	% (w/v)	paraformaldehyde dissolved at 60 °C under stirring in 1 x PBS
Phosphate buffered saline	1.36	M	NaCl

(PBS 10 x, Morphology)	0.1	M	Na ₂ HPO ₄
	27	mM	KCl
	18	mM	KH ₂ PO ₄
			→ pH 7.4
PBST	0.1	% (v/v)	Tween 20 in 1 x PBS
Saline sodium citrate buffer (SSC, 20 x)	3	M	NaCl
	0.3	M	<i>tri</i> -sodium citrate
			→ pH 7.4
TAE (50x) (DNA-gels)	2	M	Tris-Acetat, pH 8,0
	100	mM	EDTA
TE (10x)	0,1	M	Tris-HCl, pH 7,5
	10	mM	EDTA

3. Experimental procedures

3.1 Various molecular biological methods

If not otherwise indicated, standard biological techniques were carried out as described (Sambrook et al., 1989). Methods for cDNA cloning, probes for in situ hybridization and northern blotting and generation of mRNA overexpression constructs, are described in more detail.

3.1.1 Photometric quantification of nucleic acids

DNA, RNA and oligonucleotides were measured directly in aqueous solutions. The concentration was determined by measuring adsorption at $\lambda=260$ nm against blank and then evaluated via factor. The absorption of 1 OD (A) is equivalent to approximately 50g/ml dsDNA, 40 g/ml RNA and 30 g/ml for oligonucleotides. Interference by contaminants was recognized by the calculation of ratio. The ratio $A_{260} / 280$ is used to estimate the purity of nucleic acid, since proteins absorb at 280 nm. Pure DNA should have a ratio of 1.8, whereas pure RNA should give a value of approximately 2.0. Absorption at $\lambda=230$ nm reflects contamination of the sample by substances such as carbohydrates, peptides, phenols or aromatic compounds. In the case of pure samples, the ratio $A_{260} / 230$ should be approximately 2.2.

3.1.2 DNA agarose gel electrophoresis

To analyze restriction digests, quality of nucleic acid preparations, etc. horizontal agarose gel electrophoresis was performed. Gels were prepared by heating 0.8-2.5 % (w/v) agarose (Invitrogen, *electrophoresis grade*) in *Tris-acetate* buffer (TAE), depending on the size of fragments to be separated. DNA samples were adjusted to 1 x DNA sample buffer and were subjected to electrophoresis at 10 V/cm in BIO-Rad gel chambers in 1 x TAE running buffer. Afterwards, gels were stained in 0.5 μ g/ml ethidium bromide in 1 x TAE solution for approximately 20 min. Thermo-photographs of transilluminated gels were taken, or bands

were made visible on an UV-screen ($\lambda=360$ nm) and desired fragments were cut out with a scalpel. Extraction of DNA fragments from agarose plugs is described under 3.4.3.

3.1.3 Restriction of DNA

Restriction enzyme digestions were performed by incubating dsDNA molecules with an appropriate amount of restriction enzyme(s), the respective buffer as recommended by the supplier(s), and at the optimal temperature for the specific enzyme(s), usually at 37°C. In general, 20 μ l digests were planned. For preparative restriction digests the reaction volume was scaled up to 100 μ l. Digest were composed of DNA, 1 x restriction buffer, the appropriate number of units of the respective enzyme(s) (due to glycerol content the volume of the enzyme(s) added should not exceed 1/10 of the digest volume), and the sufficient nuclease-free H₂O to bring the mix to the calculated volume. After incubation at the optimal temperature for a reasonable time period (mostly 2-3 hrs or overnight), digests were stopped by incubation for 20 min at 65°C. If reaction conditions of enzymes were incompatible to each other, DNA was digested successively with the individual enzymes. Between individual reactions, DNA was purified, see (3.4.2).

3.1.4 Sequencing of DNA

Sequence determination of dsDNA was performed by the sequencing facility of the ZMNH (Dr. W. Kullmann, M. Daeumigen). Fluorescent-dye labelled chain- termination products (ABI Prism Dye Terminator Cycle Sequencing Ready Reaction Kit, Perkin Elmer, Wellesly, MA, USA) were analyzed with an ABI Prism 377 DNA Sequencer (Perkin Elmer). For preparation, 0.8-1 μ g of DNA was diluted in 7 μ l ddH₂O and 1 μ l of the appropriate sequencing primer (10 pM) was added.

3.1.5 Maintenance of bacterial strains

Strains were stored as glycerol stocks (LB-medium, 25% (v/v) glycerol) at -80°C. To regrow particular strains, an aliquot of the stock was streaked on an LB-plate containing the

appropriate antibiotics and incubated overnight at 37°C. Plates were stored up to 6 weeks at 4°C.

3.1.6 Precipitation of DNA

The salt concentration of an aqueous DNA solution was adjusted by adding 1/10 volume of sodium acetate, pH 5.2. 2.5 volumes of cold ethanol, -20°C were added and the samples mixed well. Following incubation on ice for 30 min, samples were centrifuged for 15 min (16000 x g, RT). For optimal purity, the pellet was loosened from the tube during inverting and was broken up in ethanol. After removal of the supernatant, a quick 1-2s centrifugation step was performed and residual ethanol was aspirated. Supernatants were removed and DNA pellets air dried (approximately 5 min at RT). DNA was resuspended in an appropriate volume of prewarmed water.

3.1.7 Production of competent bacteria

DH5 α bacteria were streaked on LB-agar dishes and grown overnight at 37°C with constant shaking. 50 ml of LB broth were inoculated with 5 colonies and grown at 37 °C under constant shaking (>200 rpm) until the culture had reached an optical density (OD₆₀₀) of .035-0.45. Growth of bacteria was stopped by a 5 min incubation step on ice. Cells were pelleted at 1000 x g for 15 min (4°C) and – after removal of the supernatant – resuspended in 17 ml prechilled RF1 (4°C). Following a 15 min incubation on ice, the centrifugation was repeated. The cell pellet was resuspended in 4 ml prechilled RF2 (4°C) and incubated again for 15 min on ice. Bacteria as 50 – 100 μ l aliquots were frozen in liquid nitrogen and stored at -80°C. Transformation capacity/efficacy of cells was tested by a transformation with a distinct quantity (pg-ng) of purified supercoiled plasmid DNA.

RF1

100mM RbCl

50 mM MnCl₂

30 mM KOAc

10 mM CaCl₂

→ pH 5.8 (with 0.2 M acetic acid)

RF2

10 mM MOPS (pH 6.8)

10 mM RbCl

75 mM CaCl₂

150 g/l glycerol

3.2 Cloning in plasmid vectors

3.2.1 Preparation / enzymatic manipulation of insert DNA

Four different kinds of insert DNA fragments were cloned (see item list below). If the insert DNA did not contain ends compatible with the pre-cleaved vector, several strategies were followed to overcome this problem; methods performed are briefly described below the item list.

Plasmid DNA fragments. For cloning of distinct regions of plasmid DNA, donor molecules were digested with appropriate restriction enzyme(s). Even though direct ligation using DNA from inactivated restriction digest was possible, mostly complete digests were applied to agarose gel electrophoresis, appropriate bands were cut out and DNA was eluted from agarose plugs, thus avoiding unwanted by-products during subsequent ligation reactions. Non complementary overhanging ends were converted to blunt ends prior to ligation using the Klenow enzyme.

Pfu DNA polymerase-derived products. Due to the 3'→5' exonuclease activity, a major fraction of DNA species amplified with *PfuTurbo*[®] DNA polymerase does not contain an additional adenosine at the 3'-end. These products were directly cloned with vector DNA that was cut with enzymes generating blunt ends or subjected to Topo cloning. Before ligating DNA from PCR reactions, DNA was cleaned up or DNA fragments were purified.

Taq DNA polymerase-derived products. PCR products amplified with Taq DNA Polymerase, HotStarTaq[™], or enzymes of the Advantage[™] product family DNA polymerases were directly subjected to TA cloning. The latter two products are actually mixtures that contain minor amounts of a proofreading polymerase, but TA cloning was still possible.

PCR products with introduced restriction sites. Frequently, the ends of insert DNA did not contain suitable restriction enzyme sites, i.e. when a donor cDNA was designated for cloning into a certain reading frame of an expression vector. Restriction enzyme sites were generated by PCR at the desired location. For this technique, restriction sites were designed into the 5'-

end of the PCR primers. Because certain restriction enzymes inefficiently cleave recognition sites located at the end of a DNA fragment, usually four additional bases were introduced 5' to the restriction site. PCR products were gel-purified, digested with the appropriate restriction enzymes, and purified with spin columns.

Converting a 5'-overhang to a blunt end terminus

Non compatible 5'-overhanging ends were blunted for ligation using Klenow enzyme (DNA polymerase I Large Fragment, Roche). 2U were directly added to a 20 μ l heat-inactivated restriction digest complemented to a final concentration of 40 μ M of each dNTP and incubated for 30 min at 37°C. The reaction was terminated by incubation at 70°C for 10 min and fragments were directly used for ligation reactions.

3.2.2 Enzymatic manipulation of vector DNA prior to cloning

When used as vectors, plasmids were digested at one locus either by a single restriction enzyme or by two at a multi-cloning site to achieve insertion of target DNA in a defined orientation. Digestion reactions were carried out as described under 3.1.2 using 5-10 μ g of plasmid DNA as starting material. When digestions were verified as complete and correct by agarose gel electrophoresis, complete restriction digests were subjected to preparative agarose gel electrophoresis and appropriate bands representing digested vectors were cut out and vector DNA was extracted from agarose plugs. To prevent self-circularization by DNA ligase, SAP buffer (Boehringer Ingelheim) and 1 U SAP (shrimp alkaline phosphatase) per 100 ng plasmid DNA were added to remove 5'-phosphates. The reaction was incubated at 37°C for 2 h and terminated by incubation at 70°C for 10 min. The plasmid DNA was used for ligation without further purification.

3.2.3 Ligation of plasmid vector and insert DNA

Ligation of DNA fragments was performed by mixing 50 ng vector DNA with the fivefold molar excess of insert DNA. 1 μ l of T4-Ligase and 2 μ l of ligation buffer (Roche) were added and the reaction mix was brought to a final volume of 20 μ l. The reaction was incubated either for 2 h at room temperature (sticky ends) or overnight at 16°C (blunt ends). The reaction mixture was used directly for transformation without any further purification.

3.2.4 TA cloning

Two different systems were employed for TA cloning of PCR products containing an additional adenosine at their 3'-ends. If the amount of product after a RACE-PCR, was only in the range of 50 ng or below, the highly efficient vaccinia topoisomerase-I based TOPO[®] cloning system (Invitrogen) was applied. PCR fragments were inserted into the vectors pCR[®]2.1-TOPO or pCR[®]II-TOPO following the manufactures instructions. Blunt-end derived PCR fragments were cloned in pCR[®]II-Blunt TOPO (Invitrogen). If availability of DNA fragments was not restricted, TA cloning of PCR products was performed with the pGEM[®]-T vector followed the manufacturer's instructions.

3.2.5 (Re-) Transformation of DNA into bacteria

10 ng of plasmid DNA or 20 µl of a ligation mixture were added to 100 µl of competent DH5α and incubated for 30 min on ice. After a heat shock (2 min, 42°C) and successive incubation on ice (3 min), 800 µl of LB-medium were added to the bacteria and incubated at 37°C for 30 min. Cells were then centrifuged (10000 x g, 1 min, RT) and the supernatant removed. Cells were resuspended 100 µl LB medium and plated on LB plates containing the appropriate antibiotics. Colonies formed after incubation at 37°C for 12-16 h.

3.3 Purification of nucleic acids

3.3.1 Plasmid DNA purification from bacterial cultures

Mini-scale plasmid isolation

3 ml LB/Amp-Medium (100 µg/ml ampicillin) were inoculated with a single colony and incubated over night at 37°C with constant agitation. Cultures were transferred into 2 ml Eppendorf tubes and cells were pelleted by centrifugation (12,000 rpm, 1min, RT). Plasmids were isolated from the bacteria using the GFX *micro* plasmid prep system (APB), according to the manufacturer's protocol. The DNA was eluted from the columns by addition of 50 µl

Tris-HCl (10 mM, pH 8.0) with subsequent centrifugation (12,000 rpm, 2 min, RT). Plasmid DNA was stored at 20°C.

Plasmid DNA isolation from 15-ml cultures

To rapidly obtain higher amounts of DNA, the Macherey-Nagel Nucleospin kit was used. 15 ml LB/Amp-Medium (100 µg/ml ampicillin) were inoculated with a single colony and incubated over night at 37°C with constant agitation. Cultures were transferred into 15 ml Falcon tubes and cells were pelleted by centrifugation (12,000 rpm, 1min, RT) in an Eppendorf centrifuge. Plasmids were isolated from the bacteria according to the manufacturer's protocol with the exception that twice the suggested amount of buffers were used. DNA was eluted from the columns by adding 50 µl of prewarmed (70°C) Tris/Cl (10 mM, pH 8.0) with subsequent centrifugation (12,000 rpm, 2 min, RT) twice. Finally, the DNA concentration was determined as described in 3.1..

Plasmid DNA isolation from 500 ml-cultures (Maxipreps)

For preparation of large quantities of DNA, the Qiagen Maxiprep kit was utilized. A single colony was inoculated in 2 ml LB/amp (100 µg/ml ampicillin) medium and grown at 37°C for 8 h with constant agitation. Afterwards, this culture was added to 500ml LB/amp medium (100 µg/ml ampicillin) and the culture was incubated at 37°C with constant agitation overnight. Cells were pelleted in a Beckmann centrifuge (6,000g, 15 min, 4°C) and DNA was isolated as described in the manufacture's protocol. Finally, the DNA pellet was resuspended in 600 µl of prewarmed (70°C) Tris-HCl (10 mM, pH 8.0) and the DNA concentration was determined.

3.3.2 PCR/DNA fragment purification

For purification of DNA fragments the silica matrix-based High Pure PCR-Purification kit (Roche) was used according to the manufacturer's protocol. The DNA was eluted from the column by addition of 50 μ l prewarmed (70°C) Tris-HCl (10 mM, pH 8.0). The DNA-concentration was determined using the undiluted eluate.

3.3.3 DNA fragment extraction from agarose gels

For isolation and purification of DNA fragments from agarose gels, ethidiumbromide-stained gels were illuminated with UV-light and the appropriate DNA band was excised from the gel with a clean scalpel and transferred into an Eppendorf tube. The fragment was isolated utilizing the silica matrix-based QIAquick Gel Extraction kit (Qiagen) following the manufacturer's protocol. The fragment was eluted from the column by addition of 50 μ l prewarmed (70°C) Tris-HCl (10 mM, pH 8.0). The DNA-concentration was determined using the undiluted eluate.

3.3.4 Total RNA isolation from zebrafish brain tissue

Total RNA was purified using the silica-gel-membrane technology as adopted in Qiagen's RNeasy[®] system. All buffers used were provided by the manufacturer. Adult zebrafish brains were quickly isolated and frozen in liquid nitrogen. 250 mg brain tissue was homogenized in 4 ml buffer RLT with a rotor-stator homogenizer for 60 s at maximum speed. The total RNA was isolated following the manufacturer's protocol. Finally, total RNA was eluted in 200 DEPC-treated water. Integrity of the purified total RNA was assessed by spectrophotometry (scan from λ =200-350nm) and agarose electrophoresis (even under non denaturing conditions, identical to the procedure described in section 3.1.1. for DNA). Total RNA samples were stored at -80°C.

3.3.5 Purification of mRNA

Poly A⁺ mRNA was isolated from total RNA samples with Qiagen's Oligotex[®] system (Midi). 30 µl vortexed and preheated (37°C) Oligotex-dT₃₀ suspension were added to 500 µg total RNA in a volume up to 500 µl DEPC-H₂O. Purification was performed as described in the manufacturer's protocol. Poly A⁺ mRNA was eluted from spin columns with 25 µl provided elution buffer. Purified mRNA was stored at -80°C.

3.4 Nucleic acid amplification

The *in-vitro* amplification of DNA fragments using the polymerase chain reaction (PCR) was usually performed in a MJ PTC-200 DNA ENGINE[™] classic thermal cycler. Routinely, PCR reactions were set up by adding the following ingredients to a 0.2 ml thin-walled tube (Biozym Diagnostik GmbH, Hessisch-Oldendorf, D): the template DNA (typically plasmid or first strand cDNA), the primers flanking the region(s) to be amplified, dNTPs, buffer and DNA polymerase. Primer sequences were selected manually or electronically determined with the PrimerSelect software from the Lasergene software suite (DNASTAR inc. WI, USA). Selected primer sequences were evaluated with the Oligo Calculator (<http://www.basic.nwu.edu/biotools/oligocalc.html>) which employs the nearest neighbor algorithm to determine annealing temperatures. Routinely, 20-50 µl reactions were performed. The enzymes, that were used during these experiments are as follows (in brackets typical PCR reactions are cited): (a) *Taq* DNA polymerase (“general” PCR reactions), (b) *PfuTurbo*[®] DNA polymerase (PCR to amplify DNA for further cloning steps), (c) HotStarTaq[™] DNA polymerase (RACE-PCR, RT-PCR, general amplification from first strand cDNA, cloning of difficult amplicons), (d) Advantage[™]-DNA polymerase (RACE-PCR), (e) Advantage[™]-GC 2 DNA polymerase (GC-rich templates, RACE-PCR). Table 3.1 shows cycling parameters for the DNA polymerases (a) – (e). Number of cycles (25-35 up to 40) required for optimum amplification varied depending on the amount of starting material and the efficiency of each amplification step. In certain experiments (e.g., RACE-PCR), a touchdown strategy (Don et al., 1991) was adopted. A final incubation step at the extension temperature ensured fully double stranded molecules from all nascent products. Following cycling, typically 5-10 µl aliquots up to complete reactions were analyzed by agarose gel electrophoresis to detect amplified products. In instances where the yield from a single PCR

was insufficient (e.g., RACE-PCR), the reaction was purified and an aliquot was used as template for a second PCR with the same or a nested primer set (nested PCR).

	(a) "Taq"	(b) "Pfu"	(c) "HotStar"	(d) "Adv-2"	(e) "Adv-GC"
(01)	1:00, 94°C to 5:00, 95°C	1:00, 94°C to 1:00, 98°C	15:00, 95°C	1:00, 95°C	3:00, 94°C
(02)	0:30, 94°C to 1:00, 96°C	1:00, 94°C to 1:00, 98°C	0:30, 94°C to 1:00, 94°C	0:30, 95°C to	0:30, 94°C to
(03)	0.30-1:00 T_{NB}	1:00 T_{NB}	0.30-1:00 T_{NB}	3:00 (1-5 kb) 68°C	3:00 (1-5 kb) 68°C
(04)	72°C 1 min per kb	72°C 1 min per kb	72°C 1 min per kb	Goto2, 25-35 x	Goto2, 25-35 x
(05)	Goto2, 25-40 x	Goto2, 25-40 x	Goto2, 25-40 x	> 05:00, 72°C	> 05:00, 72°C
(06)	> 05:00, 72°C	> 05:00, 72°C	> 05:00, 72°C	4°C, for ever	4°C, for ever
(07)	4°C, for ever	4°C, for ever	4°C, for ever	End	End
(08)	End	End	End		

Table 3.1.: **PCR cycling parameters.** PCR programs shown were general starting points, when using the above mentioned DNA polymerases. T_{NB} , primer melting temperature calculated with the nearest neighbor algorithm.

3.4.1 Generating RNA by *In-vitro* transcription

To generate *in-vitro* transcribed RNAs, 5-10 µg of plasmid DNA containing the desired insert and a T3, T7 or SP6 polymerase promoter were digested with restriction endonucleases overnight, at positions that were located 3' of the designated RNA polymerase promoter and 3' of the to be transcribed strand of DNA. By doing this, the DNA polymerase transcribed only the strand of interest and no vector-specific sequences. Linearized DNA was purified using the MiniElute PCR purification kit according to manufacturers instructions (Qiagen). In order to obtain Digoxigenin (DIG) labeled RNA probes for *in-situ* hybridization, transcription of the desired templates was performed with Ambion's Megascript system. For the generation of DIG-labeled RNAs, the DIG-UTP mix shown below was used instead of NTPs provided by the manufacturer.

DIG-UTP mix (10x)

10 mM	ATP
10 mM	CTP
10 mM	GTP
6.5 mM	UTP
3.5 mM	DIG-11-dUTP (Roche)

In case of mRNA to be used for overexpression studies, the mMessage mMachine kit (Ambion) was employed. 20 μ l *in-vitro* transcriptions were in both cases essentially performed as recommended by the manufacturer. Generated mRNAs were purified by LiCl precipitation, analysed on a denaturing agarose gel and stored at -80°C .

3.5 cDNA cloning**3.5.1 First strand synthesis, RT-PCR**

For reverse transcription *in-vitro*, an RNA-dependent DNA polymerase activity and a hybrid-dependent exoribonuclease (RNase H) activity of the reverse transcriptase enzyme (RT) were utilized to produce single-stranded cDNA from RNA. Routinely, Omniscript™ RT was used to produce first strand cDNA from 50 –500 ng of total RNA as starting material. Sensiscript™ RT has been used for starting amounts below 50 ng of total RNA. After denaturing total RNA samples for 5 min at 65°C , the following reactions were set up by adding all further components by a master mix. First strand synthesis occurred during a 60 min incubation at 42°C .

1 x	Omniscript™ RT buffer
0,5 mM	each dNTP (5mM dNTPs supplied)
0.5 μ M	primer (mostly oligo-dT ₂₃₋₃₀)
0.2 U/ μ l	Omniscript™ RT (40 U/ μ l)
0.5 U/ μ l	rRNasin® (40 U/ μ l)
ad 20 μ l	DEPC-treated H ₂ O

First strand cDNA was stored at -20°C or directly subjected to PCR reactions (RT-PCR) as described in section 3.5.

3.5.2 Rapid amplification of cDNA ends

To clone the 5'- and 3'-ends of cDNA sequences, two slightly different technologies of Rapid amplification of cDNA ends (RACE) were employed. RACE facilitates the cloning of full-length cDNA sequences when only a partial clone is available. Two different systems for the amplification of cDNA ends were utilized, the RNA Ligase mediated Rapid Amplification of cDNA ends (RLM-RACE, Ambion) and the *classic* RACE (Invitrogen). RACE reactions were performed following the manufacturer's instructions. Zebrafish brain poly A⁺ mRNA was used as template for gene-specific RT-PCR in both cases. As a DNA polymerase, Qiagen's HotStarTaq™ or products of the Advantage™ product family (BD Biosciences Clontech) were utilized. Gene specific primers (GSP1, GSP2 and GSP3) were designed to fulfil the requirements of cycling parameters as recommended by the manufacturer. Amplified products were purified in a gel, directly sequenced or subjected to TA cloning.

3.5.3 Cloning of cDNAs for myelin protein zero, tenascin-r and tenascin-c

Isolation of a zebrafish P0 cDNA

Clone fj35f03 (UCDMp611K0617), which exhibits sequence homology to known P0 molecules from other species was obtained from the Resource Center and Primary Database (RZPD; Berlin, Germany), and the sequence confirmed. To verify that the clone contains the complete open reading frame (ORF) we performed 5'- and 3'- RACE (Rapid Amplification of cDNA Ends) procedures. Total RNA from adult zebrafish brains was isolated using the RNeasy® system (Qiagen, Hilden, Germany) and reversely transcribed using either random hexamers or an oligo-dT anchor primer, followed by PCR. The 5' end of P0 was verified by 5' RACE using the RNA Ligase Mediated Rapid Amplification of cDNA Ends (RLM-RACE®; Ambion, Austin, Texas) system according to the manufacturer's instructions. Primers RLM1 and RLM2 and nested gene specific primers P0R1 5'-GGTGGCCGCCGATGTCAGGT-3' and P0R2 5'-ATTGCGTCCTTAGCCCCATCTG-3' were used. To verify the 3' end, a 3' RACE was carried out using a combination of nested 3'-oligo-dT coupled adapter primers and two nested gene-specific primers (P031: 5'-GGTTCTATCCTGATCAAG -3', P032: 5'-CTTCAATATGTATTTCAGTCC -3'). Furthermore the entire ORF was amplified from cDNA preparations from adult zebrafish brain using primers outside the ORF (P0up: 5'-ACGTATACTGACCTGCGGGGAGAT-3',

P0low: 5'-TGAAAGTAGAAAAATGACCAGAAA-3'). All amplified PCR products were cloned into the pCR2.1TOPO vector (Invitrogen, Groningen, Netherlands), analyzed by digestion with restriction enzymes and sequenced.

Isolation of a zebrafish tenascin-r cDNA

To isolate the zebrafish tenascin-R cDNA, we performed degenerate RT-PCR with oligonucleotide primer sequences based on the conserved FNIII-like domains of human, rat and chicken tenascin-R using the Consensus-Degenerate Hybrid Oligonucleotide Primer (CODEHOP) program (Rose et al., 1998). Total RNA from adult zebrafish brains was prepared and reverse transcribed using either random hexamers or an oligo dT primer, followed by PCR [P1: 5'-CGTGGAGGTGCAGTGGGA(R)CC(N)TT)-3', P2: 5'-GGCGGAGATTCCGACTCC(R)TA(Y)TC(N)GT-3'), yielding a partial tenascin-R fragment. A degenerate 5' oligonucleotide primer based on the EGF-like repeats of tenascin-R [P3: 5'-GCCTTTCGAGTGCCGG(Y)T(N)GA(R)GT(N)AC-3'] and a gene specific 3' primer (PS3: 5'-CCACTCCACAAACGCAACCGTGT-3') located in the most 5' end of the cloned tenascin-R fragment were used to clone a second tenascin-R fragment which contained a more 5' part of the molecule. Based on this sequence, a 5' RACE was performed according to manufacturer's instructions. Nested anchor primers AAP and AUAP and gene-specific nested primers (PSN3: 5'-TGCCATTGCGGACTCCACTGACT-3', PSN4: 5'-GGCTCCACTCCACAAACGCAACC-3') located in the most 5' end of the newly cloned tenascin-R fragment were used. To obtain the 3' end of tenascin-R, a 3' RACE was carried out with a combination of nested 3'-oligo-dT coupled adapter primers and two nested 5' gene-specific primers (PSN1: 5'-CGCCTTCAGCCTACTCTGAGCCA-3', PSN2: 5'-GCAATGGCACTGAGAGTGGA-3') located in the most 3' end of the cloned tenascin-R fragment. All amplified PCR products were cloned into the pCR2.1TOPO vector (Invitrogen), analyzed with restriction enzymes and sequenced.

To detect possible paralogs of tenascin-R in zebrafish three additional degenerate primer pairs derived from consensus sequences of also the newly cloned zebrafish tenascin-R were used. Primer pairs were: [S1: 5'-GGCGAGGACGAGATGCT(N)(R)C(N)GA(R)TA(Y)A-3'; LS1: 5'-TGATGGTGTGATGTTGGTCCAGT(Y)(N)CC(N)GG(N)AC-3'], [S2: 5'-GGAGTCTGCGTTCGAGGG(N)(S)A(N)TG(Y)(R)T-3'; LS2: 5'-GGGACAGGGGAGGCTG(N)A(R)(N)C(K)(R)AA-3'], [S3: 5'-

CACGTACACCCTGACCGAC(Y)T(N)(S)A(R)CC(N)GG-3'; LS3: 5'-CTCGATGTCGGCGATAGG(N)GG(N)(R)(S)CCA-3'].

Molecular cloning of a full-length cDNA for zebrafish tenascin-c

Two partial clones containing three FN-III domains and the fibrinogen knob belonging to the 3'-end of tenascin-c have been described (Qiao et al., 1995; Tongiorgi et al., 1995b). During a low stringency screen of a 20-28 hpf zebrafish library with the 444bp long cDNA insert of pGEX-EGF/S (Xiao et al., 1996) a partial clone containing the 14.5 EGF like domains of tenascin-c but not the complete 5'-end (unpublished, but see Weber et al., 1998) was obtained. To isolate the complete zebrafish tenascin-c cDNA, total RNA from adult zebrafish brains was prepared and reverse transcribed using an oligodT primer and RT-PCR was performed with primers (TNCover1: 5'-CTGGGCTTTACTGGCGATGAC-3' and TNCover2: 5'-CTCTTGGCTGTGTCTCGGAATG-3') derived from the most 5'-and 3'-ends of both partial sequences. To obtain the 5'-end of zebrafish tenascin-c rapid amplification of cDNA ends using the 5'RACE system (Invitrogen) was performed according to manufacturer's instructions. Total brain RNA was reverse transcribed using gene-specific primer TNCrace1 (5'-GCCATTGACGCACCTTCC-3') and RT-PCR was performed using nested anchor primers AAP and AUAP and gene-specific primers (TNCrace2: 5'-CTGTCCAAGGCTCGTCGCATAC-3'; TNCrace3: 5'-GCCTCCAGCATTTCAGCCTATT-3'). All amplified PCR fragments were cloned into the pCR2.1TOPO vector (Invitrogen), restriction analyzed and sequenced.

Alignments of the deduced amino acid sequences of all three cloned genes were done using the ClustalW method implemented in the BioEdit suite available through <http://www.mbio.ncsu.edu/BioEdit/bioedit.html>. The modular architecture of the proteins was predicted by searching the Protein Families Database of Alignments and Hidden Markow Models (Bateman et al., 2000) and the transmembrane domain was predicted using the TransMembrane Hidden Markow Model (TMHMM) algorithm (Sonnhammer et al., 1998). The signal peptide was identified using the PSORT program (Nakai and Horton, 1999).

3.6 Purification and labeling of nucleic acid probes

cDNA probes used for northern blot analysis were ^{32}P -dCTP labeled with the Megaprime™ system (APB). 25 ng of the designated cDNA probe were filled up with DEPC- H_2O to 31 μl . As recommended by the manufacturer, 5 μl random primer solution were added. Mixtures were denatured by boiling for 3 min and cooled to RT for 10 min. 10 μl labeling buffer, “2 U Klenow enzyme (1U/ μl) and 30 μCi ^{32}P -dCTP were added. Labeling occurred during incubation at 37°C. The labeled probes were separated from unincorporated radioactivity with ProbeQuant™ G-50 micro column (APB), which contain pre-equilibrated Sephadex™ G-50 grade F. The overall process was monitored by scintillation counting. Prior to use in hybridisation experiments, labeled probes were stored at -20°C . Directly before applying probes to prehybridized blots, molecules were denatured by boiling for 5 min.

3.7 Analysis of nucleic acids by hybridization

3.7.1 Northern blot analysis

A tenascin-R cRNA probe, 500 bp in length, was generated by PCR using adult brain cDNA as template (N1: 5'-GGTGATTGACAGCGACATTA-3', N2: 5'-GTCCTTGGTAGAGAAAGG-3'). A probe specific for myelin protein zero was generated by PCR using gene-specific primers P0U1: 5'-ATGCTGTCCGTACTGGCACTGA-3' and P0L1: 5'-GATACGCTGTTTTTGCTGTGATC-3'. All probes α - ^{32}P labeled using the Megaprime™ DNA labeling kit (Amersham Pharmacia Biotech). The tenascin-C probe has been described (Tongiorgi et al., 1995b). Denaturing electrophoresis of total RNA samples and capillary blotting using a Hybond™ N⁽⁺⁾ membrane were performed according to standard procedures (Sambrook et al., 1989). Briefly, total RNA 30 μg in a volume of 7 μl was complemented with 3 μl 10xMOPS and 20 μl F/FA mix. RNA was denatured by incubating samples for 10 min at 65°C. 3 μl 10 x RNA loading buffer were added. A thin, low percentage gel (0.7 % agarose, length 15 cm) containing 0.7 M formaldehyde in 1 x MOPS buffer was cast and pre-run for 30 min at 100 mV. Samples were loaded and the gel was run until bromphenol blue had moved 3-4 cm into the gel. Buffer was circulated from anode to cathode every 30min. After the run, the gel was washed in deionized water for 15 min followed by two washes with 2 x SSC for 15min each. A capillary blot was set up and the RNA transferred overnight using 10 x SSC as transfer buffer. The membrane was rinsed in 2

x SSC to remove residual agarose and the RNA was crosslinked to the membrane by UV-irradiation (0.07 J/cm^2). Air-dried membranes were prehybridized in ULTRAhyb™ hybridization solution (Ambion) at 68°C . A radioactively labeled cDNA probe was denatured (5 min, 100°C) and added to an equal volume ULTRAhyb™ as used for prehybridization (approx. 5×10^6 cpm/ml). The hybridization mix was added to the blots covered by ULTRAhyb™. Hybridization was carried out at 68°C overnight. Membranes were washed 3 x 15 min with 2 x SSC, 0.5 g/l SDS at RT and 2 x 40 min with 0.1 x SSC, 1 g/l SDS at 50°C . Blots were wrapped in plastic wrap and exposed to X-ray films (BioMax Light-1 film, Kodak St. Louis) at -80°C with the help of intensifying screens. Exposure lasted from 12 h to several days.

Mops (10 x)

500 mM MOPS

10 mM EDTA

→pH to 7.5 (with 5 N NaOH)

RNA loading buffer (10 x)

400 g/l sucrose

2 g/l bromophenol blue

2 g/l xylene cyanol

F/FA mix

75 % formamide, deionized

25 % formaldehyde (37 % solution)

3.7.2 RNA in situ hybridization (ISH) on cryosections

Digoxigenin (DIG)-labeled RNA sense and anti-sense probes for tenascin-R mRNA were generated from a 3.2 kb C-terminal fragment containing also the 3'UTR. To obtain a probe specific for myelin protein zero, the complete ORF of zebrafish P0 was amplified by PCR using primers P0U and P0L (see cDNA cloning) and cloned into the pGEM-T EASY vector (Promega, Madison, WI). Digoxigenin (DIG)-labeled RNA sense and antisense probes were generated using the Megascript™ system (Ambion) according to the manufacturer's instructions (see 3.5.1.). The tenascin-C probe has been described (Tongiorgi et al., 1995b). To perform non-radioactive detection of mRNAs, $14 \mu\text{m}$ sections were cut from fresh-frozen tissue on a cryostat and mounted on glass slides. The sections were fixed in 4% paraformaldehyde in phosphate-buffered saline (pH 7.3) overnight. The next day, sections were washed three times in 1 x PBS, treated with 0.1 M HCl for 20 min, acetylated in 0.1 M

triethanolamine containing 0.25 % acetic anhydride and dehydrated in an ascending ethanol series. Finally, sections were air dried and prehybridized for 3 hours at 37°C with hybridization mix. Hybridization with the DIG-labeled probes occurred at 55°C overnight in humid chambers. DIG-labeled probes were diluted 1:250-1:1000 in hybridization buffer. After hybridization, sections were washed twice in 0.2 x SSC at 55°C, followed by three washing steps in 0.2 x SSC containing 50 % formamide (for each 90 minutes at 55°C). To prevent unspecific binding, sections were incubated in blocking buffer for 30 min before anti-DIG AP-conjugated antibodies (Roche Diagnostics, Mannheim, Germany), diluted 1:2000 in blocking buffer, were applied overnight at 4°C. To remove unbound antibody, sections were washed twice in DIG-buffer 1 for 15 min. The washing solution was poured off and the sections were equilibrated for 5 min with DIG-buffer 3. Signal was developed in the dark with DIG-buffer 3 containing 0.35 g/l 4-nitroblue tetrazolium chloride (NBT, Roche Diagnostics), 0.175 g/l 5-bromo-4-chloro-3-indolyl phosphate (BCIP, Roche Diagnostics) and 0.25 g/l levamisole (Sigma-Aldrich) until signals became visible under a stereomicroscope. Sense probes, developed in parallel under the same conditions as the anti-sense probes, did not show any labeling. Finally, sections were washed in 1 x PBS and coverslipped.

Hybridisation buffer

25 ml deion. formamide
 5 ml 10x "Grundmix"
 3.3 ml 5M NaCl
 2.5 ml 2M DTT
 4.7 ml DEPC-H₂O
 10 ml dextran sulfate

10 x "Grundmix"

2 ml 1 M Tris ph 7.5
 200 µl 0.5 M EDTA
 2 ml 50 x Denhardt's solution
 2 ml tRNA (25 mg/ml)
 1 ml poly A⁺-RNA (10 mg/ml)
 2.8 ml DEPC- H₂O

DIG-buffer 1

100 mM Tris
 150 mM NaCl
 →pH 7.5

Blocking buffer

1 % (w/v) Blocking reagent (Roche Diagnostics)
 0.5 % (w/v) BSA
 in DIG-buffer 1

DIG-buffer 3

10 mM MgCl₂
 100 mM Tris
 100 mM NaCl →pH 9.5

3.7.3 Whole mount RNA in situ hybridization

To detect the expression patterns of mRNAs in 16-24 hpf zebrafish embryos, non-radioactive whole mount in situ hybridization was performed. Embryos at the desired developmental stages were deeply anesthetized in 0.1% aninobenzoic acid ethyl methyl ester (MS222, Sigma-Aldrich), dechorionated and fixed overnight in 4% PFA at 4°C. The following day, the embryos were washed with PBST and incubated in 100% methanol for 30 min at -20°C. Methanol was removed by subjecting the embryos to a descending methanol series (75, 50 and 25 % methanol in PBST). Afterwards embryos were washed in PBST. To achieve penetration of the riboprobes, embryos were digested with 1.4 µg/ml Protinase K (Roche Diagnostics) in PBST for 10 min at RT, followed by two washes in 2 mg/ml glycine in PBST. Embryos were post-fixed in 4% PFA for 20 min at RT. PFA was removed by PBST washes and embryos were prehybridized with hybridization buffer at 55°C for 3 hours. Hybridization with the DIG-labeled probes occurred at 55°C overnight. DIG-labeled probes were diluted 1:250-1:1000 in hybridization buffer. After hybridization, sections were washed twice in with 2 x SSCT containing 50% formamide for 30 min, followed by a washing step in 2 x SSCT for 15 min and two washing steps with 0.2 x SSCT for 30 min. All washing steps were made at 55°C. To prevent unspecific binding of the anti-DIG AP-conjugated antibodies, embryos were incubated for 30 min in blocking buffer. Anti-DIG AP-conjugated antibodies (Roche Diagnostics, Mannheim, Germany) were diluted 1:2000 in blocking buffer and applied overnight at 4°C. To remove unbound antibody, sections were washed six times in 1 x PBST for 20 min. The washing solution was poured off and signal was developed in the dark with BCIP/NBT tablets (Sigma-Aldrich) until signals became visible under a stereomicroscope. Sense probes, developed in parallel under the same conditions as the anti-sense probes, did not show any labeling. Finally, embryos were washed in 1 x PBS. Embryos were cleared in an ascending glycerol series (30, 50 and 70 % glycerol in 1 x PBS). The yolk sack was removed and embryos were mounted in 70 % glycerol.

whole mount hybridisation buffer

5 ml deion. formamide

2.5 ml 20 x SSC

10 µl Tween®

100 µl 100 mg/ml yeast RNA (Sigma Aldrich)

2.38 ml DEPC-H₂O

10 µl 50 mg/ml Heparin

3.7.4 Screening of a zebrafish cDNA library

The 444bp cDNA insert of clone pGEX-EGF/S (Xiao et al., 1996), which encodes the 4.5 EGF repeats of rat TN-R (Fuss et al., 1993), was labeled with digoxigenin (PCR DIG Probe Synthesis Kit, Roche Diagnostics, Mannheim, Germany) and used to screen an adult zebrafish brain library (a gift from Dr. J. Ngai, UCSF, San Francisco), as previously described (Sambrook et al., 1989). Replica filters were hybridized under low stringency conditions in 30% formamide, 6X SSC, 5X Denhardt's solution, 0.5% SDS and 100 µg/ml sonicated herring sperm DNA (Roche Diagnostics) at 42°C. Filters were washed twice for 5 min in 2X SSC, 0.1% SDS at 42°C, followed by two washes for 15 min in 1X SSC, 0.1% SDS at 42°C. The corresponding signals were developed on BioMax Light-1 (Kodak, St. Louis, MI) according to the manufacturer's instructions (Roche Diagnostics).

3.8 Immunohistochemistry

3.8.1 Indirect immunofluorescence on sections

To perform indirect immunofluorescence 14 µm sections were cut from the designated fresh-frozen tissue on a cryostat and mounted on glass slides. Sections were air-dried and surrounded with a Pap-Pen (Kisker, Steinfurt, D) to minimize the amount of the used antibodies. Sections were fixed in methanol for 10 min at -20°C and rehydrated in 1 x PBS for 10 min. To prevent unspecific binding of the primary antibodies, sections were incubated in the appropriate preimmune-serum for 30 min at RT. Sections were incubated with the primary antibodies in a humid chamber containing 1 x PBS at 4°C overnight. Sections were washed four times with 1 x PBS to remove unbound antibodies. To visualize the primary antibodies, fluorescence-labeled secondary antibodies (Dianova, Hamburg, D) were diluted 1:200 in 1 x PBS and applied to the sections for 45 min at RT in the dark. Sections were washed four times with 1 x PBS to remove unbound secondary antibodies and coverslipped with elvanol. Sections that had previously been reacted for *in situ* hybridization were processed in the same way except for the methanol step.

3.8.2 Whole mount immunohistochemistry

To detect the expression patterns of proteins in 16-24 hpf zebrafish embryos, whole mount immunohistochemistry was performed. The chorions of animals at the desired developmental stages were removed using two fine forceps and embryos were fixed in 4% PFA containing 1% (v/v) DMSO for 45 min at RT. The embryos were washed in 1 x PBS and incubated with blocking buffer to prevent unspecific binding of the primary antibody for 30 min at RT. Older animals (33 hpf) were digested with 1 mg/ml collagenase for 5 min at RT and washed in 1 x PBS before adding the blocking buffer. Primary antibodies were diluted in blocking buffer and applied to the embryos overnight at 4°C. Unbound primary antibody was removed by three washing steps with 1 x PBS for 15 min each. To visualize the primary antibodies fluorescence or HRP labeled secondary antibodies were diluted 1:200 in blocking buffer and applied to the embryos overnight at 4°C. Unbound secondary antibody was removed by three washing steps with 1 x PBS for 15 min each. To visualize the HRP signals, embryos were incubated in 0.5 mg/ml diaminobenzidine in 1 x PBS for 20 min at 4°C. The brownish precipitate was developed in 5-10 min by adding 0.035% H₂O₂ in 1 x PBS. Finally, the staining solution was removed, embryos were washed in 1 x PBS. Embryos were cleared in an ascending glycerol series (30, 50 and 70 % glycerol in 1 x PBS), and embryos were mounted in 70 % glycerol.

3.8.3 Tracing of optic axons

For simultaneous visualization of the optic projection and tenascin-R protein distribution, optic nerves were labeled with biocytin, as described (Becker et al., 2000a). Animals were perfused with 4% paraformaldehyde, their brains were embedded in 4% agar and sectioned at 40 µm with a vibratome (Leica, Hamburg, Germany). Biocytin was detected with Cy2-coupled streptavidin (Dianova), tenascin-R was detected using different primary antibodies and Cy3-coupled secondary antibodies (Dianova). The sections were mounted in Mowiol and viewed under a laser scanning microscope (Zeiss, Oberkochen, Germany) using Argon and Krypton lasers, with appropriate emission and detection wavelengths.

3.9 Zebrafish surgery

3.9.1 Optic nerve crush and enucleation

For lesions of the optic nerves of adult zebrafish, individuals were anesthetized by immersion in 0.033% aminobenzoic acid ethylmethylester (MS222, Sigma-Aldrich) for 5 minutes. The left eye was gently lifted from its socket and the exposed intraorbital nerve was crushed behind the eyeball under visual control using watchmaker's forceps as previously described (Becker et al., 2000). A translucent stripe across the otherwise opaque optic nerve at the site where the forceps had been applied indicated a successful crush of the nerve. For the enucleation experiments, individuals were anesthetized as described above and the left eye was removed using fine scissors. After surgery, gills were flushed with tank water by gently pulling the fish through the water. Fish resumed breathing within a few seconds.

3.9.2 Spinal cord transection

Spinal cord transections were performed as described previously (Becker et al., 1997). Briefly, fish were anaesthetized, scales were removed from the flanks of the fish at the level of the spinal cord, a longitudinal incision was made and the vertebral column was exposed by pushing the muscle tissue aside. Then the vertebral column was cut with micro-scissors at a level halfway between the dorsal fin and the operculum, corresponding to the eighth vertebra. The wound was sealed with a drop of histoacryl (B. Braun Melsungen, Germany). After surgery, fish were revived as described above for optic nerve lesions and were allowed to survive the spinal cord transection for 14 days.

3.10 Perturbation of gene expression by injection of mRNAs, proteins or morpholinos into freshly fertilized zebrafish eggs

The zebrafish offers the possibility to analyze the functions of genes during early development *in vivo* by injecting reagents directly into the freshly fertilized egg. Three different methods to perturb gene functions were used.

RNA overexpression:

RNA overexpression leads to an ectopic expression of the desired protein in almost every cell of the developing embryo. Cells, for example neurons, which normally do not express the designated gene e.g. a receptor for repulsive guidance cues are forced to express this gene and their axons may respond to their environment in a way that differs from wildtype embryos thereby giving insights into the protein's function, for example see (Shoji et al., 1998). Furthermore, cells which normally express the designated gene are forced to synthesize higher amounts of the protein which also can give information about the protein's function.

Plasmid construction for RNA injection:

An overexpression vector containing the secretion signal and the 14.5 EGF-like repeats of zebrafish tenascin-c was generated in the following manner. Total brain poly A⁺ mRNA was isolated and reverse transcribed with an oligodT primer. RT-PCR was performed using primers TNCEGFBamHI (5'-CGGGATCCATGGGGATGCGAGGCCTGCTGCT-3') and TNCEGFClal (5'-CCATCGATCGCAGTCATCGCCAGTAAAGCCCA-3'). The obtained product was inserted into the *BamHI* and *Clal* sites of pCS2MT (Rupp et al., 1994) to generate pCS2TNCEGFmyc. To exclude non-specific effects which could be generated by the myc-tag himself, we generated vector pCS2TNCLSmyc which contains the secretion signal of tenascin-c in front of the myc-tag in the following manner. pCS2MT was cut with *BamHI* and *XhoI* to remove the myc-taq. The myc-tag was reamplified using pCS2MT as template and primers TNCLS1 (5'-CTGTCTAGTGCTGGCCTGGTGAAACATCGATTTAAAGCTATGGAG-3') and pCS2MTlow 363-384 (5'-CTATAGTTCTAGAGGCTCGAGA-3'). Primers TNCLS2 (5'-CTGCTGGCCTCTATGGCAGTGGCTGTTTTAGTTCATCTGTCTAGTGCTGGCCTG-3') and TNCLS3 (5'-CGCGGATCCATGGGGATGCGAGGCCTGCTGCTGGCCTCTATGGCAGTG-3') each in combination with pCS2MTlow 363-384 (see above) were successively used to add the localization signal of tenascin-c in front of the myc-tag. The resulting fragment was digested with *BamHI* and *XhoI* and inserted into the corresponding sites of pSC2MT.

In *vitro* synthesis of capped mRNA from the linearized pCS2TNCEGFmyc and pCS2TNCLSmyc was carried out as described in chapter 3.5.1 and mRNA was used without further purification. The RNA concentration was determined spectrophotometrically.

Concentrations between 1 and 2 $\mu\text{g}/\mu\text{l}$ were used for injections.

RNA Injection:

Freshly fertilized eggs were harvested and disinfected with 1 x HBSS containing 0.5 % PFA. Eggs were washed three times with 1 x HBSS and arranged in a line in a petri dish containing 2 % agarose. Usually 0.5 μl 5% rhodamine dextran ($M_w = 10000$) were added to a 3 μl aliquot of mRNA solution to visualize the amount of injected liquid. A glass micropipette (3 μm , GB 150F-8P, Sciences Products GmbH, Hofheim, D) was filled with the RNA solution by capillary forces and subjected to a micromanipulator. RNA was injected with a Picospritzer (PLI-100, Medical systems Corp., Greenvale, USA) at 6 psi and 90 msec directly into the yolk of 1-4 cell staged eggs. Finally, injected eggs were incubated in 1 x HBSS at 28.5°C until the desired developmental stage was reached and embryos were subjected to phenotypic analysis.

Morpholino technology:

Antisense oligonucleotides are widely used to inhibit the translation of proteins in a variety of model systems. The first antisense oligonucleotides like RNA and single-stranded DNA were derived from natural origins. Later developed oligonucleotides were chemically synthesized and several modifications were added to improve stability and specificity (Summerton et al., 1997). Morpholino phosphorodiamidates, a new generation of antisense oligonucleotides which were originally developed for therapeutic approaches (Arora et al., 2000) are the first viable sequence specific gene inactivation method in the zebrafish. Morpholinos are synthetic DNA analogues which contain a morpholine ring in lieu of the standard ribose sugar moiety and contain a neutral backbone. Morpholinos are very resistant to a variety of nucleases, they show a low toxicity and have a high affinity to RNA (Summerton et al., 1997). Morpholino phosphorodiamidates function in a RNase H independent manner, which makes them different from other antisense oligonucleotides. A morpholino selected against the leader sequence or nearby bases of an mRNA can bind to it and sterically inhibit scanning of the mRNA by the 40S ribosomal subunit (Egger and Larson, 2001). Since protein synthesis of specific genes is not completely inhibited by morpholino application, the effect will be referred to as a *knockdown*. The efficacy of morpholinos is restricted to target sites within the leader and sequences surrounding the start codon (Summerton, 1999), a bound morpholino does not appear capable of altering activity of the ribosomal complex once translation is

initiated. Thus, only a small fraction of the transcribed RNA sequences bound by morpholinos within a cell will result in a deleterious effect on gene function.

To establish morpholinos in the zebrafish, phenotypes of known mutants such as no-tail (Schultemerker et al., 1994) were copied. The morpholinos were injected into fresh fertilized eggs and shown to phenocopy the mutations (Nasevicius and Ekker, 2000). Morpholinos were used with great success in many studies to gain information of gene function (Erter et al., 2001; Solomon and Fritz, 2002). They are also useful to analyze gene function in the fruitfly *Drosophila melanogaster*, the frog *Xenopus laevis* and in cell culture systems. Unspecific effects of morpholinos were also described (Nasevicius and Ekker, 2000), these effects are due to hybridization of the morpholino to sequences similar to the target or are dose dependent (Ekker and Larson, 2001).

300 nmol lyophilized morpholinos specific for Tenascin-c or a randomized control morpholino (see appendix for sequences) were delivered and resuspended in 37,5 µl Danieau solution to obtain a stock solution of 65 ng/nl (8 mM). The stock solutions were split in 3 µl aliquots and stored at -20°C. Morpholinos were adjusted with Danieau solution to obtain concentrations between 8 and 16 ng/nl and were injected into 1-4 cell staged eggs as described above for the mRNA overexpression studies.

Injection of protein fragments:

Embryos (14-16 hpf) were dechorionated and embedded in low melting agarose (Sigma-Aldrich). Embryos were injected at the interface between notochord and somite at the level of the 10th trunk segment using a glass micropipette (3 µm opening) attached to a Picospritzer. Recombinant protein fragments containing the EGF-like repeats or the FN-III like domains 6-8 (Species und reference) of TN-C were dissolved in vehicle solution (10 x PBS, containing 5 % rhodamine dextran) and embryos were injected with approximately 10 nl solution. This procedure has been estimated to result in an 100-fold dilution of injected substances within the embryo (Bernhardt and Schachner, 2000). Finally, injected embryos were incubated in 1 x HBSS at 28.5°C until the desired developmental stage was reached and embryos were subjected to phenotypic analysis.

3.11 Quantitative analysis

3.11.1 Quantitative analysis of trunk ventral motor growth

The first 16 (24 hpf) or 18 (33 hpf embryos) pairs of trunk ventral motor axons were analyzed in whole mounted embryos under a 40x objective. Ventral motor nerves were scored as truncated when they were missing completely or did not grow beyond the horizontal myoseptum. Abnormal branching of the nerves was only scored at the level of the horizontal myoseptum and dorsal to it. This is because naturally occurring small branches were occasionally observed in the ventral third of the nerve at the latest time point analyzed. Nerves that had rostral and caudal branches or appeared bifurcated were scored as bifurcations. Embryos from at least two independent experiments were scored for each treatment and time point, amounting to 14-50 embryos for most treatments.

3.11.2 Quantification of cells expressing P0 mRNA

Numbers of cell profiles labeled by in situ hybridization in the lesioned, unlesioned, and enucleated optic tracts and in the lesioned and unlesioned spinal cords of adult zebrafish, were quantified using the NeuroLucida imaging software (MicroBrightfield Europe, Magdeburg, Germany) installed on an Axioskop (Zeiss, Oberkochen, Germany). The area of the optic tract at the level of the parvocellular superficial pretectal nucleus or the complete spinal cord was outlined and the number of P0 mRNA expressing cells within this area was determined in control and lesioned tissues in one section for three animals each at different time points after the lesion. To facilitate comparison, numbers of labeled cells were expressed as cells per mm².

3.11.3 Quantification of neurite outgrowth

The effect of substrate borders on axon outgrowth from retinal explants was quantified as described (Becker et al., 1999; Becker et al., 2000b). Since fascicles accumulated at the border at the end of the incubation period, interactions of individual fascicles with the substrate border could not be counted. Therefore, border interactions were scored by counting explants for which the vast majority of axon fascicles were prevented from crossing the substrate border at the end of the incubation period. Values were expressed as percentage of

all explants extending axon fascicles that had contacted the substrate border. Neurite outgrowth on homogeneous substrates was quantified by determining the mean number of axon fascicles exceeding 400 μm in length (one explant diameter) per explant after two days *in vitro*, as described (Becker et al., 1999; Becker et al., 2000b).

3.12 Organotypic retinal cell culture

3.12.1 Preparation of *in vitro* substrate

Substrates were essentially prepared as has been described elsewhere (Becker et al., 1999). All solutions were prepared in PBS, all incubations were performed at room temperature and all washes were done three times in PBS, unless indicated differently. Tissue culture wells with a glass bottom (MatTek, Ashland, MA) were coated with poly-D-lysine (0.5 mg/ml) in borate buffer (120 mM H_3BO_3 , 20 mM $\text{Na}_2\text{B}_4\text{O}_7$, pH 8.3) for 2 hours, washed and air-dried. Wells were then incubated with nitrocellulose dissolved in methanol according to Lagenaur and Lemmon (1987). Wells were again coated with poly-D-lysine for 2 hours, washed and air-dried. For the preparation of homogeneous substrates, proteins (BSA, tenascin-R) were coated at a concentration of 100 $\mu\text{g}/\text{ml}$ as 25 μl droplets overnight. For the preparation of substrate borders, two different methods were used to demarcate the border. In most experiments, a 10 μl India ink spot was precoated that was immediately aspirated, as described previously (Becker et al., 1999). The solution with test protein (8 μl) was then applied on this spot, and incubated overnight. The test protein border exactly matched the ink border, as shown by immunofluorescence detection of test protein (Becker et al., 1999). In some experiments an 8 μl droplet of protein solution mixed with 100 $\mu\text{g}/\text{ml}$ BSA-rhodamine (Molecular Probes, Eugene, OR) was coated directly to visualize the substrate border under fluorescent light and yielded identical results (Becker et al., 2000b). After washing, laminin (Sigma, St. Louis, MO) was coated on the surface of the entire well for both homogeneous substrates and substrate borders at a concentration of 1.7 $\mu\text{g}/\text{ml}$ overnight. Wells were washed and immediately used for explant culture. Test proteins and laminin were never allowed to dry out throughout the coating procedure.

3.12.2 Retinal explant culture

Adult zebrafish or goldfish received a bilateral conditioning optic nerve crush 7 days prior to retinal explant preparation, as previously published for serum-free amphibian retinal explant culture (Becker et al., 1999). Animals were deeply anesthetized, decapitated and the eyes were collected in Hank's balanced salt solution (HBSS). Eyes were quickly rinsed in 70% ethanol, the retinae were dissected and chopped into 400x400 μm squares on a tissue chopper (McIlwain, Gomshall, Great Britain). Squares were washed in HBSS and L-15 tissue culture medium (Gibco, Karlsruhe, Germany) containing N2 supplements (Sigma) and transferred to a medium-filled tissue culture well. Explants were oriented with fine forceps to attach them to the culture substratum with the vitreous side down at a distance of approximately 200 μm from the substrate border. Culture wells were placed in a humidified chamber and neurites were allowed to grow out at 26°C for 2-4 days.

3.13 Western blot analysis

Cross-reactivity of the rabbit polyclonal anti-EGF-L and the mouse monoclonal 597 antibodies with zebrafish tenascin-R was determined by Western blot analysis as described earlier (Becker et al., 1999). Protein extracts of adult zebrafish brains were separated by SDS-PAGE, blotted on nitrocellulose and probed with antibodies. Antibody binding was detected with an HRP-coupled anti-rabbit secondary antibody (Dianova, Hamburg, Germany) and visualized with a chemiluminescent substrate (Super Signal, Pierce, Rockford, IL), according to the supplier's instructions. Blots were exposed on Kodak X-O-MAT film for 5 to 40 sec.

4. Results

In the first section of the results, the cloning of myelin protein zero (P0) and its characterization during development and regeneration of the CNS in the zebrafish *Danio rerio* will be described.

4.1 Expression of protein zero is increased in lesioned axon pathways in the central nervous system of adult zebrafish

4.1.1 Molecular cloning of protein zero (P0) cDNA in zebrafish

To identify homologs of P0 in zebrafish, we screened the zebrafish EST database using BLAST (Altschul et al., 1990) and obtained clone fj35f03 which showed a high degree of homology to P0 molecules of other species. Nucleotide sequencing of this clone revealed a single ORF of 612 bp which was independently confirmed by 5'- and 3'-RACE procedures on cDNA preparations from adult zebrafish brain. The sequence was additionally confirmed by PCR using primers that bracket the ORF (see Experimental procedures). The start codon was predicted based on preceding stop codons near the N-terminal end of the deduced protein. The full length gene encodes a deduced protein of 204 amino acids and consists of a large N-terminal extracellular region containing an Ig-like domain (residues 1-147), a transmembrane domain (residues 148-170) and a short cytoplasmic region (residues 171-204). Alignment of the zebrafish amino acid sequence with those of human (Hayasaka et al., 1991), mouse (You et al., 1991), chicken (Barbu, 1990), and shark P0 (Saavedra et al., 1989), as with a trout P0 homolog designated IP1 (Stratmann and Jeserich, 1995), indicated significant structural homology among the six molecules (Fig. 3). The highest overall identity of amino acid sequences is 76% between the zebrafish gene and trout IP1 (Table 1). The degree of amino acid identity between the zebrafish molecule and the other P0 molecules is between 35-40%. Sequence conservation is highest (50%) in the extracellular Ig-like domain. Based on structural and amino acid similarities with P0 of other species and following the established nomenclature for zebrafish (Mullins, 1995), we tentatively named the gene P0 (Genebank Accession No.: AJ489219).

Fig. 3. Zebrafish P0 shares structural homologies with P0 molecules of other vertebrate species.

The deduced amino acid sequence of zebrafish P0 is aligned with trout IP1, as well as shark, human, mouse and chicken P0. The overall structure includes one immunoglobulin (Ig) domain and a single transmembrane domain (TM) followed by a short intracellular part. Black and gray boxes represent identical and similar amino acids, respectively.

Table 1. Zebrafish P0 is related to other known P0 molecules. Numbers indicate percentage of amino acid identity.

	Zebrafish	Trout (IP1)	Shark	Human	Mouse	Chicken
Zebrafish	100	77	36	38	38	41
Trout (IP1)		100	40	40	41	41
Shark			100	43	49	48
Human				100	84	65
Mouse					100	73
Chicken						100

Northern Blot analysis on RNA isolated from adult zebrafish brains demonstrated expression of a 2.6 kb transcript of P0 in the adult zebrafish brain (Fig. 4).

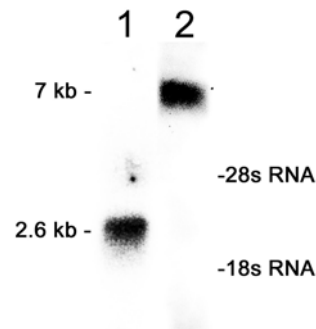


Fig. 4. P0 is expressed in the adult zebrafish brain.

A total RNA sample, isolated from adult brain tissue was hybridized with a ^{32}P -labeled cDNA probe specific for zebrafish P0, yielding a band at 2.6 kb (lane 1). A probe specific for tenascin-C labels a band at 7 kb after stripping of the blot (lane 2). The positions of the 28 and 18 sRNAs, which migrate at 4 and 1.6 kb, respectively, are indicated on the right.

4.1.2 Expression of zebrafish P0 mRNA during development in the hindbrain and spinal cord is associated with myelination

We analyzed early embryos at 16-24 hours post-fertilization (hpf) by whole mount in situ hybridization to investigate whether P0 is expressed before myelination, as suggested by studies in amniotes (Bhattacharyya et al., 1991). We found alternating stripes of cells expressing P0 mRNA in the hindbrain of whole mounted embryos with sharp boundaries of expression between these stripes at 16-18 hpf (Fig. 5A). These expression domains apparently correspond to rhombomers. Rhombomer 5 (identified by its location adjacent to the otic vesicle; Kimmel, 1993) expressed particularly high levels of P0 mRNA. At 24 hpf, the domains of P0 mRNA expression were enlarged and less defined (data not shown). Clearly, the expression in rhombomers at these early stages cannot be related to myelination, since axons are only beginning to grow out at 16-18 hpf (Metcalf et al., 1990; Ross et al., 1992; Wilson et al., 1990).

To determine the time course of P0 mRNA expression during later development, we analyzed expression of P0 mRNA in cross-sections of whole animals at 2, 3, 5 and 28 days post-fertilization. At 2 days, P0 mRNA expression could not be detected in any tissue (data not shown). At 3 days, single intensely P0 mRNA expressing cells were located close to the midline of the hindbrain, where myelination begins in the trout (Jeserich et al., 1990). P0 expressing cells had increased in number and the domain of P0 mRNA expressing cells had

expanded rostrally, caudally and laterally by 5-6 days (Fig. 5B). Comparison with immunolabeling of myelin sheaths using O1 and O4 antibodies at 6 days confirmed co-localization of the P0 mRNA signal with the first labeled myelin sheaths in the medial longitudinal fascicle (Fig. 5B,C,D). The density of cells along the descending pathway declined towards the spinal cord, which did not show any P0 mRNA containing cells (Fig. 5E) or O1/O4-immunopositive myelin sheaths (not shown) at that stage. In 4 to 6-week-old zebrafish, substantial numbers of P0 mRNA expressing cells were found all over the hindbrain and spinal cord, where cells were mainly found in white matter tracts (Fig. 5F). In the adult, this expression pattern was maintained (Fig. 7L).

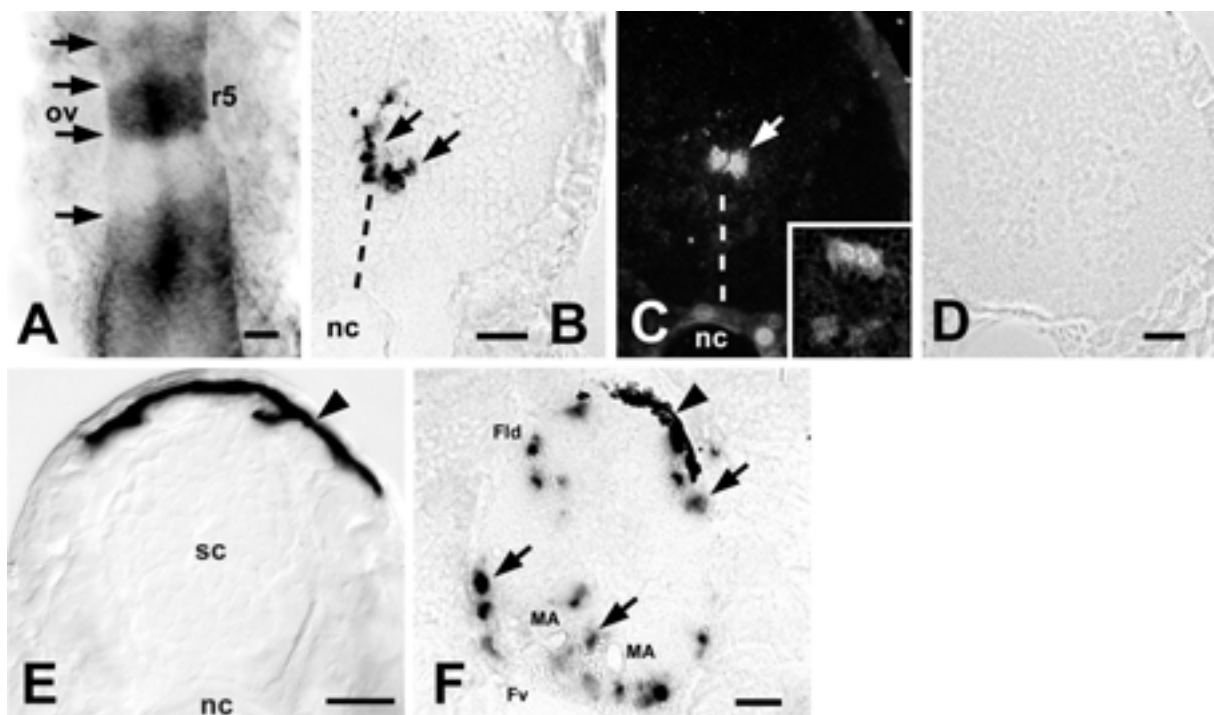


Fig. 5. Zebrafish P0 is expressed during development of the hindbrain and spinal cord.

A: A dorsal view of a whole mount preparation of an 18 hpf embryo is shown; anterior is up. P0 mRNA is expressed in hindbrain areas corresponding to rhombomeres. Arrows point out the sharp expression boundaries characteristic of rhombomere labeling. The position of rhombomere 5, which is located adjacent to the otic vesicle (ov) is indicated (r5). B-D: In cross-sections through the hindbrain of 5-day-old zebrafish, P0 mRNA expressing cells are concentrated around the ventromedial midline (arrows in B). In 6-day-old zebrafish, myelin is detected in the same area by immunofluorescence with the O4 (arrow in C) and the O1 (inset in C) antibodies. D is the phase contrast image corresponding to C. The dotted line in B and C indicate the midline of the brain; nc, notochord. E,F: In cross-sections through the spinal cord (sc) of a 5-day-old zebrafish (E) there are no P0 mRNA positive cells. In the spinal cord of a 6-week-old zebrafish (F), P0 mRNA positive cells are mainly located in the white matter. Arrows in F indicate some of the labeled cells. Arrowheads in E and F point to melanocytes covering the dorsal spinal cord. Fld, dorsal part of the lateral funiculus; Fv, ventral funiculus; MA,

Mauthner axon; nc, notochord. Scale bars in A = 50 μm ; in B = 25 μm ; in D = 25 μm for C, inset in C, and D; in E = 50 μm ; in F = 50 μm .

4.1.3 P0 mRNA is expressed during development of the optic system and in other areas of the CNS

In the developing optic system, the first P0 mRNA positive cells were detected in 5-day-old larvae at the chiasm (Fig. 6A), a location in which the first oligodendrocytes can be expected from studies on myelin development in the optic system of the trout (Jeserich and Jacque, 1985). At this developmental stage, P0 mRNA expressing cells were not detected in the optic nerve, tract or tectum (data not shown). In sections of 4 to 6-week-old whole animals, high numbers of P0 mRNA expressing cells were also present in the optic nerve (Fig. 6B), tract (Fig. 6C) and tectum, but not in the retina (not shown).

In the adult optic system, this expression pattern was maintained. Single cells expressing P0 mRNA were also detected in the intraretinal part of the adult optic nerve, but never in the retina (Fig. 6D,E). A high number of P0 mRNA expressing cells, which were arranged in longitudinal rows, were detectable in the optic tract (Fig. 6F). P0 mRNA positive cells were also accumulated in the superficial layer of the optic tectum, where myelinated axons of retinal ganglion cells invade the tectum (Fig. 6G). Some P0 mRNA expressing cells were also found in the periventricular cell layer of the tectum (Fig. 6G). Double labeling with an antibody to GFAP indicated that there was no detectable expression of P0 mRNA in GFAP immunopositive somata of radial astrocytes at the ventricular surface of the tectum or elsewhere (not shown). However, while the antibody against GFAP labels radial astrocytes throughout the brain, astrocytes in the optic nerve are not labeled (Nona et al., 1989), such that a possible overlap of the P0 signal with astrocytes in the optic nerve could not be assessed.

In other areas of the adult CNS, in situ hybridization revealed highest densities of P0 mRNA expressing cells in heavily myelinated areas, such as the brainstem (Tomizawa et al., 2000). Individual tracts have been shown to be myelinated in the brain of adult (4 to 6 months post-fertilization) zebrafish, e.g. the medial and lateral longitudinal fascicles (Tomizawa et al., 2000). These tracts were also identifiable in our in situ hybridizations by their prominent appearance in differential interference contrast optics, and were always decorated with P0 mRNA expressing cells. In thicker tracts, such as the lateral longitudinal fascicle, P0 mRNA positive cells were also found deep within these axon bundles (Fig. 6H). In sum, the developmental sequence of appearance of P0 mRNA expressing cells in the CNS and their

association with myelinated tracts during development and in the adult suggests that P0 mRNA expressing cells are mostly oligodendrocytes. Early P0 mRNA expression in rhombomeres is a notable exception from this rule.

4.1.4. P0 mRNA is expressed in the PNS

In the developing PNS, no P0 mRNA labeled cells were detected in 5-day-old larvae or earlier stages. In cross-sections through whole 4-week-old juvenile fish, P0 mRNA expressing cells were detected underneath the epidermis of the trunk at the level of the horizontal myoseptum, corresponding to the position of the posterior lateral line nerve (Fig. 6I). In situ hybridization on longitudinal sections through cranial nerves demonstrated glial cells expressing P0 mRNA in the adult PNS (Fig. 6J). Although clearly detectable, labeling in PNS was less intense than in the CNS during development and in the adult. Other tissues outside the nervous system, such as muscle, skin or intestine were negative for P0 mRNA labeling.

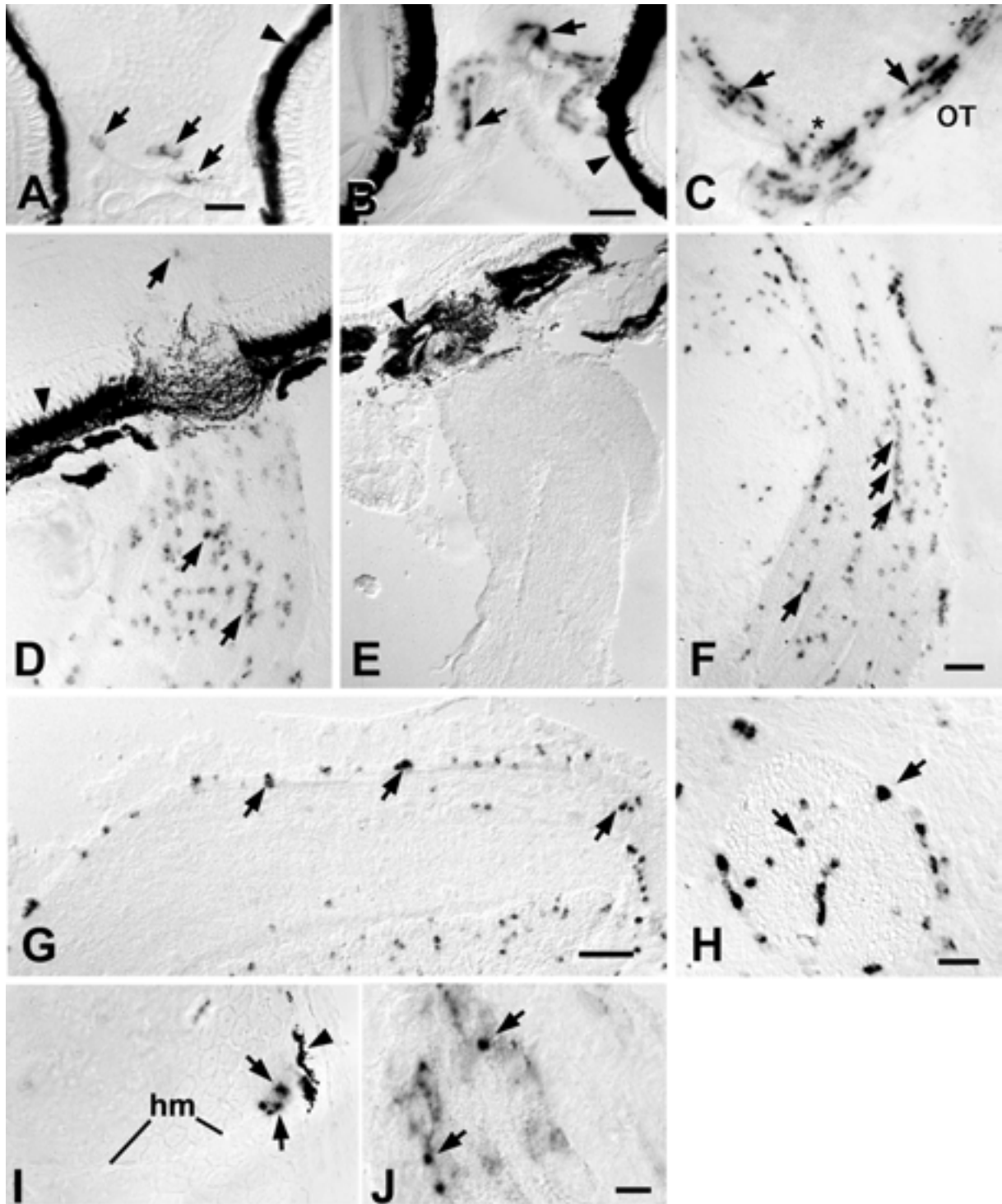


Fig. 6. Zebrafish P0 mRNA is expressed during development of the optic system and other areas of the nervous system.

A-C: In cross-sections of whole animals (dorsal is up) the first P0 mRNA expressing cells (arrows in A) are detectable in the optic chiasm at five days of development. The medial margins of both eyes are included in the section and the arrowhead points to pigment epithelium. At six weeks of development numerous cells in the optic nerves (arrows in B), and in a more caudal section in the chiasm (asterisk in C) and the optic tracts (ot; arrows in C) express P0 mRNA. Arrowheads in A,B point to retinal pigment epithelium. **D,E:** In longitudinal sections through the adult optic nerve with the attached retina (retina is up), cells expressing P0 mRNA are

located in the extraretinal optic nerve and a few cells are also found in the intraretinal part of the optic nerve (arrows), but not in the retina proper. In situ hybridization with a sense probe (E) shows no specific labeling of the adult optic nerve. Arrowheads depict retinal pigment epithelium. **F:** In cross-sections through the adult diencephalon (lateral is right), numerous P0 mRNA positive cells are arranged in longitudinal rows (arrows) in the optic tract. **G:** In cross-sections through the adult tectum (dorsal is up, lateral is left and the medial border of the tectum is just included at the right margin of the photomicrograph), P0 mRNA expressing cells are accumulated in the layer of myelinated retinal ganglion cell axons (arrows). **H:** P0 mRNA expressing cells are accumulated in and around the cross-sectioned lateral longitudinal fascicle in the CNS of adult zebrafish (dorsal is up, lateral is left). The ovoid shape of the heavily myelinated tract is visible through differential interference contrast. Arrows indicate two of the labeled cells. **I:** In cross-sections through the trunk of a 4-week-old juvenile zebrafish (lateral is right), P0 mRNA expressing cells (arrows) are found underneath the epidermis at the level of the horizontal myoseptum (hm) in the mid-trunk region in the position of the posterior lateral line nerve. Arrowhead indicates a melanocyte. **J:** P0 mRNA expressing cells (arrows) are found in a vertically oriented longitudinal section through an adult cranial nerve. Scale bars in A = 50 μm ; in B = 20 μm ; in F = 50 μm for C-F; in G = 50 μm ; in H = 25 μm ; in J = 10 μm for I,J.

4.1.5 P0 mRNA is upregulated in the lesioned optic pathway

After an optic nerve crush, regrowing retinal ganglion cell axons have reached the tectum by 2 weeks post-lesion and the retinotopic map has been restored by 4 weeks post-lesion (Becker et al., 2000a). Based on data from the closely related goldfish, remyelination is expected to begin by 3-6 weeks post-lesion (Ankerhold and Stuermer, 1999). To investigate P0 expression during post-lesion axon regrowth and de- and remyelination, P0 in situ hybridization signals were compared between lesioned and unlesioned optic pathways of the same animals on the same slides (optic nerves) or even in the same tissue sections (tracts, tecta) at 2, 7, 14, 28, 56, 128, 180 days after the lesion ($n \geq 3$ animals for each time point). In these preparations, the signal was “underdeveloped” to avoid saturation of labeling, which would otherwise obscure differences in labeling intensities between the control and lesioned tissues. Signal development was usually stopped when the expression in the control pathway was just beginning to become recognizable under a stereo microscope. Therefore, expression intensities in control tissues depicted in Fig. 7 appear lower than those demonstrated in Fig. 6. After an optic nerve crush, the retina remained unlabeled. In the optic nerve, cells located distal (near the brain) and proximal (near the retina) to the lesion site showed increased labeling intensity of P0 mRNA (Fig. 7A), compared to cells in unlesioned control nerves (Fig. 7B) at 7 and 14 days after the lesion, the only time points analyzed for the optic nerve. In the optic tract (Fig. 7E-H) and tectum (Fig. 7C,D), labeling of P0 mRNA was also increased. In the tectum, this increase was restricted to the main layer of myelinated optic axons (Fig.

7C,D). Labeling was more intense in the lesioned tract and tectum already at 2 days post-lesion and remained elevated for at least 180 days (the latest time point investigated) compared to the unlesioned control side. Labeling intensities appeared highest at 1 to 2 months post-lesion.

To investigate whether the increased detectability of P0 mRNA was due to an increase in cell numbers expressing the message, we counted P0 mRNA positive cell profiles in the lesioned and in the contralateral control optic tracts (Fig. 7N). Sections through unlesioned optic tracts of adult animals did not show any detectable differences in the number of labeled profiles between the left and right tracts (left: 1650 ± 170 profiles/mm²; right: 1616 ± 96 profiles/mm²). At 2 (lesioned side: 2030 ± 348 profiles/mm²; unlesioned side: 1212 ± 297 profiles/mm²), 7 (lesioned side: 2091 ± 183 profiles/mm²; unlesioned side: 1711 ± 311 profiles/mm²) and 14 days post-lesion (lesioned side: 2018 ± 215 profiles/mm²; unlesioned side: 1320 ± 412 profiles/mm²), when increased labeling intensity of P0 mRNA was clearly visible, the number of P0 mRNA positive cell profiles was moderately elevated and differences between the lesioned and the control side were not statistically significant. In animals in which the optic nerves were allowed to regenerate for 28 (lesioned side: 2656 ± 193 profiles/mm²; unlesioned side: 1011 ± 88 profiles/mm²; Mann-Whitney-U test: $p=0.0015$) or 56 days (lesioned side: 2232 ± 192 profiles/mm²; unlesioned side: 790 ± 50 profiles/mm²; Mann-Whitney-U test: $p=0.0146$), we counted an approximately 2.5-fold higher number of P0 mRNA positive cell profiles in the lesioned tracts than in the unlesioned contralateral control tract. Thereafter, at 4 (lesioned side: 2825 ± 177 profiles/mm²; unlesioned side: 1900 ± 92 profiles/mm²) and 6 months post-lesion (lesioned side: 2550 ± 27 profiles/mm²; unlesioned side: 1900 ± 344 profiles/mm²), profile numbers were still slightly increased, but differences to controls were no longer statistically significant. Thus, counts of cell profiles confirm strongest expression of P0 mRNA in the lesioned optic tract at one to two months post-lesion.

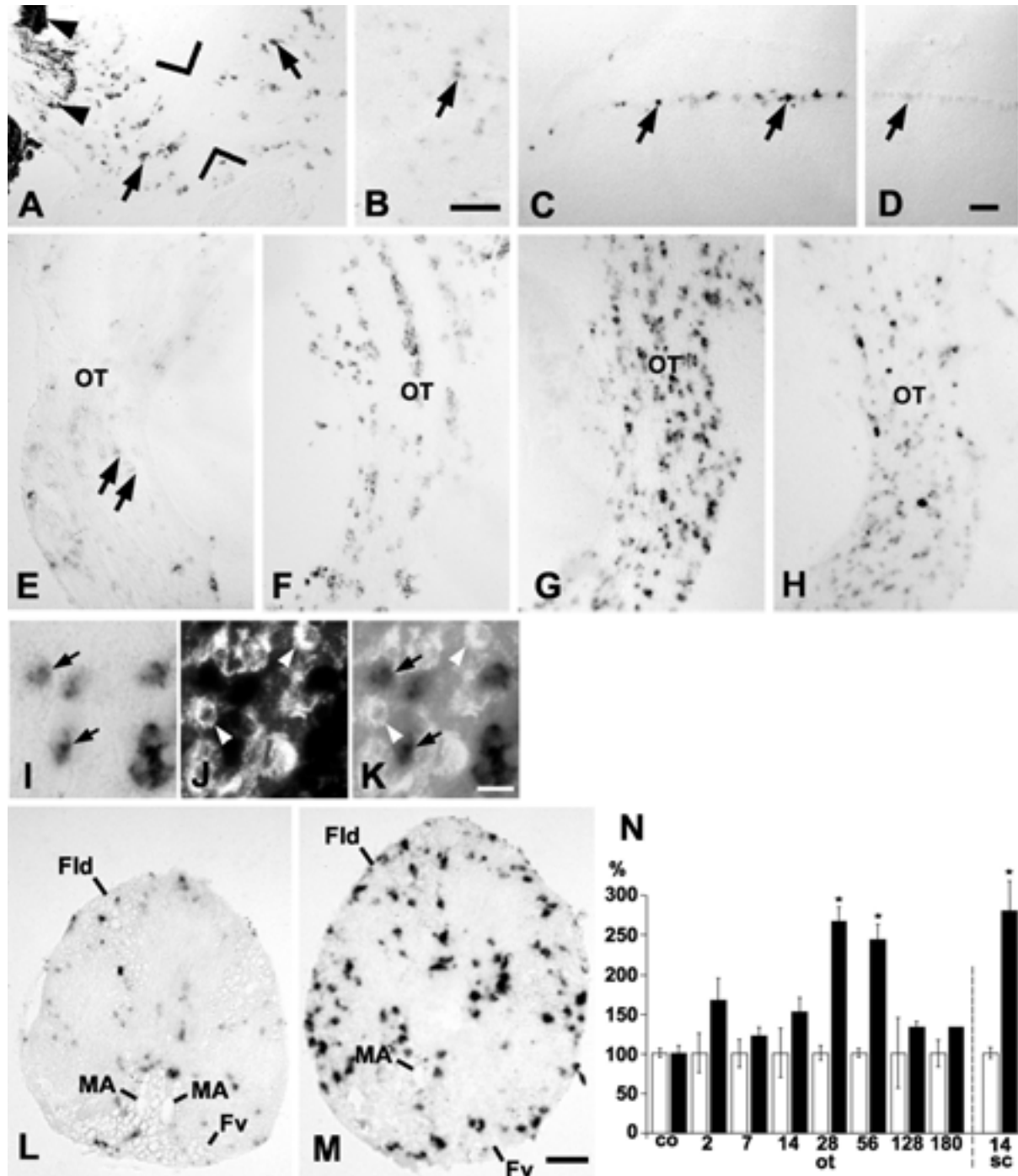


Fig. 7. P0 mRNA is upregulated after lesions of the optic nerve and spinal cord. A,B: In longitudinal sections (retinal side left) through the lesioned optic nerve (A, seven days post-lesion) the intensity of P0 mRNA labeling is increased proximal and distal to a lesion site (open arrowheads in A), compared to the unlesioned control nerve (B; oriented in the same way as the lesioned nerve, but not including the retinal pigment epithelium). Arrows point to some labeled cells, arrowheads in A indicate retinal pigment epithelium C,D: In cross-sections through the optic tectum (dorsal is up; lateral is right in C and left in D), increased expression of P0 mRNA is detectable in the layer of myelinated optic fibers (arrows in C), compared to the unlesioned control side of the same tissue section (arrow in D) 28 days after an optic nerve crush. E-H: Detecting P0 mRNA in cross-sections through the diencephalon in the unlesioned (E; dorsal is up; lateral is left) and lesioned optic tract (OT) at 7 (F), 28 (G) and 128 (H) days post-lesion (dorsal is up; lateral is right) indicates increased labeling after an optic nerve crush. Tracts depicted in E and G are unlesioned and lesioned side from the same tissue section.

Arrows in E depict some of the cells showing basal expression of P0 mRNA. I-K: Double labeling of P0 mRNA (I) and immunofluorescence for microglial cells/macrophages (J) in the lesioned optic tract reveals no overlap in the overlay of both signals (K) at 28 days post-lesion. Arrows point to the same P0 mRNA expressing cells, and arrowheads to the same microglial cells/macrophages in I-K. L,M: In cross-sections through the spinal cord (complete sections are shown; dorsal is up) caudal to a spinal transection (M), P0 mRNA expression is strongly increased, compared to the unlesioned spinal cord (L). Note that in M only one Mauthner axon is indicated. The other one has probably collapsed, such that it cannot be located in cryosections. For abbreviations, see Fig. 3. N: The number of P0 mRNA positive cell profiles, expressed as percent of controls, are given for different post-lesion time points indicated in days on the x-axis for the unlesioned left control side (open bars) and the lesioned right side (black bars) of the optic tract (OT). A comparison between left and right optic tract of unlesioned animals is also given (co). For the spinal cord (sc) the unlesioned (open bar) and lesioned situation (black bar) is compared. Error bars represent standard errors of the mean. Asterisks indicate statistical significance ($p < 0.05$). Scale bars in B = 50 μm for A and B; in D = 50 μm for C and D; in K = 100 μm for I-K; in M = 50 μm for E-H,L,M.

To find out whether increased expression of P0 mRNA depends on the presence of regenerating axons, animals were enucleated and expression of P0 mRNA was analyzed at 7 ($n = 3$ animals), 11 ($n = 3$ animals) and 28 days ($n = 5$ animals) post-lesion. Enucleation led to a clearly increased detectability of P0 mRNA in the lesioned optic pathway at 7 and 11 days post-lesion (Fig. 8A,B), similar to the increased expression after optic nerve crush. At 28 days post-lesion, when labeling intensity was highest after a crush of the optic nerve, labeling was still more intense than in the contralateral control tract after enucleation. However labeling intensity had decreased compared to 7 days after enucleation (Fig. 8C). Quantification of P0 mRNA positive cell profiles (Fig. 8D) indicated a moderate 1.35-fold elevation of profile numbers compared to the control side at 7 days post-lesion (lesioned side: 2460 ± 335 profiles/ mm^2 ; unlesioned side: 1827 ± 129 profiles/ mm^2 ; Mann-Whitney-U test: $p < 0.05$; $n = 3$ animals). At 28 days post-lesion, when numbers of P0 mRNA positive profiles were elevated approximately 2.5-fold after optic nerve crush, numbers of P0 mRNA positive profiles were not significantly elevated over values for the contralateral control tract after enucleation (lesioned side: 2199 ± 321 profiles/ mm^2 ; unlesioned side: 1592 ± 84 profiles/ mm^2 ; Mann-Whitney-U test: $p > 0.05$; $n = 4$ animals). Thus after enucleation animals show a similar increase in P0 mRNA expression at early post-lesion time points (7 to 11 days post-lesion) as after optic nerve crush, but fail to show the additional increase of expression at 28 days post-lesion. This suggests that the late, but not the early phase of P0 mRNA upregulation in glial cells of the optic nerve depends on the presence of regenerating axons.

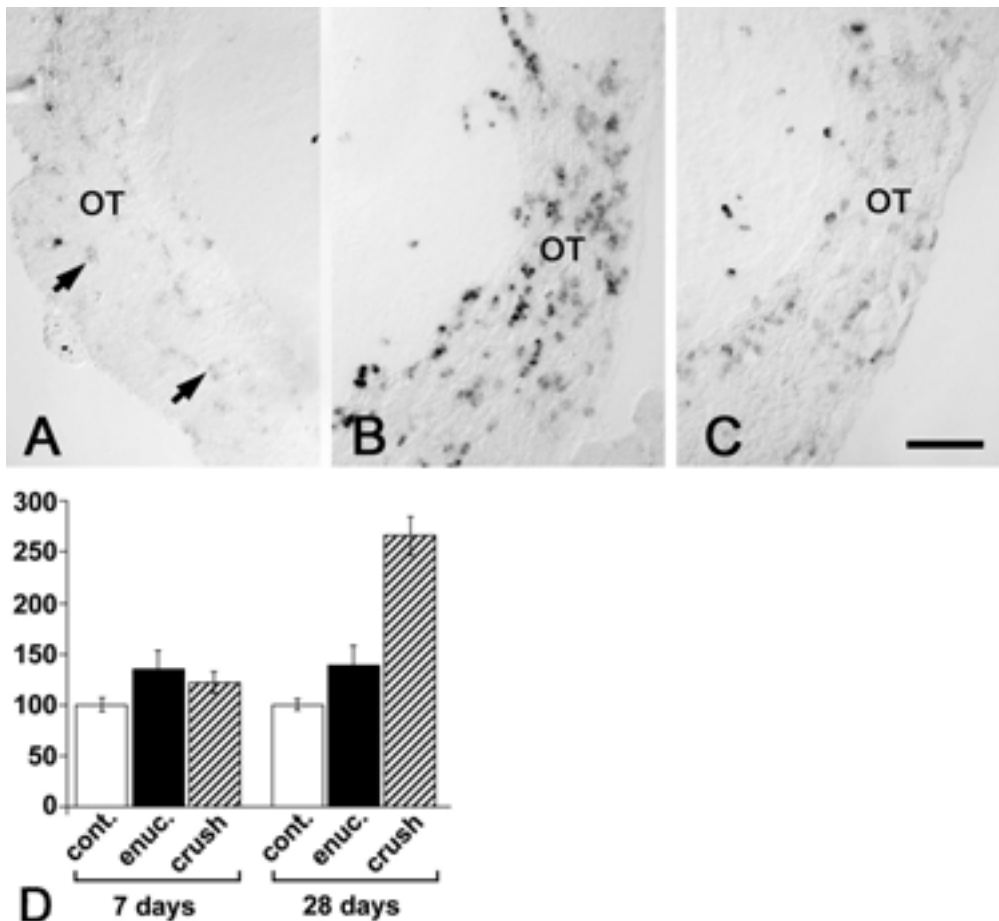


Fig. 8. After enucleation, expression of P0 mRNA in the optic pathway follows a time course of upregulation that differs from that after optic nerve crush.

A-C: Cross sections through the diencephalon including the optic tract (OT) are shown; dorsal is up; lateral is left for (A) and right for (B,C). At 7 days after enucleation (B) labeling of P0 mRNA is clearly increased compared to the contralateral control tract in the same tissue section (A). By 28 days after enucleation (C) expression of P0 mRNA was still higher than in unlesioned control tracts, but lower than at 7 days after enucleation. **D:** The number of P0 mRNA positive cell profiles, expressed as percent of controls, are compared between the contralateral control tract (cont.), the tract after enucleation (enuc.) and after optic nerve crush (crush), 7 and 28 days after the lesion. While profile numbers were similar at 7 days post-lesion, there was a significant ($p < 0.05$) increase in P0 mRNA positive cell profiles only after optic nerve crush, but not after enucleation at 28 days post-lesion. Bar in C = 75 μm for A-C.

Regenerating axons co-localized with P0 mRNA expressing cells in the lesioned optic pathway as shown by double labeling of P0 mRNA positive cells by in situ hybridization and of regenerating axons using the linc antibody at 14 and 28 days after optic nerve crush (Fig. 9). Axons labeled by the antibody were mostly regenerating optic axons and not persisting disconnected axons, since labeling by the linc antibody was almost completely absent in animals that were enucleated 28 days before analysis (not shown).

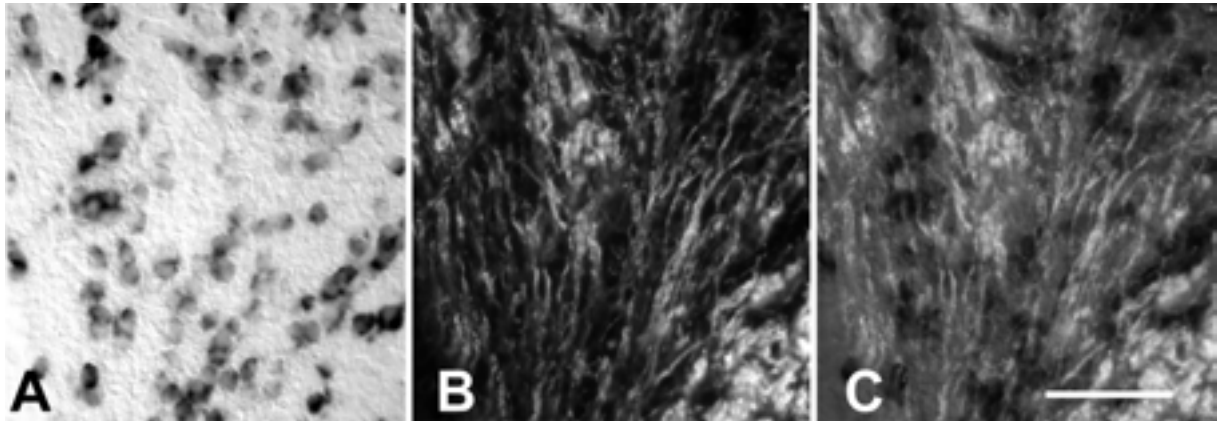


Fig. 9. Regenerating axons are co-localized with glial cells expressing high levels of P0 mRNA.

High power magnifications of the optic tract in the cross-sectioned diencephalon 28 days after optic nerve crush are shown; dorsal is up, lateral is right. Sections were double-labeled for P0 mRNA (A) to reveal P0 mRNA positive glial cells and with the linc antibody (B) to show regenerating axons. The overlay (C) indicates co-localization of glial cells and axons. Bar in C = 50 μ m for A-C.

Microglial cells/macrophages are also strongly increased in number after a CNS lesion in zebrafish (Becker and Becker, 2001). To exclude that this cell type contributed to the population of P0 mRNA expressing cells we performed double labeling experiments for P0 mRNA and an immunohistochemical marker for microglial cells/macrophages (4C4). We analyzed the optic tract one month post-lesion, the interval at which highest numbers of cells expressing P0 mRNA were observed. Despite an increased number of microglial cells/macrophages being present in the lesioned versus the contralateral control pathway, essentially no overlap between the P0 mRNA signal and the microglial cell/macrophage marker occurred (Fig. 7I-K).

In sum, we observed a rapid increase in P0 mRNA labeling intensity in the lesioned optic pathway during the time of axon regrowth (2 to 14 days post-lesion). A significant increase in the number of P0 mRNA positive cell profiles was observed 1 to 2 months after optic nerve crush, but not after enucleation. This increase in cell numbers, which was not due to microglial cells/macrophages, probably correlates with remyelination of regenerating axons.

4.1.6 Expression of P0 mRNA is increased in the lesioned spinal cord

To analyze the behavior of P0 mRNA expressing cells in other lesioned pathways of the CNS, we performed whole spinal cord transections. We determined expression of P0 mRNA in the spinal cord 0 to 1 mm caudal to the lesion, where descending axons from the brainstem regenerate. We detected an increase of P0 mRNA expression in both labeling intensity and the

number of P0 mRNA positive cell profiles compared to sections of unlesioned spinal cord reacted on the same microscopic slide 14 days after a lesion (Fig. 7L-N). P0 mRNA expressing cells were located mainly in the peripheral white matter. In the lesioned spinal cord, the number of P0 mRNA expressing cells was increased 3-fold over non-lesioned spinal cord (lesioned spinal cord: 1068 ± 148 profiles/mm²; unlesioned spinal cord: 382 ± 32 profiles/mm²; Mann-Whitney-U test: $p=0.0495$). Thus, not only the optic pathway, but also axon pathways in the spinal cord react to a lesion with increased expression of P0 mRNA.

Results part two

In the second part of the results, the cloning of TN-R and functional characterization during development and regeneration of the CNS in the zebrafish *Danio rerio* will be described.

4.2 Evidence for a role of TN-R as a repellent guidance molecule for regenerating optic axons in adult fish

In this study, we mostly use both zebrafish and goldfish two closely related teleost species, since a large body of data on optic nerve regeneration already exists for goldfish (Bernhardt, 1999; Stuermer et al., 1992). However, cloning of TN-R and localization of TN-R mRNA was done only in the zebrafish, which is more amenable to genetic analysis. Immunohistochemical localizations and *in vitro* tests of axon growth were done in both species.

Some of the experiments belonging to this study (organotypic retinal cell culture, western blotting and tracing of optic axons) were performed by Dr. Catharina Becker and Dr. Thomas Becker, but were added to clarify the role of TN-R during development and regeneration of the optic projection in zebrafish.

4.2.1 Zebrafish possess a TN-R gene

To clone the zebrafish TN-R gene, degenerate primers against highly conserved residues in the fibronectin type III-like (FN III) domains of known TN-R genes from other species using the (CODEHOP; Rose et al., 1998) were designed (see Experimental procedures). RT-PCR on total RNA isolated from adult zebrafish brains yielded a 700 bp partial clone, which, based on comparisons with mammalian and avian TN-R orthologs, contained the FNIII domains 2-4. By combining 5'- and 3'- RACE technologies, we cloned the full length coding sequence for TN-R (Fig. 10). Full length TN-R encodes a deduced protein of 1351 amino acids. The start codon was predicted from the presence of stop codons preceding the N-terminal end of the deduced protein and the presence of a signal peptide at the N-terminus. The general domain structure of zebrafish TN-R, comprising a cysteine-rich domain, 4.5 epidermal growth factor-like (EGF) repeats, followed by 9 FN III domains and a fibrinogen globe at the C-terminus, is identical to that of orthologs in other vertebrate species. Alignment of deduced amino acid sequences (Fig. 10) indicated that zebrafish TN-R is approximately 60% identical to each of

the species orthologs of TN-R in chicken (restrictin: Nörenberg et al., 1992), human (Leprini et al., 1996) and rat (Fuss et al., 1993).

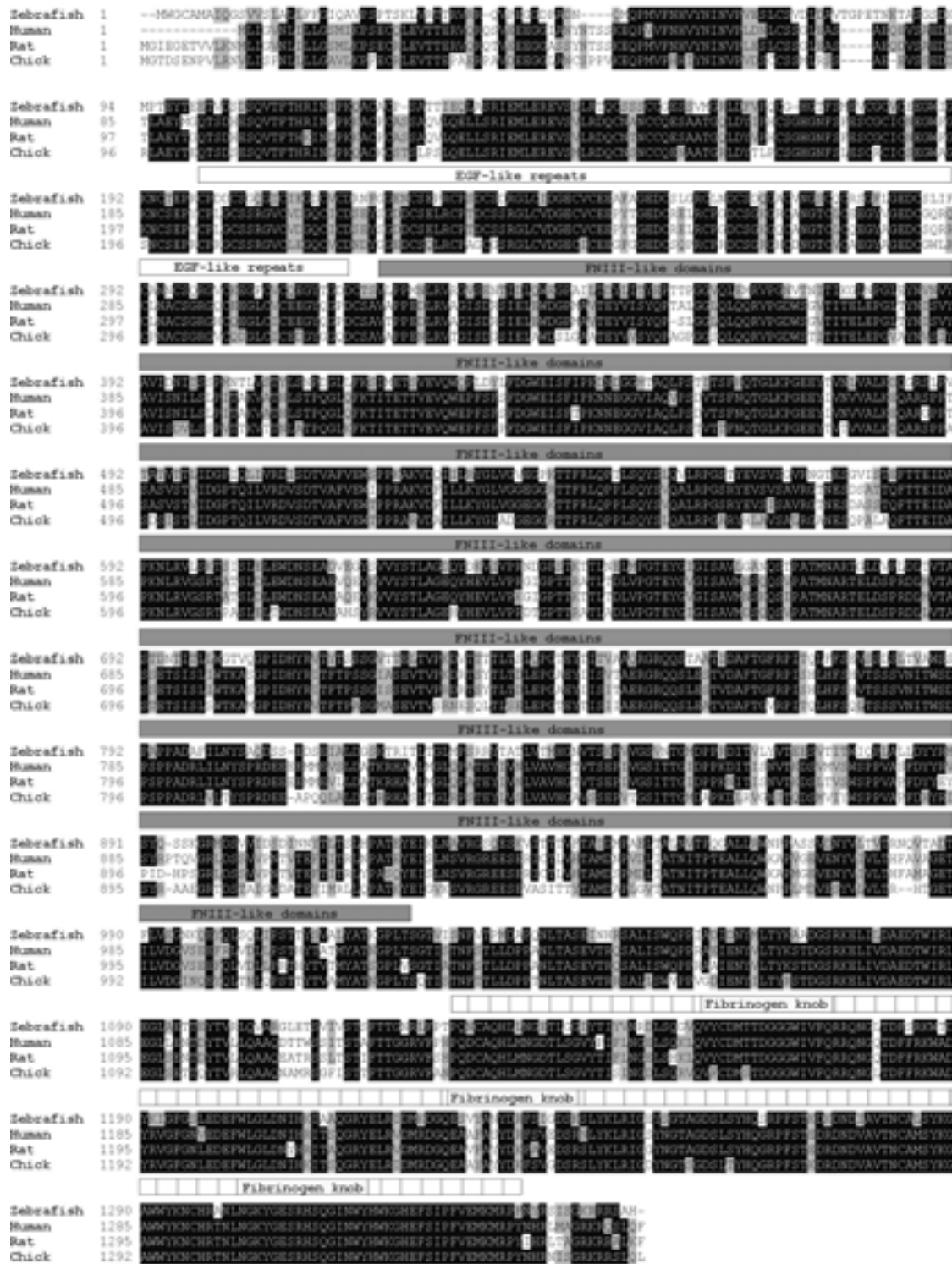


Fig. 10. Amino acid sequence of TN-R in zebrafish compared to that of human, rat and chick.

Identical amino acids are highlighted in black, similar amino acids in gray. Epidermal growth factor-like repeats (EGF-like), fibronectin type III-like domains (FNIII-like) and the fibrinogen knob are indicated.

Due to genome duplication events that involve large chromosome sections in ray finned fish (Postlethwait et al., 1999), the zebrafish genome often contains two copies of the mammalian orthologs, e.g. of hox transcription factors (Amores et al., 1998) or the recognition molecule L1 (Tongiorgi et al., 1995a). We designed three degenerate primer pairs, derived also from TN-R of zebrafish in addition to the previously described TN-R molecules, to search for further TN-R paralogs. Two of these primer pairs (S2/LS2 and S3/LS3, see Experimental procedures) yielded PCR products, which were, however, identical to the sequence already cloned. Screening an adult zebrafish brain library with a cDNA probe derived from rat TN-R under conditions of low stringency did also not detect a second TN-R paralog in zebrafish. Likewise, a computer screen of the genomic sequences available so far (Sanger Institute, University of Cambridge, UK) was negative. Although we could not find evidence for the existence of a second TN-R paralog in zebrafish, this possibility can presently not be excluded.

The conserved modular architecture of the deduced amino acid sequence of the cloned zebrafish molecule and the high degree of amino acid conservation strongly suggests that we have isolated a TN-R ortholog in zebrafish. Following the established nomenclature for zebrafish (Mullins, 1995) we named the gene TN-R.

4.2.2 TN-R mRNA and protein are present in the brain of adult zebrafish

To investigate whether TN-R is expressed in the adult brain of zebrafish Northern and Western blot analyses were performed on mRNA and protein isolated from adult brains. Northern Blot analysis detected an 11 kb transcript, which is similar in length to the 12 kb TN-R transcript found in adult mouse brain tissue (Weber et al., 1999). The transcript for the related molecule tenascin-C migrated at 7 kb (Weber et al., 1998), suggesting specificity of the TN-R signal (Fig. 11A).

Western blot analysis with polyclonal (anti-EGF-L, not shown) and monoclonal antibodies (antibody 597; Fig. 11B) raised against TN-R of other vertebrate species cross-reacted with zebrafish TN-R and revealed the characteristic double bands at 160 and 170 kD (160 and 180 in mice; Bartsch et al., 1993). Antibodies against tenascin-C labeled two bands of higher molecular weight between 200 and 250 kD, indicating that TN-R antibodies did not cross-react with the related tenascin-C protein (Fig. 11B). We conclude that TN-R mRNA and protein are present in the adult brain of zebrafish and that antibodies raised against TN-R of other species specifically recognize the protein in zebrafish.

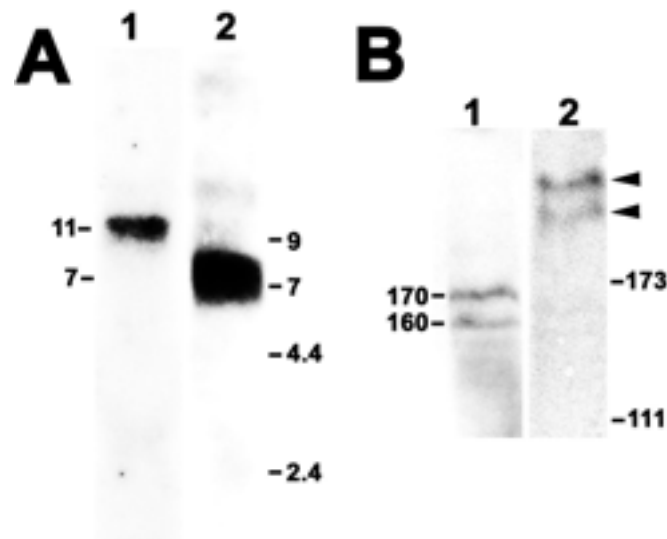


Fig. 11. TN-R mRNA and protein is expressed in the adult zebrafish brain.

A: Northern blot analysis of total RNA isolated from adult zebrafish brains yielded a band at 11 kb (lane 1). A probe to tenascin-C labeled a major band at 7 kb (lane 2). Calculated lengths of transcripts are indicated on the left; positions of molecular markers are indicated on the right. **B:** Western blot analysis of total protein from brains of adult zebrafish using antibody 597 to TN-R (lane 1) yielded two labeled protein bands at 160 and 170 kD (indicated on the left). A polyclonal antibody to tenascin-C labeled bands of 200 and 250 kD (arrowheads). Molecular weight markers are indicated on the right.

4.2.3 Newly generated optic axons in the adult encounter TN-R as a homogeneous substrate in the retina

In the following, the distribution of TN-R protein (zebrafish and goldfish) and mRNA (only zebrafish) along the unlesioned and lesioned (2, 7, 14, 28 and 56 days post-lesion) optic pathway by immunohistochemistry and *in situ* hybridization will be described, as it may be relevant for interactions with newly growing and regenerating axons in adult fish. Regenerating axons start to grow from their severed stumps at the lesion site (Bernhardt, 1989), while newly growing axons have their origin in the periphery of the retina, where new retinal ganglion cells are continuously added in adult fish. From here axons have to grow to their exit point in the center of the retina (Stuermer and Bastmeyer, 2000). Therefore, the distribution of TN-R along the intraretinal pathway of optic fibers can only be relevant for axons of newly generated retinal ganglion cells in unlesioned animals.

In the retina of unlesioned adult animals we found intense and homogeneously distributed TN-R immunoreactivity in the optic fiber layer through which newly generated optic axons have to grow (Fig. 12B). In the optic nerve head this immunoreactivity tapered off, creating a

downhill gradient of TN-R for axons exiting the retina (Fig. 12A). Intense TN-R immunoreactivity was also found in the outer plexiform layer of the retina (Fig. 12B), which is not in contact with optic axons. Expression of TN-R in the outer plexiform layer is highly conserved in evolution (Schachner et al., 1994).

Corresponding to the immunohistochemical data, two layers of TN-R mRNA expressing cells were present in the adult retina, at the outer margin of the inner nuclear layer and in a more diffuse band towards the vitreal margin of the inner nuclear layer (Fig. 12C). The outer row of cells corresponds to the position of horizontal cells, which express TN-R also in other vertebrates (Bartsch et al., 1993). The inner row of labeled cells is located in the layer of Müller cell somata. These cells span the whole width of the neuroretina and may transport the protein along their processes into the optic fiber layer.

After an optic nerve crush, no changes in protein or mRNA expression in the retina were detected. Protein expression patterns were not different between zebrafish and goldfish.

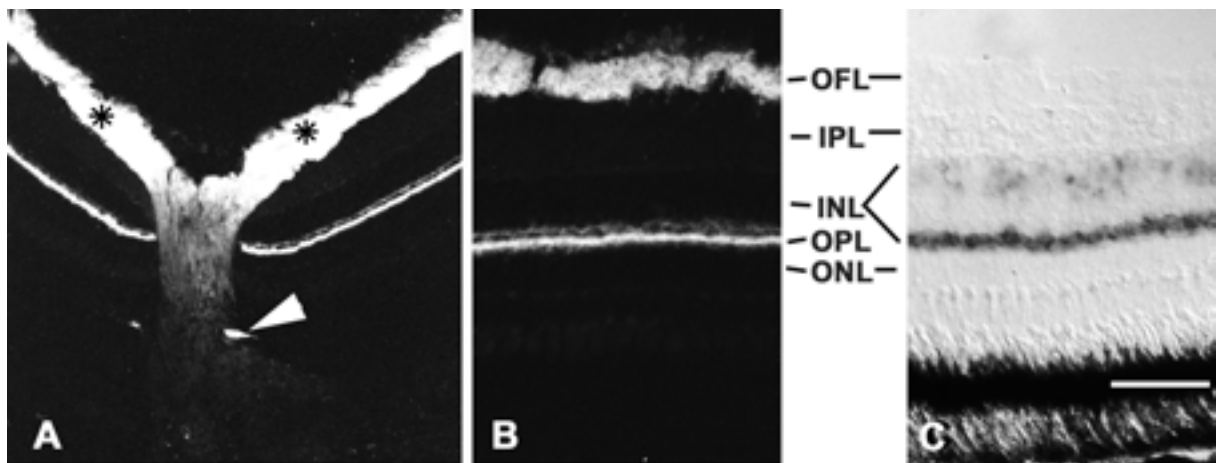


Fig. 12. Axons of newly added retinal ganglion cells in adult fish have to grow through the TN-R-immunopositive optic fiber layer in the retina.

A-C: Cross sections through the retina of unlesioned adult zebrafish are labeled with TN-R antibodies (A,B) or mRNA probes (C). The vitreal side of the retina is up. At low magnification of a section through the optic nerve head (A) intense TN-R immunoreactivity in the optic fiber layer (asterisks), which tapers off in the optic nerve head, is observed. The outer plexiform layer (OPL) is labeled in addition to the optic fiber layer (OFL), as seen in A and at higher magnification in B. The arrowhead in A indicates non-specific labeling of connective tissue. (C) TN-R mRNA is present in two layers within the inner nuclear layer (INL). IPL = inner plexiform layer; ONL = outer nuclear layer. Bar in C = 100 μ m for A and 50 μ m for B,C.

4.2.4 TN-R expression is low in the normal and lesioned optic nerve and tract in adult fish

In the unlesioned optic nerve and tract of zebrafish and goldfish TN-R immunoreactivity was low, e.g. compared to the diencephalic neuropil (Fig. 13A,E) or the retina (Fig. 12). A punctate staining pattern was observed at high magnification (Fig. 13G). The dots of immunoreactivity in the fish optic nerve and tract could represent nodes of Ranvier, the sites at which TN-R immunoreactivity is particularly strong in the optic nerve of mice (Bartsch et al., 1993). However, in contrast to the optic nerve of fish, the optic nerves of mice (Bartsch et al., 1993; Becker et al., 2000b) and salamanders (Becker et al., 1999) are intensely labeled by TN-R antibodies throughout the tissue. In these species, this is probably due to the presence of TN-R also on other cellular elements, such as myelin sheaths and unmyelinated axons (Bartsch et al., 1993). In the spinal cord white matter of zebrafish and goldfish, where fibers of much larger diameter are found, an accumulation of TN-R immunoreactivity at nodes of Ranvier was even more apparent (Fig. 13J).

In the unlesioned optic nerve of zebrafish and goldfish there are discrete zones in which newly added axons grow. These zones can be labeled with antibodies to the neural cell adhesion molecule NCAM (Bastmeyer et al., 1990) and also with an antibody to polysialic acid (own unpublished observations), a specific glycoepitope of NCAM. To find out whether there might be a stronger expression of TN-R in these growth zones we labeled alternating cross sections of the optic nerve with antibodies to TN-R and polysialic acid. However, there was no conspicuous TN-R immunoreactivity in growth zones of the optic nerve (data not shown).

After an optic nerve crush, there was no increase of TN-R immunoreactivity at the crush site in zebrafish or goldfish at any time point investigated (Fig. 13C). The density of TN-R immunoreactive putative nodes of Ranvier was strongly reduced at 1 week post-lesion (Fig. 13H). Punctate labeling gradually increased again between 4 and 12 weeks post-lesion (Fig. 13I). This time course mirrors that of remyelination of regrowing axons after Wallerian degeneration (Ankerhold and Stuermer, 1999; Colavincenzo and Levine, 2000) and is therefore consistent with the possibility that these small dots are nodes of Ranvier.

TN-R mRNA expression was detectable in sparsely distributed cells in the unlesioned nerve and tract of zebrafish (Fig. 13B,K). Two days after an optic nerve crush, no change in TN-R mRNA expression was observed. The density of cells expressing TN-R mRNA was increased between 1 and 4 weeks after the lesion (Fig. 13D,M) and had returned to a density comparable to that in unlesioned control animals by 8 weeks post-lesion (Fig. 13N). This time

A-D: Longitudinal sections through the optic nerve double labeled for TN-R protein (A,C) and mRNA (B, D) of an unlesioned (A,B) and a crushed nerve at seven days post-lesion (C,D) of adult zebrafish are shown; retina is up. TN-R immunoreactivity is low in the unlesioned extraretinal optic nerve (A) and is even lower in the lesioned nerve (C). The density of TN-R mRNA expressing cells is low in the unlesioned nerve. Arrows in B indicate labeled cells. In the lesioned nerve, the number of cells expressing the mRNA is increased proximal and distal to the lesion site, which is indicated for C and D by an arrow in D. **E,F:** Cross sections through the diencephalon of adult zebrafish including the unlesioned (E) and lesioned (F; seven days post-lesion) optic tract (OT) are shown. Arrows indicate the lateral border of the optic tract. In both situations immunofluorescence in the tract is considerably lower than in the adjacent diencephalon. **G-I:** At higher magnification of the unlesioned optic tract (G) small dots of immunoreactivity, probably representing nodes of Ranvier, are apparent. These dots have mostly disappeared by seven days post-lesion (H) and reappear by 60 days post-lesion (I). Brightness and contrast in G-I have been enhanced for optimal visualization of the weak immunoreactivity at putative nodes of Ranvier. **J:** In a longitudinal section through the adult spinal cord white matter of a zebrafish (fibers are oriented horizontally), TN-R immunoreactivity is accumulated at nodes of Ranvier of large diameter fibers (arrows). **K-N:** Cross sections through the diencephalon including the unlesioned (K) and lesioned zebrafish optic tract (OT) at 7 (L), 28 (M) and 56 (N) days post-lesion are shown. The density of mRNA expressing cells is increased at 7 and 28 days post-lesion and has returned to a density comparable to that in the unlesioned control tract by 56 days post-lesion. Arrows in K and N indicate some of the few TN-R mRNA positive cells. Bar in N = 100 μm for A-F, K-N; bar in I = 25 μm for G-J and 9 μm for J.

4.2.5 Optic axons encounter TN-R in a border-like situation in the brain

Patterns and intensities of immunoreactivity in structures bordering the trajectories of optic axons in the brain did not differ between the unlesioned and lesioned situation in zebrafish and are therefore described together. In contrast to the optic pathway itself, structures bordering it expressed higher levels of TN-R immunoreactivity. The ventral diencephalon bordering the optic tract expressed higher levels of TN-R immunoreactivity than the optic tract, resulting in a sharp boundary of TN-R expression at the tract/diencephalon interface (Fig. 13E,F). A similar border-like distribution of TN-R immunoreactivity was observed in the pretectum of fish with unlesioned and lesioned optic nerves (Fig. 14). Here, axons have to choose between retinorecipient and non-retinorecipient brain nuclei: Moderate to high TN-R immunoreactivity was observed in the non-retinorecipient lateral part of the dorsal accessory optic nucleus (IDAO), the magnocellular superficial pretectal nucleus (PSm), the posterior pretectal nucleus (PO) and the accessory pretectal nucleus (APN), with the latter being most intensely labeled (Fig. 14B). Analyzing this immunoreactivity in conjunction with the trajectories of optic fibers revealed a border-like encounter of optic axons with these structures (Fig. 14A-D). Large neurons at the border of non-retinorecipient brain nuclei were

strongly labeled by TN-R antibodies. Optic axons were always located in areas that were only weakly TN-R immunoreactive, both in lesioned and unlesioned animals (Fig. 14A-C) with optic fibers passing TN-R immunopositive nuclei in close apposition (Fig. 14D). Adjacent retinorecipient pretectal brain nuclei, such as the parvocellular superficial pretectal nucleus (PSP), the medial part of the dorsal accessory optic nucleus (mDAO) or the central pretectal nucleus (CPN) were only weakly TN-R immunopositive, compared to non-retinorecipient brain nuclei (Fig. 14B). TN-R mRNA was prominently detected in those large neurons, which were also labeled by TN-R antibodies in the accessory pretectal nucleus and in the magnocellular superficial pretectal nucleus in unlesioned and lesioned zebrafish (Fig. 14E-G). Periventricular cell layers in the diencephalon showed a uniform mRNA signal of low intensity (not shown), corresponding to the uniform immunoreactivity detected in the diencephalic fiber layers (cf. Fig. 13E,F).

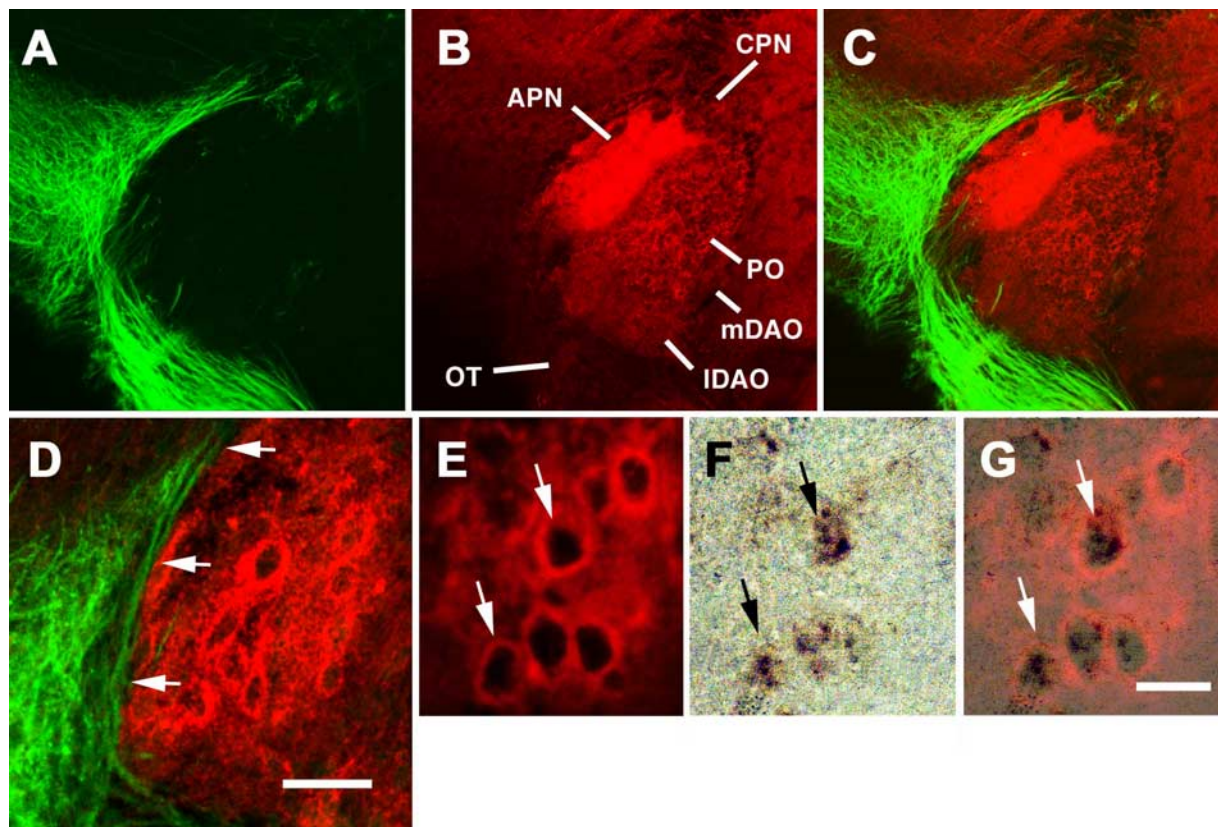


Fig. 14. TN-R borders the pathway of optic axons in the pretectum.

Cross sections through the pretectum of adult zebrafish double labeled for either optic axons (green) and TN-R immunoreactivity (red) in A-D, or for TN-R immunoreactivity (red) and TN-R mRNA (brown) in E-G are shown; dorsal is up; lateral is left. **A-C:** A single section through the pretectum of an animal that received an optic nerve crush three weeks prior to analysis is shown, with only optic axons (A), only TN-R immunoreactivity (B), or both (C) being depicted. Optic axons avoid the non-retinorecipient accessory pretectal

nucleus (APN), posterior pretectal nucleus (PO) and the lateral part of the dorsal accessory optic nucleus (IDAO) which express TN-R protein at different levels. Immunoreactivity in the optic tract (OT), in the retinorecipient central pretectal nucleus (CPN) and in the retinorecipient medial part of the dorsal accessory optic nucleus (mDAO) is particularly low. **D:** At higher magnification of the lateral border of the accessory pretectal nucleus, optic fibers (green) contacting the border of TN-R immunoreactivity (red) are obvious (arrows). **E-G:** In the accessory pretectal nucleus large neurons are particularly strongly labeled by TN-R antibodies (E). TN-R mRNA is also detected in this nucleus (F). Superimposing fluorescence and light microscopic images reveals colocalization of mRNA and protein (G). Arrows in E-G point to the same cells. Bar in D = 33 μm for D and 100 μm for A-C; bar in G = 25 μm for E-G.

Optic axons grow into and terminate in the optic tectum, their main target, in a layer-specific pattern. TN-R immunoreactivity (Fig. 15A) and optic fiber receiving layers (Fig. 15B) appeared to exclude each other in the tectum of unlesioned animals. TN-R immunoreactivity bordered the stratum fibrosum et griseum superficiale, the widest layer of optic axons, dorsally and ventrally. A few fibers also grew into narrow deeper tectal layers that appeared to express lower levels of TN-R immunoreactivity than surrounding layers (Fig. 15B). After an optic nerve crush, this pattern was unchanged at all post-lesion intervals analyzed (TN-R immunoreactivity: Fig. 15C; optic fiber layers: Fig. 15D), despite massive degeneration of severed optic fibers in the tectum during the early phase of regeneration (one to two weeks post-lesion). Mutually exclusive labeling of TN-R immunoreactivity and traced optic fibers in the tectum could also be shown densitometrically by measuring relative labeling intensities of traced optic axons and TN-R protein in double labeled tissue sections (Fig. 15E). Some cells located primarily in deep fiber layers, which were probably not relevant to optic axon guidance were intensely TN-R immunopositive in the tecta of unlesioned (Fig. 15A) and lesioned zebrafish (Fig. 15C). The appearance of these cells was reminiscent of inhibitory interneurons in the mammalian cortex that are decorated by perineuronal nets that contain TN-R (Brückner et al., 2000; Weber et al., 1999). Consistent with the presence of TN-R protein in the tectum, we found TN-R mRNA throughout the deep cellular layer and in a few intensely labeled cells in deeper layers of the tectal neuropil in unlesioned and lesioned animals (Fig. 15F,G). The intensely labeled cells correspond in their location to the strongly TN-R immunopositive cells (cf. Fig. 15A,C). Hybridizations with a sense probe did not yield any signal (Fig. 15H).

In lesioned and unlesioned adult goldfish, patterns of immunoreactivity closely resembled those found in zebrafish in the entire optic pathway (not shown). Patterns of mRNA expression were not analyzed because the relatively large gene was only cloned in zebrafish and hence no RNA probe specific to goldfish TN-R was available.

Summarizing the distribution of TN-R in relation to optic axons throughout the optic pathway, we find that both regenerating and newly growing adult optic axons encounter TN-R in the ventral diencephalon, pretectum and tectum in a border like fashion in zebrafish and goldfish. Axons of newly generated retinal ganglion cells are additionally confronted with intense TN-R immunoreactivity in their intraretinal path.

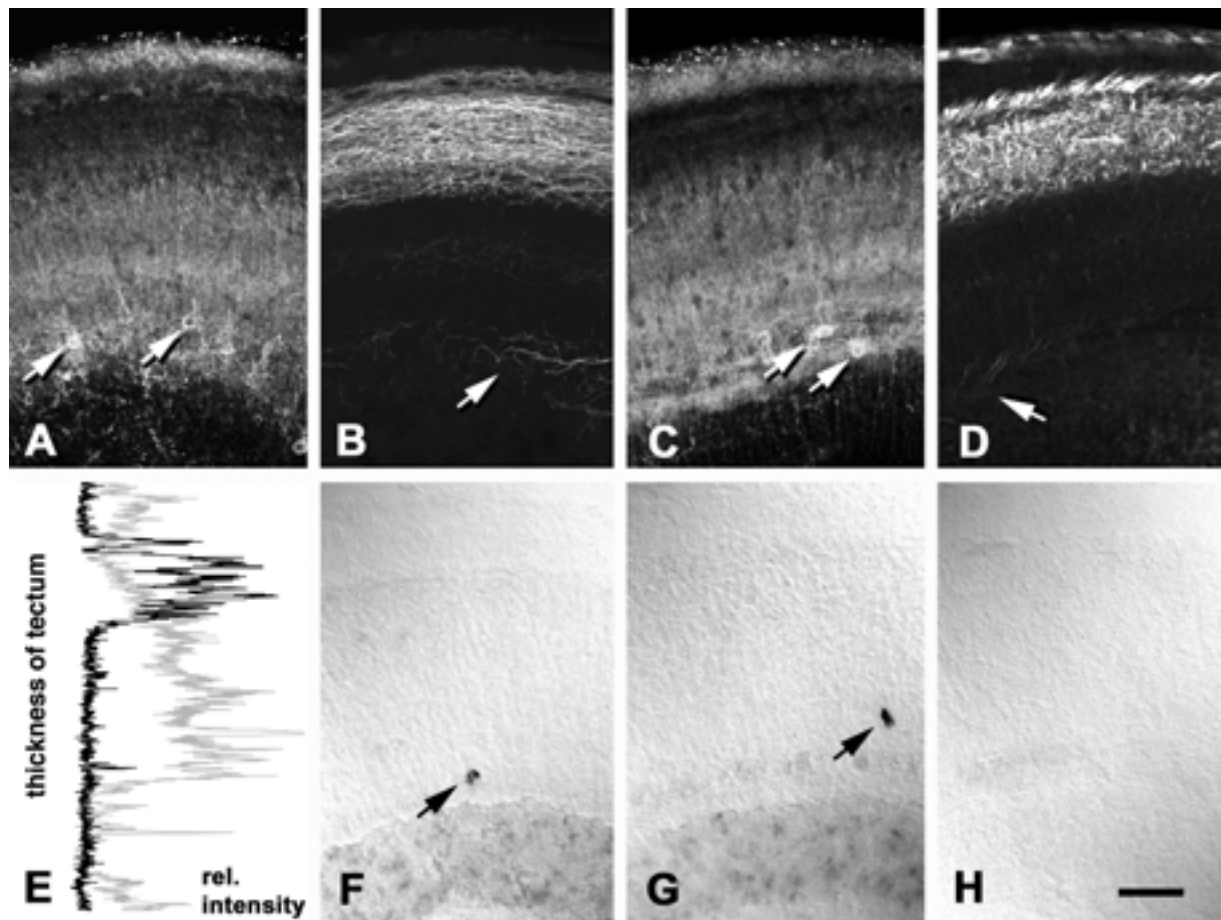


Fig. 15. TN-R is excluded from the optic fiber layer in the tectum.

Cross sections through the tectum of adult zebrafish are shown; dorsal is up. Tecta were either double labeled for TN-R immunoreactivity (A,C) and optic axons (B,D) or single labeled for TN-R mRNA (F,G) in unlesioned animals (A,B,F) and those that received an optic nerve crush three weeks prior to analysis (C,D,G). E shows a plot of relative fluorescence intensity of TN-R (gray) and optic fiber labeling (black) in a tectal cross section; dorsal is up. The section in H has been hybridized with a sense mRNA probe as a negative control for F,G. TN-R immunoreactivity is selectively low in optic fiber receiving layers of the tectum (A-E) with no differences between the lesioned and unlesioned situation. TN-R mRNA is homogeneously expressed in the periventricular cell layer in the tectum of lesioned and unlesioned fish (F,G). Expression of mRNA is particularly strong in scattered cells (arrows in F,G), the positions of which correspond to neurons with intense perisomatic immunoreactivity (arrows in A, C). In addition to the majority of optic axons that grow into the tectum superficially, some fibers also grow in deeper layers of the tectum (arrows in B, D). Bar in H = 50 μ m for A-D, F-H.

4.2.6 TN-R is present during development of the optic projection

To elucidate the possible relationship between TN-R expression and guidance of optic axons during development in comparison to regeneration, we analyzed expression patterns of TN-R mRNA and protein in 3-5 day-old zebrafish larvae, and in 4-6 week-old juvenile zebrafish. The first optic fibers reach the optic tectum by 44 hours post-fertilization and establish retinotopic innervation by 3 days of development (Stuermer, 1988). At 3-5 days of development, strong TN-R immunoreactivity was detected in the outer plexiform layer of the retina, but not in the optic fiber layer (Fig. 16A,C). No conspicuous labeling was apparent in the optic nerve and tract in 3-5 day-old larvae (not shown). In the brain, distinct neuropil areas were labeled in 3-5 day-old larvae. In particular, the optic neuropil of the tectum appeared to be free of TN-R immunoreactivity, creating a border situation for growing optic axons towards deeper tectal layers (Fig. 16A). TN-R mRNA was intensely labeled in only one band of cells located at the outer margin of the inner nuclear layer of the retina and was diffusely labeled in the central cellular layer of the diencephalon and midbrain by three to five days of development (Fig. 16B,D).

By four to six weeks of development, when the optic projection is still rapidly growing, patterns of immunoreactivity and mRNA labeling in the retina and optic pathway resemble the adult pattern (not shown). At this time of development TN-R was also detectable in the optic fiber layer of the developing retina.

Thus, with the exception of the non-detectable TN-R immunoreactivity in the optic fiber layer in the retina of 3-5-day-old larvae, the expression pattern of TN-R during development resembled that in the adult optic pathway. This suggests similar, although not identical, interactions of optic axons with TN-R in developing and adult fish.

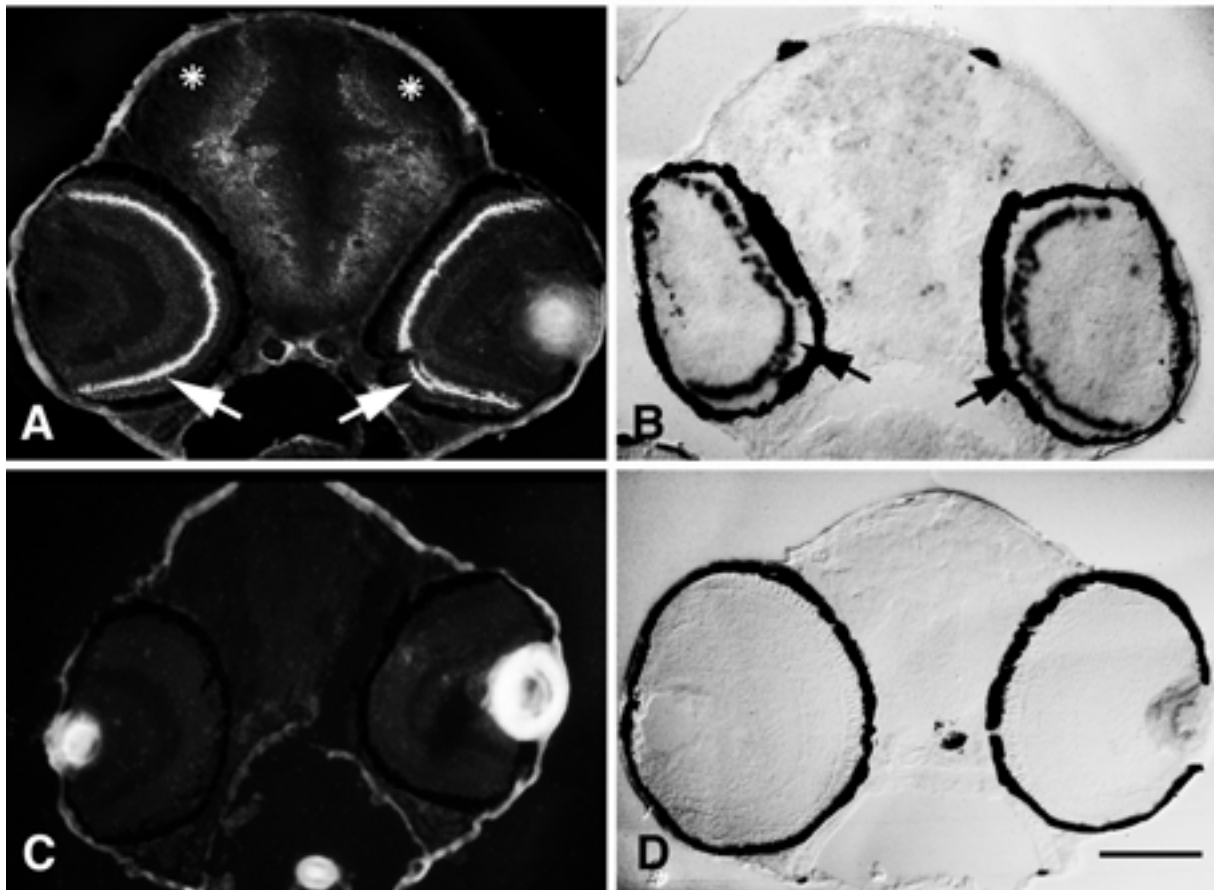


Fig. 16. TN-R is expressed during development of the optic projection.

Cross sections through 5-day-old zebrafish larvae are labeled with antibodies (A,C) or mRNA probes (B,D); dorsal is up. TN-R immunoreactivity is found in the outer plexiform layer of the retina (arrows in A), but not in the optic fiber layer of the retina. TN-R immunoreactivity is present in the brain, but the optic fiber receiving layer of the tectum (asterisks in A) is selectively free of immunoreactivity, similar to the adult tectum. TN-R mRNA is labeled in the inner nuclear layer of the retina (arrows in B) and diffusely in the brain. In F a section incubated with non-immune serum is shown. In D a section hybridized with sense cRNA probe is shown. Bar in D = 100 μm for A-D.

4.2.7 Axonal reactions to TN-R *in vitro* depend on the way the molecule is presented

Regenerating optic axons encounter TN-R always in a border-like situation in the brain, whereas axons of newly generated retinal ganglion cells grow through a TN-R immunopositive territory in the retina in older zebrafish larvae and adult zebrafish and goldfish *in vivo*. To mimic both situations, axons from retinal explants of adult goldfish and zebrafish were cultured next to a substrate border of TN-R (brain situation). Goldfish axons were additionally tested on a homogeneous TN-R substrate (retinal situation). Axon outgrowth from adult zebrafish retinal explants on a homogeneous substrate could not be

tested due to poor attachment of the explants to the substrate. In all preparations, laminin was present throughout the culture dish in concentrations that promote growth of fish optic axons. In agreement with previously reported behaviors of optic axons of adult mice and salamanders (Becker et al., 1999; Becker et al., 2000b), zebrafish and goldfish optic axons were mostly unable to cross a substrate border of TN-R. Instead, they appeared to turn and grow along such a border. Since results from goldfish and zebrafish did not differ, they were pooled. Of all explants confronted with TN-R, $79\% \pm 8.2\%$ s.e.m. ($n = 80$ explants) showed inhibition of the vast majority of their axonal fascicles at a TN-R substrate border (Fig. 17C). In contrast, a control substrate border of BSA was ignored by growing axons (Fig. 17A). Axonal fascicles of $13\% \pm 3.8\%$ s.e.m. of the explants ($n = 55$ explants) were deflected at a BSA border. The differences between TN-R and BSA substrates are statistically highly significant (Mann-Whitney U, $P < 0.01$; Fig. 17E).

As an additional control, we tested the reaction of zebrafish optic axons to substrate borders that had been treated with chondroitinase. TN-R binds chondroitin sulfate proteoglycans (Xiao et al., 1997) and has been suggested to carry chondroitin sulfates itself (Probstmeier et al., 2000). Chondroitin sulfates are capable of eliciting similar reactions in optic axons as those observed here (Becker and Becker, 2002). Chondroitinase treatment efficiently abolished the avoidance reaction when pure chondroitin sulfates are coated. However, chondroitinase did not alter the reaction of zebrafish optic axons to a TN-R substrate border. Four out of four explants showed deflection of axonal fascicles at the border of a chondroitinase treated TN-R substrate spot. This indicates that deflection of axons at a TN-R substrate spot is not due to potentially present chondroitin sulfates.

On a homogenous substrate of TN-R in conjunction with laminin, axon growth from goldfish retinal explants was massive (Fig. 17D). This is in sharp contrast to adult optic axons of mice and salamanders, which are inhibited in this situation (Becker et al., 1999; Becker et al., 2000b). Compared to a BSA control substrate (Fig. 17B), goldfish axons grew in a more fasciculated manner on a TN-R containing substrate. Growth of these fascicles on TN-R substrates was more rapid than on BSA containing substrates. After two days *in vitro*, explants on a TN-R substrate extended a mean number of $11.2 (\pm 1.25$ s.e.m.) axonal fascicles exceeding more than $400 \mu\text{m}$ in length ($n = 58$ explants). This was significantly more (Mann-Whitney U, $P < 0.05$) than on BSA control substrates (7.9 ± 0.92 s.e.m. fascicles per explant; $n = 50$ explants; Fig. 17E). The difference in axon growth promotion between TN-R substrates and controls may be even greater, since the higher degree of fasciculation on TN-R substrates leads to lower numbers of countable fascicles, although the number of individual

axons that are promoted in their growth may be higher. Thus, growth of adult goldfish optic axons is compatible with and even promoted by a homogeneous TN-R substrate.

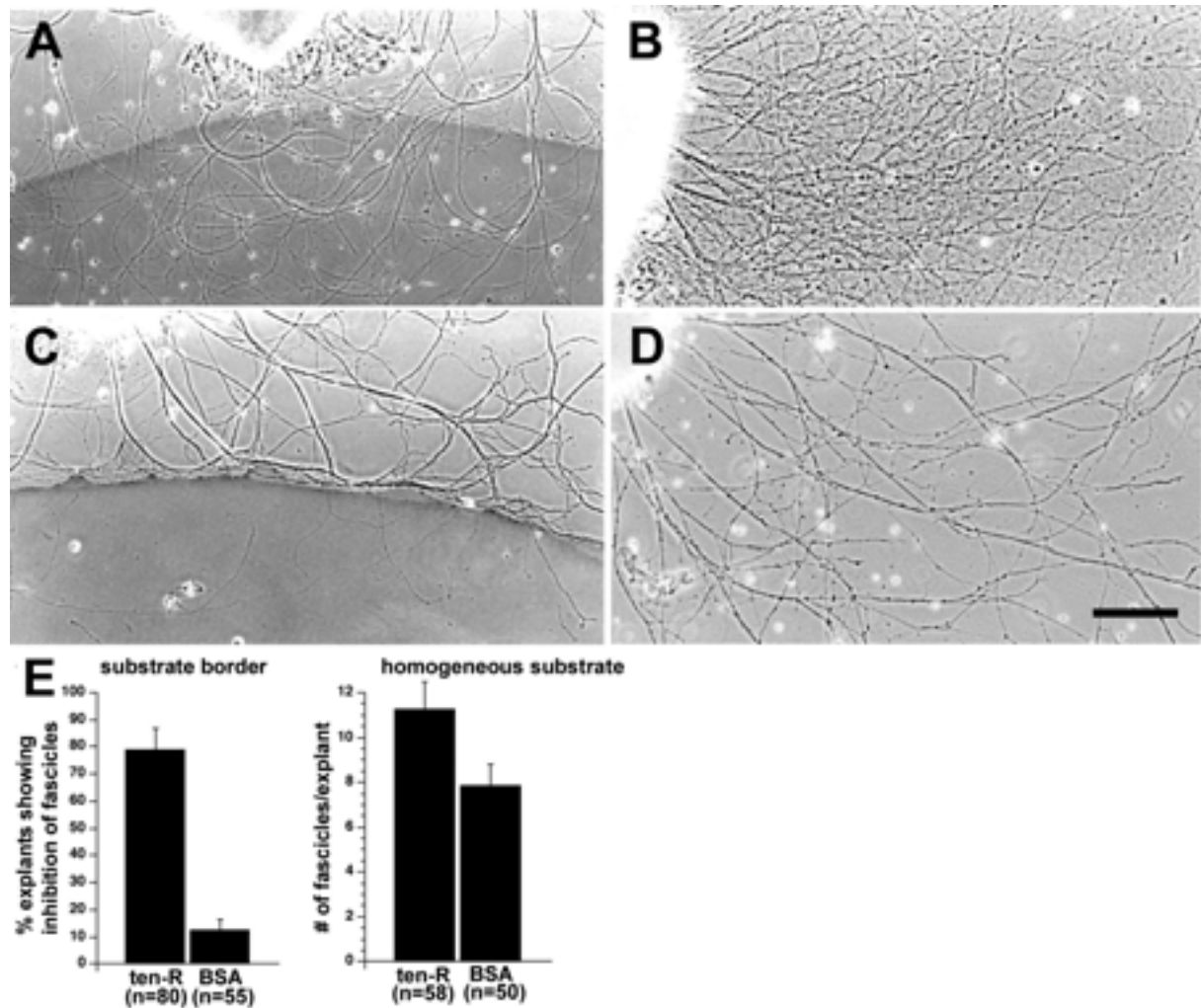


Fig. 17. Retinal axons are repelled by a TN-R substrate border, but their growth is promoted by a homogeneous substrate *in vitro*.

A,C: Goldfish axons growing from retinal explants (located at the top of each panel) readily cross a substrate border of BSA (A), but are mostly repelled at a TN-R border (C) at four days *in vitro*. Spots of test substrates appear dark due to the addition of india ink. **B,D:** Goldfish retinal explants (top left corner) placed on homogeneous test substrates exhibit profuse axon outgrowth on BSA (B) and TN-R (D) substrates at four days *in vitro*. Note that axon growth on TN-R is more fasciculated than on BSA. **E:** Quantitative analysis of axon outgrowth shows that axon fascicles are repelled by TN-R substrate borders significantly more often than at BSA borders, while on a homogeneous TN-R substrates axon growth is enhanced compared to BSA substrates. Bar in D = 200 μm for A, C and 100 μm for B, D.

Results part three

In the third section of the results, the cloning of tenascin-C and its in vivo function during outgrowth of ventral motor axons in the trunk of the zebrafish *Danio rerio* will be described.

4.3 Tenascin-C is involved in outgrowth of motor axons in the trunk of zebrafish

4.3.1 Molecular cloning of a full-length tenascin-C cDNA in zebrafish

Two partial sequences of the zebrafish TN-C cDNA containing the FN-III domains 6-8 and the fibrinogen knob of the 3'-end had previously been described (Tongiorgi et al., 1995b); (Qiao et al., 1995). A further partial sequence containing the 14.5 epidermal growth factor (EGF)-like domains at the 5'-end of TN-C was further obtained during a low stringency screen with a probe containing the EGF-domains of rat TN-R (see Experimental procedures). To obtain the full length zebrafish TN-C cDNA, we used these two sequences to generate primers which bridge the gap between both partial sequences. Since the obtained sequence was missing a signal peptide and further parts of the 5'-end as revealed by sequence alignment with other known TN-C homologs, we performed a 5'-RACE to clone the full-length coding sequence of TN-C. Full length TN-C encodes a deduced protein of 1711 amino acids. The start codon was predicted from the presence of stop codons preceding the N-terminal end of the deduced protein and the presence of a signal peptide at the N-terminus. The general domain structure of zebrafish TN-C, comprising a cysteine-rich domain, 14.5 EGF repeats, followed by 8 FN III domains and a fibrinogen globe at the C-terminus, is identical to that of homologs in other vertebrate species. Alignment of the zebrafish molecule with those of human (Leprini et al., 1996), mouse (Saga et al., 1991; Weller et al., 1991) and chicken (Jones et al., 1989) TN-C indicated significant structural homology among the four molecules (Fig. 18). The highest overall identity of amino acid sequences is 49% between the zebrafish and chicken sequences. The degree of amino acid identity between zebrafish and human TN-C is 42% and to the mouse TN-C 45%. Based on structural and amino acid identities with TN-C of other species we could confirm the obtained sequence data of (Tongiorgi et al., 1995b) and (Qiao et al., 1995). Following the established nomenclature for zebrafish (Mullins, 1995), we tentatively named the gene *tenascin-c*.

Fig. 18. Amino acid sequence of tenascin-C in zebrafish compared to that of human, mouse and chicken. Identical amino acids are highlighted in black, similar amino acids in gray. Epidermal growth factor-like repeats (EGF-like repeats, white boxes), fibronectin type III-like domains (FNIII-like domain, grey boxes) and the fibrinogen knob are indicated (hatched boxes).

4.3.2 TN-C immunoreactivity is localized in the pathway of outgrowing motor axons in the trunk during development of the zebrafish

Immunoreactivity of TN-C and chondroitin sulfate proteoglycans in the trunk of the developing zebrafish have previously been described. (Bernhardt et al., 1998, Tongiorgi, 1999; Bernhardt and Schachner, 2000). To analyze the expression patterns of TN-C and chondroitin sulfates in the trunk of the zebrafish during outgrowth of ventral motor axons in more detail we used confocal microscopy to visualize the spatial relationship of these molecules to outgrowing motor axons. An antibody directed against zebrafish TN-C (Tongiorgi, 1999) and also an antibody generated against chicken TN-C (Bartsch et al., 1995), which has been shown to cross-react with zebrafish TN-C (Bernhardt et al., 1998), were used to detect TN-C immunoreactivity. Both antibodies always labeled the same structures in the developing zebrafish. At 16 hpf, TN-C immunoreactivity was detected in the posterior half of each body segment, in the segment borders and around the notochord (Fig. 19A) as described previously (Bernhardt et al., 1998; Tongiorgi, 1999). Expression of TN-C protein in the trunk during later developmental stages was dynamically regulated. In 22-24 hpf old embryos, TN-C immunoreactivity was no longer confined to the posterior half of each body segment, but was concentrated at the horizontal myoseptum which is a critical choice point in the pathways of outgrowing motor axons (Beattie et al., 2002). TN-C immunoreactivity appeared as fibrils in the preparations (Fig. 19B). Expression of TN-C protein at the horizontal myoseptum could be detected before axon outgrowth as revealed by confocal image stacks through caudal parts of the trunk of 22.5 hpf embryos (n=8, Fig. 19C, E and F). In more rostral parts of the trunk this pattern of TN-C immunoreactivity was maintained even when ventral motor axons had already grown beyond the horizontal myoseptum into ventral parts of the trunk (Fig. 19 G, I and J). The expression of TN-C in the segment borders and around the notochord remains unchanged between 16 and 22.5 hpf (Fig. 19E and I). In the same confocal image stacks analyzed for TN-C immunoreactivity, chondroitin sulfate (detected by the CS56 antibody) was distributed all over the somite in addition to the segment borders and the notochord at 22.5 hpf (Fig. 19D, H, F and J). Confocal image stacks of a 22 hpf embryo were rotated and embryos were analyzed from a dorsal view. In this orientation the association of outgrowing

motor axons with TN-C immunoreactivity was also obvious (Fig. 19K, N, M). Chondroitin sulfate immunoreactivity was detected at the surface of the notochord and around a putative sclerotomal cell in this preparation (Fig. 19L) as described previously (Bernhardt et al., 1998). In summary, TN-C immunoreactivity was co-localized with outgrowing motor axons at their choice point at the horizontal myoseptum. In contrast to the widespread distribution of chondroitin sulfate immunoreactivity, TN-C immunoreactivity was further localized at the horizontal myoseptum before motor axons grown out, thereby pointing to a potential guidance function of this molecule for motor axons.

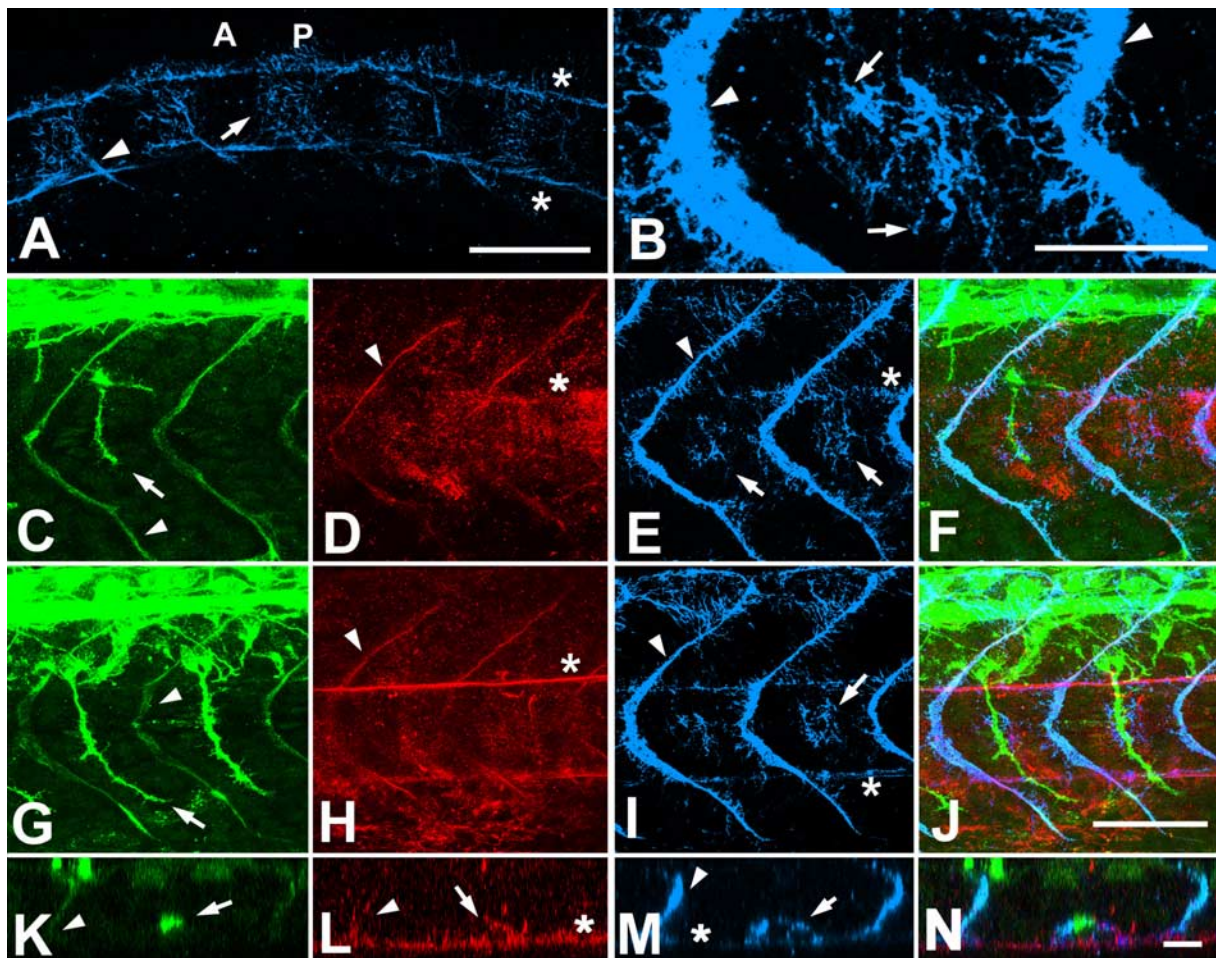


Fig. 19. TN-C immunoreactivity is localized at the level of the horizontal myoseptum in the pathway of outgrowing motor axons. In A-J, lateral views of confocal image stacks of whole mounted zebrafish embryos are shown at mid-trunk levels. In K-N horizontal views of one body segment are shown. Rostral is to the left in A-N, dorsal is up in A-J. Lateral is up in K-N. Axons are labeled in green. Note that the HNK-1 antibody also recognizes the vertical myosepta (arrowheads in C, G and K). Immunoreactivity for TN-C is shown in blue and chondroitin sulfates are labeled in red. **A:** A side view of trunk segments of a 16 hpf old embryo is shown. TN-C immunoreactivity is located in the posterior half (P) of each body segment (arrow), at the vertical myosepta (arrowhead) and at the upper and lower border of the notochord respectively (asterisks). **B:** A high magnification of a trunk segment at the level of the horizontal myoseptum of a 22.5 hpf embryo is shown. TN-C

immunoreactivity, which appears as fibrils is located at level of the horizontal myoseptum (arrows) and at the vertical myosepta (arrowheads). **C-F:** In caudal parts of the trunk of a 22.5 hpf embryo a ventral motor axon just reaching the horizontal myoseptum is shown (arrow in C). Note that in the adjacent caudal segment no axon has grown out, yet. In this preparation, chondroitin sulfate immunoreactivity, is distributed all over the somite and is concentrated in the vertical myosepta (arrowhead in D) and around the notochord (asterisk in D). TN-C immunoreactivity is localized at the level of the horizontal myoseptum (arrows in E) and at the vertical myosepta (arrowhead in E) and around the notochord (asterisk in E). The overlay in F clearly demonstrates that TN-C immunoreactivity is localized at the horizontal myoseptum around the outgrowing axon. Immunoreactivity for chondroitin sulfate is also broadly distribution around the axons. **G-J:** In more rostral segments of the same embryo, which are more mature due to a developmental gradient within the embryo, ventral motor axons have grown beyond the horizontal myoseptum to their ventral target areas (arrow in G). The patterns of chondroitin sulfate- and TN-C- immunoreactivity appeared unchanged in this preparation compared to more immature, caudal segments (H, I and overlay in J). **K-N:** A horizontal section through a 22.5 hpf embryo at the level of the horizontal myoseptum is shown. The motor axon is located in the middle of the body segment (arrow in K) adjacent to the notochord which is strongly immunopositive for chondroitin sulfates (asterisk in L). The vertical myosepta (arrowhead in L) and a putative sclerotomal cell (arrow in L) are also immunopositive for chondroitin sulfates. TN-C immunoreactivity is detected in the middle of the body segment and around the putative sclerotomal cell (arrow in M, see also the overlay in N) and is also located at the vertical myosepta (arrowhead in M) and to a lower extent at the notochord (asterisk in M). The overlay in N clearly demonstrates that TN-C immunoreactivity is concentrated around the motor axon. Scale bars in A = 50 μm for A, in J = 50 μm for C-J, in B = 25 μm for B and in N = 12,5 μm for K-N.

4.3.3 Overexpression of the EGF-like domains of TN-C resulted in abnormal outgrowth of ventral motor axons

To investigate the function of TN-C during outgrowth of ventral motor axons we generated an overexpression construct containing the 14.5 EGF-like domains of zebrafish TN-C fused to a Myc-tag. This construct was named TNCEGFmyc. The EGF-like domains of mouse TN-C had been described to repel axons in vitro (Dorries et al., 1996; Jones and Jones, 2000). As a control for unspecific effects of the Myc-tag itself, the secretion signal, which directs TN-C out of the cell into the extracellular matrix was fused to a Myc-tag. This construct was named TNCLSmyc. First, we investigated the patterns of protein expression and localization of our in vitro produced mRNAs in injected zebrafish embryos. In vehicle injected embryos (Fig. 20A) no specific labeling was detected as revealed by whole mount immunohistochemistry using a FITC-labeled Myc-antibody on 24 hpf embryos. Injecting the mRNA encoding TNCLSmyc resulted in a detectable expression of the encoded protein in the vertical myosepta (Fig. 20B) of developing embryos. Ectopic expression of TNCEGFmyc in a 24 hpf

embryo was detected in a pattern that resembled the expression of endogenous TN-C. Myc-immunoreactivity was located in the pathway of the ventral motor axons, the segment borders (Fig. 20C), around the notochord and in the otic vesicle (not shown). As a control for the secretion of TNCEGFmyc and TNCLSMyc, we injected an mRNA encoding the Myc-epitope but missing the secretion signal and found labeled cells, but no signal in the vertical myosepta, suggesting that the protein was confined to the cytoplasm (Fig. 20E). Thus, we could clearly show that the proteins encoded by TNCEGFmyc and TNCLSMyc are localized in the ECM.

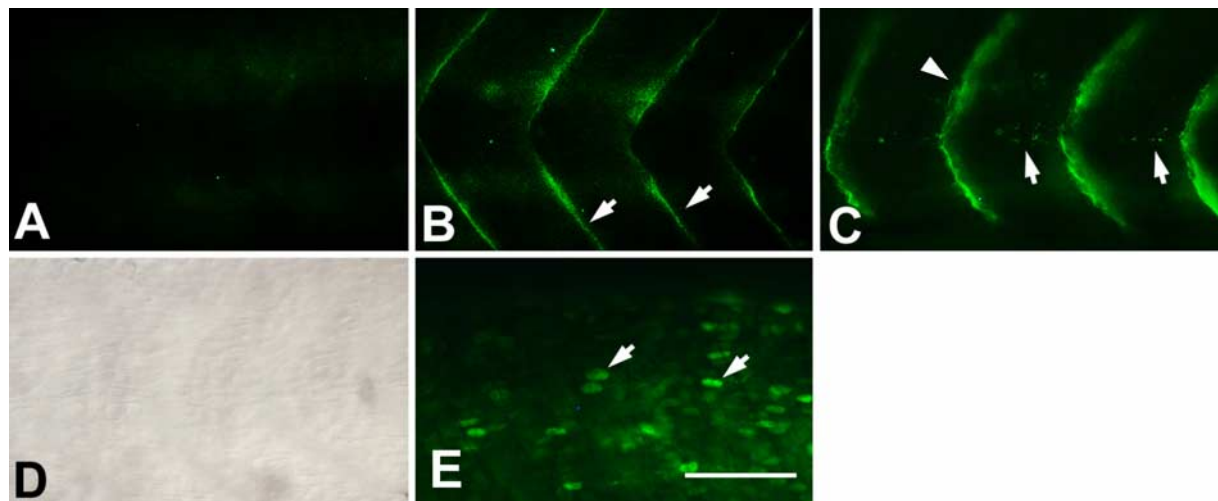


Fig.20. Injection of an mRNA encoding the EGF-like domains of TN-C leads to protein expression patterns identical to those of endogenous TN-C. Lateral views of whole mounted embryos are shown at mid-trunk level. Rostral is to the left and dorsal is up. Protein from injected mRNAs in the trunk as detected with an α -Myc antibody in 24 hpf embryos is shown. A: A zebrafish embryo injected with vehicle solution is shown. B: Expression of a control protein containing the secretion signal of TN-C fused to six Myc epitopes is detected at the vertical myosepta (white arrows). C: Injection of a mRNA encoding the 14.5 EGF-like repeats of TN-C leads to detectable protein expression in the somites at the level of the horizontal myoseptum (white arrows) and at the vertical myosepta (white arrowhead). In D the differential interference contrast image corresponding to A is shown. E: Injection of a mRNA encoding the six Myc-epitopes without the localization signal of TN-C leads to detectable protein expression in the cytoplasm of cells (white arrows). Scale bar in E = 50 μ m for A-E.

Axon growth of TNCEGFmyc-injected embryos was investigated at 24 hpf, when only the three primary motor axons per trunk hemisegment had grown out and the axon of the caudal primary motorneuron (CaP) pioneers the midsegmental pathway ventral to the horizontal myoseptum (Eisen et al., 1986; Myers et al., 1986; Westerfield et al., 1986). To analyze only those embryos, which expressed the injected mRNAs, we performed a double staining with the Myc-antibody to visualize ectopic expression of the injected mRNAs and a tubulin antibody to label axon tracts. Only those embryos showing expression of the injected mRNA

were subjected to quantification of axon growth. We did not analyze secondary motor axons, which start to grow out at 28 hpf (Ott et al., 2001; Pike et al., 1992), since expression of our injected mRNAs could not be detected anymore in 33 hpf embryos.

In uninjected and vehicle-injected control embryos and those injected with TNCLSm_{yc}, ventral motor axons usually grew straight and unbranched towards the ventral somite (Fig. 21A) In embryos injected with TNCEGF_{myc}, branched (Fig. 21B) or truncated motor nerves (Fig. 21C, D) were frequently observed. In uninjected embryos (n=40), 3.2% (37/1280) of the nerves analyzed were abnormal. In vehicle injected embryos (n=36) the frequency of aberrant ventral motor nerves was 3.6% (42/1152) and in embryos injected with TNCLSm_{yc} mRNA (n=45) it was 3.2% (46/1440). In embryos injected with TNCEGF_{myc} mRNA (n=49), we observed a doubling of the incidence of abnormal nerves to 8.8 % (137/1568). This was statistically significant compared to control embryos injected with TNCLSm_{yc} mRNA (Mann-Whitney U-test, $p < 0.0001$; Table 2; Fig. 21E). The types of aberrations after TNCEGF_{myc} mRNA injection were either complete truncations or truncations at the horizontal myoseptum. Aberrant branching of the nerves was also observed. The number of truncations in embryos injected with TNCEGF_{myc} (3.3% of all nerves analyzed; Table 2) was at least 5-fold increased compared to controls. In TNCLSm_{yc} injected embryos, 0.6% of all nerves analyzed were truncated, in vehicle injected embryos 0.4% and in uninjected embryos 0.2% of all nerves analyzed were truncated (Table 2). The rate of aberrant branches in embryos injected with TNCEGF mRNA (5.5% of all nerves analyzed) was almost doubled compared to controls (Table 1). In TNCLSm_{yc} injected embryos 2.6% of all nerves analyzed showed abnormal branches, in vehicle injected embryos 3.2% and in uninjected embryos 2.7% of all nerves analyzed revealed abnormal branches (Table 2). After injection of the TNCEGF_{myc} mRNA caudal branches occurred most frequently 42% (57 out of 137 abnormal nerves), followed by truncations 36% (50/137), bilateral branches 18% (25/137) and rostral branches 5% (7/137; Table 5). Thus at 24 hpf, expression of an mRNA encoding the EGF-like domains of TN-C induced a significantly increased rate of abnormal ventral motor nerves, which were mostly abnormal branches and truncations of the motor nerves.

Table 2. Frequency of abnormal motor nerves after injection of TNCEGFmyc mRNA analyzed at 24 hpf.

	# of analyzed embryos	Nerves scored (total)	total # of abnormal nerves	Severe truncation	Abnormally branched nerves	Mean # of abnormal nerves per embryo
TNCEGF myc	49	1568	137 (8.8%) §	50 (3.3%)	87 (5.5%)	2.9 ± 0.25
TNCLS myc	45	1440	46 (3.2%)	9 (0.6%)	37 (2.6%)	1.0 ± 0.18
vehicle	36	1152	42 (3.6%)	5 (0.4%)	37 (3.2%)	1.1 ± 0.21
uninjected	40	1280	37 (2.9%)	3 (0.2%)	34 (2.7%)	0.9 ± 0.22

§ Significant different from control groups

4.3.4 Injection of a recombinant TNCEGF fragment also leads to aberrant motor axon outgrowth

The expression of TNCEGFmyc mRNA from the early onset of development might have influenced developmental processes such as somitogenesis (Stickney et al., 2000), which starts at 10.5 hpf and thereby affect motor axon growth only indirectly. To show that the phenotypes observed after injection of TNCEGFmyc are due to direct perturbation of motor axons, we injected different TN-C fragments shown to be repellent for growth cone advance and neurite outgrowth (EGF repeats) or to confer adhesion to neurons (FNIII 6-8) in vitro (Dörries et al., 1996). These fragments were injected at the level of the 10th somite in 15-17 hpf old embryos so that early developmental processes were mostly not influenced. The axon tracts were labeled with a tubulin antibody and embryos were analyzed at 24 hpf. In uninjected embryos, vehicle injected control embryos and embryos injected with the FN 6-8 fragment, ventral motor axons usually grew straight and unbranched towards the ventral somite (Fig. 21F). In embryos injected with a protein fragment containing the EGF-like domains of TN-C (EGF-L fragment), complete truncations or truncations at the level of the horizontal myoseptum (Fig. 21G, H) were frequently observed. In uninjected embryos (n=15), 4.1 % (20/480) of the nerves analyzed were abnormal. In vehicle-injected embryos (n=15) the frequency of aberrant ventral motor nerves was 3.7 % (18/480) and in embryos injected with the FN 6-8 fragment (n=14) it was 3.5 % (15/448). Embryos injected with the EGF-L

fragment (n=18), showed an approximately 2.5 fold increase of abnormal nerves to 8.9 % (48/576). This was statistically significant compared to embryos injected with the FN 6-8 fragment (Mann-Whitney U-test, $p = 0.0034$; Table 3; Fig. 21I) and to vehicle injected controls (Mann-Whitney-, $p = 0.0092$). 5.2 % of all nerves analyzed in embryos injected with the EGF-F protein fragment (Table 3) showed complete truncations or truncations at the level of the horizontal myoseptum. This rate was almost 5-fold increased compared to control groups since, embryos injected with the FN 6-8 fragment showed 0.9%, vehicle injected embryos 1.2% and uninjected embryos 0.4% truncations of all nerves analyzed (Table 3). This rate of truncations was comparable to the number of truncations observed after injection of the TNCEGFmyc mRNA (Table 2). The rate of aberrant branches in embryos injected with the EGF-L fragment (3.7% of all nerves analyzed, Table 3) was in the range of normally occurring branches observed in controls. In embryos injected with the FN 6-8 fragment 2.5% of all nerves analyzed showed abnormal branches, in vehicle injected embryos we observed 2.5% and in uninjected controls 3.6% of all nerves analyzed were abnormally branched (Table 3). After injection of the EGF-L fragment, truncations occur most frequently 59% (30 of 51 abnormal nerves), followed by bilateral branching 22% (11/51), caudal branches 14% (7/51) and rostral branching 6% (3/51; Table 5). Thus at 24 hpf, the injection of recombinantly expressed EGF-like repeats of TN-C leads to truncations of the ventral motor nerves at similar frequencies observed after injection of TNCEGFmyc mRNA and therefore confirms these results.

Table 3. Frequency of abnormal motor nerves after injection of the EGF-L protein fragment analyzed at 24 hpf.

	# of analyzed embryos	Nerves scored (total)	total # of abnormal nerves	Severe truncation	Abnormally branched nerves	Mean # of abnormal nerves per embryo
EGF-L	18	675	51 (8.9%) §	30 (5.2%)	21 (3.7%)	2.7 ± 0.41
FN 6-8	14	448	15 (3.5%)	4 (0.9%)	11 (2.6%)	1.0 ± 0.27
vehicle	15	480	18 (3.7%)	6 (1.2%)	12 (2.5%)	1.2 ± 0.26
uninjected	15	480	20 (4.1%)	2 (0.4%)	18 (3.7%)	1.3 ± 0.33

§ Significant different from control groups

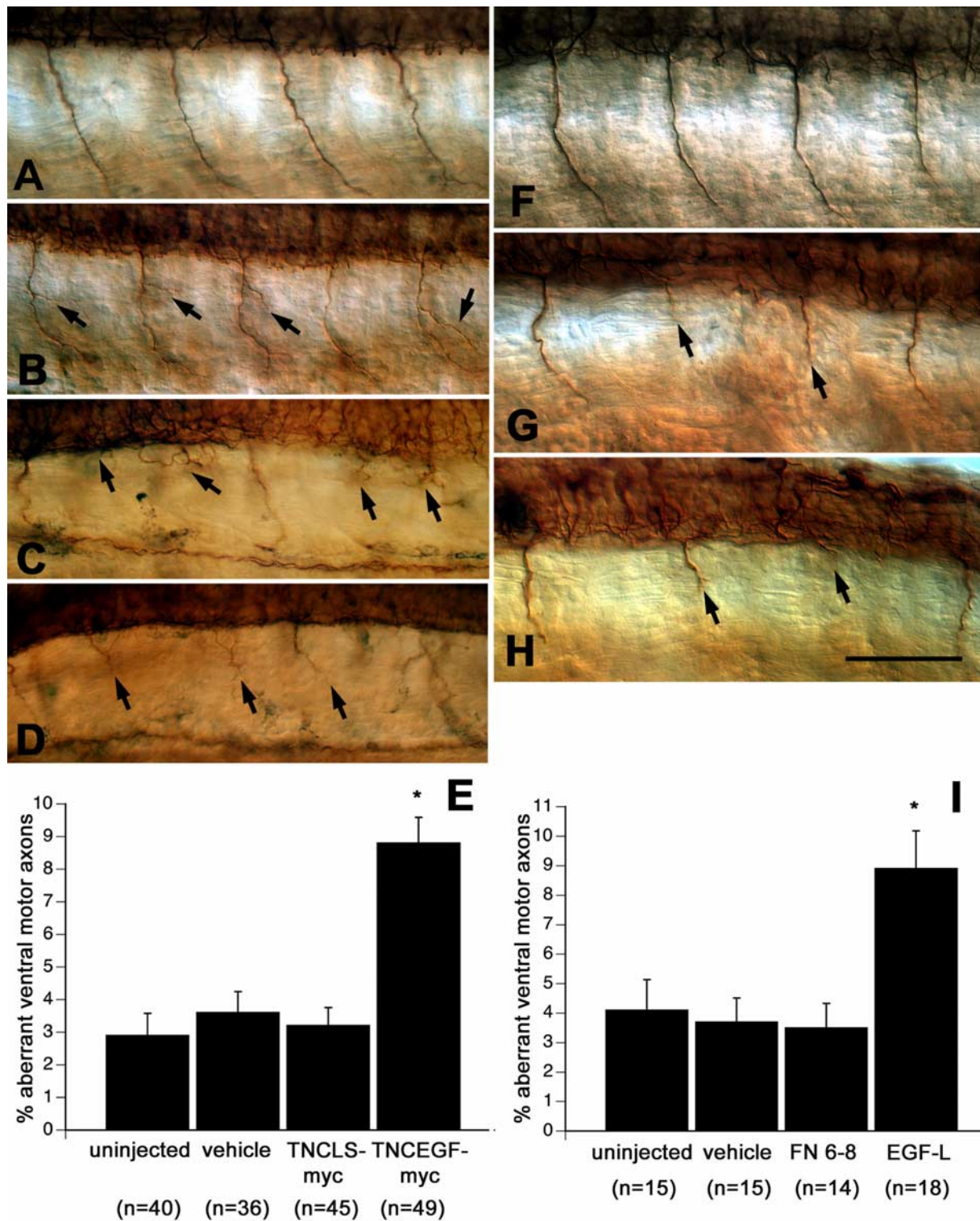


Fig.21. Overexpression of an mRNA encoding the complete EGF-like repeats of TN-C or injection of an EGF-L protein fragment leads primarily to truncated ventral motor nerves at 24 hpf. Lateral views of whole mounted embryos are shown at mid-trunk levels. Rostral is to the left and dorsal is up. **A:** In control embryos injected with the TNCLSmyc mRNA, axon trajectories are straight and unbranched at 24 hpf. **B-D:** In TNCEGFmyc-injected embryos, some nerves are branched at the level of the horizontal myoseptum (arrows in B). Truncations of axons frequently occurred at the level of the horizontal myoseptum or at their exit point from the spinal cord (arrows in C and D). **E:** In embryos injected with TNCEGFmyc mRNA, 8.8% of all ventral motor nerves analyzed per embryo are abnormal which is statistically highly significantly different from values

of control embryos injected with TNCLSmyc or other controls (asterisk, $p < 0.0001$). Values for uninjected control embryos (uninjected) and vehicle injected (vehicle) are also indicated. **F:** In embryos injected with a recombinant protein fragment containing the FN III-like domains 6-8, ventral motor nerves grow straight and unbranched. **G, H:** Injection of the EGF-like repeats of TN-C leads to truncations of ventral motor axons. Truncations of axons occurred at the level of the horizontal myoseptum or at the exit point at motor axons from the spinal cord (arrows in G and H). **I:** In embryos injected with the recombinantly expressed EGF-like repeats of TN-C (EGF-L), 8.9% of all ventral motor nerves analyzed per embryo are abnormal, which is statistically significant, compared to embryos injected with the FN 6-8 fragment (FN 6-8, asterisk, $p < 0.0034$) and also for the other controls. Values for uninjected control embryos (uninjected) and vehicle injected (vehicle) are also indicated. Scale bar in H = $50\mu\text{m}$ for A-H.

4.3.5 The overexpression of TNCEGFmyc mRNA or injection of the EGF-L fragment does not affect trunk structures, muscle pioneers and other axon trajectories.

We inspected trajectories of other nerves and tracts in the injected embryos to see whether these had been influenced by injections of the TNCEGFmyc mRNA or the EGF-L protein fragment. The posterior lateral line nerve extends along the trunk also at the level of the horizontal myoseptum from rostral to caudal in a coordinate fashion with general development. This nerve is sensitive to specific perturbations that may lead to defasciculation and/or pathfinding errors of single axon fascicles or of the entire nerve (Becker et al., 2001b; Shoji et al., 1998). We quantified the length of the lateral line nerve by identifying its segmental position in embryos labeled with the tubulin antibody. In embryos injected with TNCEGFmyc mRNA, the nerve extended in its normal position in a fasciculated manner (Fig. 22A). On average the lateral line nerve and primordia analyzed was located in segment 6.5 ± 0.14 ($n=49$) which is in the range of uninjected embryos (Fig. 22B; mean= 6.4 ± 0.18 ; $n=40$). In embryos injected with the EGF-L protein fragment the mean of all lateral line nerve and primordia analyzed was located at segment 5.3 ± 0.11 ($n=18$) and in uninjected control embryos at segment 5.7 ± 0.11 ($n=15$; not shown). The average length of the lateral line nerve and primordium between uninjected embryos and their respective control embryos were not statistically different. This indicates, that injection of the TNCEGFmyc mRNA or the EGF-L protein fragment does not influence general development of the embryos and that perturbation of TN-C function does not affect the outgrowth of the lateral line nerve.

It is possible that cells in the pathway of the ventral motor axons that are important for axon pathway choices were affected by the overexpression of TNCEGFmyc mRNA or injection of the EGF-L fragment and the effect on axon growth is an indirect one. At the level of the

horizontal myoseptum, a critical choice point for growing motor axons, the so-called muscle pioneers, are located. We specifically labeled muscle pioneers with an antibody to the engrailed protein (Melancon et al., 1997) and found no differences between uninjected (Fig. 22C; n= 5) and TNCEGFmyc mRNA injected embryos (Fig. 22D; n=6). We also could find no differences between embryos injected with the EGF-L protein fragment (n=6) and uninjected embryos (n=7) labeled with the engrailed antibody (not shown).

We also analyzed the integrity of trunk segments by immunolabeling of chondroitin sulfates in uninjected embryos and those injected with the TNCEGFmyc mRNA. In uninjected embryos (n=6), chondroitin sulfate immunoreactivity is concentrated in vertical myosepta and around the notochord, which is in agreement with previous studies (Bernhardt et al., 1998; Bernhardt and Schachner, 2000). In TNCEGFmyc mRNA injected embryos (n=7) this pattern of chondroitin sulfate immunoreactivity was unchanged (not shown). The distribution of chondroitin sulfate immunoreactivity was also unchanged in embryos injected with the EGF-L fragment (n=6) and uninjected embryos (n=5, not shown). These findings suggest that the pathway of ventral motor axons was not altered by perturbation of TN-C function.

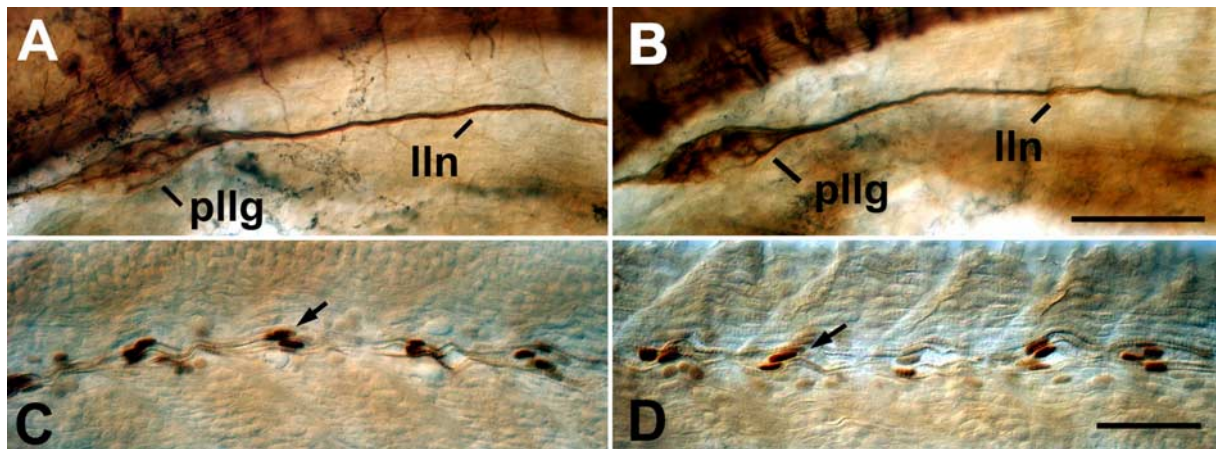


Fig.22. Trunk structures and other axon tracts are normal in TNCEGFmyc mRNA injected embryos at 24 hpf. **A,B:** A lateral view of the anterior trunk region of the zebrafish labeled with an anti-tubulin antibody is shown. The ganglion of the posterior lateral line (pll) as well as the lateral line nerve (lln) in an embryo injected with TNCEGFmyc (B) appear normal compared to an uninjected embryo (A). **C,D:** Muscle pioneer cells at the horizontal myoseptum of the trunk (arrows in C,D), visualized by immunohistochemistry for the engrailed protein, appear normal in uninjected (C) and TNCEGFmyc-mRNA-injected embryos (D). Scale bar in B = 75 μ m for A and B, in D = 50 μ m for C and D.

4.3.6 TN-C is required for motor axon pathfinding in the developing zebrafish

To further clarify whether TN-C is required in the developing zebrafish for correct ventral motor axon pathfinding, we injected one-to-two-cell-stage embryos with antisense morpholino oligonucleotides (MO), which when targeted to the startcodon of the mRNA act as an inhibitor of translation (Nasevicius and Ekker, 2000). Injection of a control morpholino with a random sequence did not influence the expression of TN-C in the trunk of 24 hpf old embryo as revealed by immunohistochemistry (n=8; Fig. 23A). A morpholino directed against TN-C strongly reduces the levels of TN-C immunoreactivity in the trunk of 24 hpf old animal (n=7, Fig.23B). TN-C immunoreactivity could not be detected in the pathway of ventral motor axons but some residual TN-C immunoreactivity was still detectable at the segment borders in the trunk of a 24 hpf old embryo (Fig. 23B). The reduction of TN-C immunoreactivity could be confirmed with both TN-C antibodies mentioned above, thereby demonstrating their specificity. The injected embryos were labeled with a tubulin antibody to visualize axon tracts and analyzed at 24-27 hpf and 33 hpf. In 24-27 hpf old embryos injected with the control MO (n=19) 3.7 % (23/608) of the nerves analyzed were abnormal, and in those injected with the TN-C MO (n=40) 2.6 % (33/1280) of the nerves showed abnormalities (not shown). This difference was not statistically different and numbers of affected nerves of both treatments were in the range of uninjected embryos which revealed 2.7% (40/1280) abnormal nerves (n=40; table 4).

At 33 hpf, when secondary motor axons had grown into the ventral motor axon pathway, we also analyzed growth of motor nerves after injection of a control MO compared to a MO specific for TN-C. In uninjected embryos (Fig. 23C; table 4) 1.1 % (11/1008) of the analyzed nerves were abnormal and in those injected with the control MO (Fig. 23D; table 4) 1.2 % (14/1152) of the analyzed nerves showed abnormalities. Embryos injected with the TN-C MO (Fig. 23E, F) showed abnormal branches of the ventral motor axons. In embryos injected with the TNC MO, a 5-fold increase of abnormal nerves to 5.9 % (75/1260) which was statistically significant compared to embryos injected with the control MO (Fig. 22 G; Mann-Whitney U-test, $p < 0.0001$; table 4) was observed. Analysis of embryos injected with the TNC-MO revealed high numbers of abnormal branches of the motor nerves (5.5% of all nerves analyzed, table 4) and only a small amount of truncated nerves was observed (0.4% of all nerves analyzed).

In embryos injected with the TNC MO, aberrant caudal branching was most frequent 80% (60 of 75 abnormal nerves), followed by rostral branching 9% (7/75), truncations 7% (5/75) and bilateral branching 4% (3/75; Table 5).

Thus, although levels of TN-C immunoreactivity in 24 hpf old embryos were reduced after injection of the TNC MO we could not observe an effect of the outgrowth of primary motor axons in the trunk. At 33 hpf, when secondary axons had joined the pathway of primary motor axons, we observed an increase in the number of aberrant branches. Reducing the level of TN-C immunoreactivity leads to abnormal branching whereas overexpression of TN-C mainly resulted in truncations.

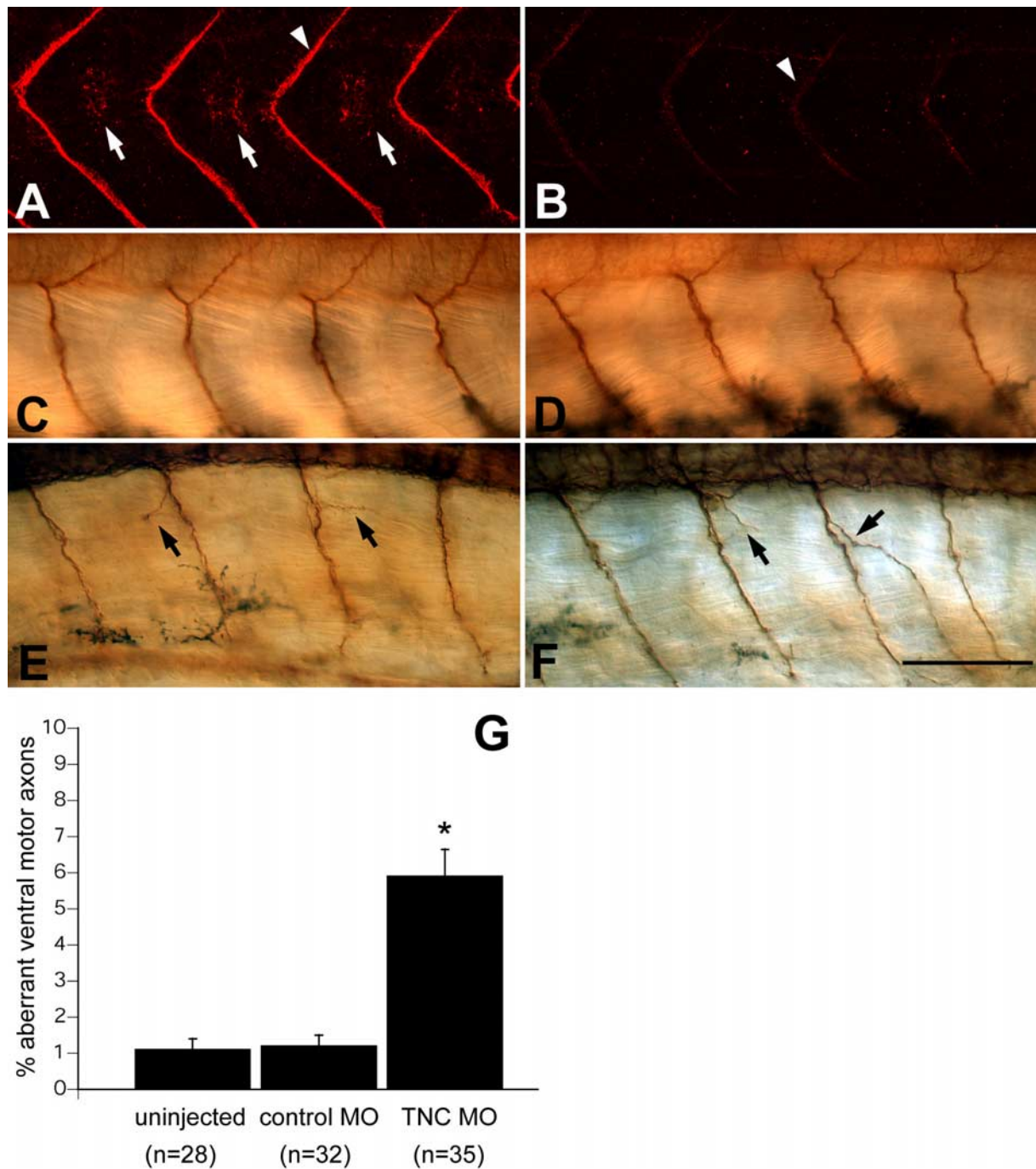


Fig.23. Injection of a morpholino (MO) specific for TN-C reduces TN-C immunoreactivity and induces branching errors of ventral motor axons. Lateral views of whole mounted zebrafish embryos are shown at mid-trunk levels. Rostral is to the left and dorsal is up. **A:** At 24 hpf, injection of control morpholino does not influence TN-C expression in the zebrafish as revealed by immunohistochemistry using the polyclonal antibody

against chicken TN-C (arrows indicate TN-C immunoreactivity at the horizontal myoseptum, the arrowhead points to TN-C immunoreactivity at the vertical myosepta). **B**: Injection of a MO specific for TN-C reduces levels of TN-C immunoreactivity in the zebrafish. Residual TN-C immunoreactivity is detectable at the vertical myosepta (arrowhead). **C,D**: In wild type (C) or control MO injected embryos (D) ventral motor nerves grow straight and unbranched at 33 hpf. **E,F**: Injection of a MO specific for TN-C leads to aberrant branches of the ventral motor nerves at 33 hpf (arrows in E and G). **G**: At 33 hpf, 5.9% of all ventral motor nerves analyzed per embryo injected with the morpholino specific for TN-C (TNC MO) are abnormal, which is statistically highly significantly (asterisk, $p < 0.0001$) different from control embryos injected with the control morpholino (control MO) and uninjected embryos. The value for uninjected control embryos (uninjected) is also indicated. Scale bar in F = 50 μ m for A-F.

Table 4. Frequency of abnormal motor nerves after injection of TNC MO analyzed at 24-27 hpf and at 33 hpf.

	# of analyzed embryos	Nerves scored (total)	total # of abnormal nerves	Severe truncation	Abnormally branched nerves	Mean # of abnormal nerves per embryo
24-27 hpf						
TNC MO 8-16 ng/nl	40	1280	33 (2.6%)	3 (0.2%)	30 (2.4%)	1.2 ± 0.41
Control MO 8-16 ng/nl	19	608	23 (3.7%)	0	23 (3.7%)	0.9 ± 0.18
uninjected*	40	1280	37 (2.9%)	3 (0.2%)	34 (2.7%)	0.9 ± 0.22
TNC MO 16 ng/nl	35	1260	75 (5.9%) §	5 (0.4%)	70 (5.5%)	2.2 ± 0.27
Control MO 16 ng/nl	32	1152	14 (1.2%)	2 (0.2%)	12 (1%)	0.4 ± 0.11
uninjected	28	1008	11 (1.1%)	0	11 (1.1%)	0.4 ± 0.12

* Uninjected embryos are taken from Table 2

§ Significant different to control embryos

Table 5. Relative frequencies of different types of aberrations after perturbation of TN-C function injecting different reagents.

	Severe truncation	Rostral branches	Caudal branches	Bilateral branches	Abnormal nerves
EGF-L 24 hpf	30 (59%)	3 (6%)	7 (14%)	11 (21%)	51
TNCEGF mRNA 24hpf	50 (36%)	7 (5%)	57 (42%)	25 (18%)	137
TNC MO 16 ng/nl 33hpf	5 (7%)	7 (9%)	60 (81%)	3 (4%)	75

4.3.7 TN-C immunoreactivity is absent from the horizontal myoseptum of *unplugged* mutants

We analyzed the distribution of TN-C immunoreactivity in the *unplugged* mutant (Granato et al., 1996) because the described phenotypes of this mutant (Zhang and Granato, 2000; Zhang et al., 2001a) resembled the phenotypes observed after perturbation of TN-C functions. Furthermore, genetic mosaic analysis has shown that *unplugged* activity is not required in the motor axons themselves, but instead in a population of adaxial cells, which might deposit guidance cues into the ECM (Devoto et al., 1996; Zhang and Granato, 2000). We also analyzed TN-C immunoreactivity in the *stumpy* mutant (Beattie et al., 2000). In this mutant, CaP axons remained stopped at the horizontal myoseptum. We performed double immunohistochemistry on 22 hpf old embryos using the HNK-1 antibody to label axon tracts and thereby identify the mutant phenotype in combination with an antibody recognizing TN-C using confocal microscopy. All embryos were analyzed using the same intensity settings of the microscope. Confocal image stacks through the trunk of *unplugged* non-homozygous clutch mates (n=11), identified by Cap axons growing unbranched beyond the horizontal myoseptum towards their ventral target areas (Fig. 24A), showed TN-C immunoreactivity at the segment borders and at the horizontal myoseptum around the axons (Fig. 24B, C) indistinguishable from wildtype control embryos. In *unplugged* mutants (n=5), identified by aberrant branches of motor axons at the horizontal myoseptum (Fig. 24D, G), TN-C immunoreactivity was not detectable around the axons at the level of the horizontal myoseptum (Fig. 24E, F, H and I). Segment borders showed lower levels of TN-C immunoreactivity (Fig. 24E, H) than non-homozygous clutch mates (Fig 24B). In *stumpy*

mutants (n=7), TN-C immunoreactivity was shown to be located around the stalled axons at the level of the horizontal myoseptum and in the vertical myosepta (Fig. 24J-L). The same pattern of TN-C protein distribution was observed in the corresponding wild types (n=4, not shown). Thus TN-C deficiency at the horizontal myoseptum in the trunk of *unplugged* but not *stumpy* mutants might contribute to the aberrant outgrowth of motor axons.

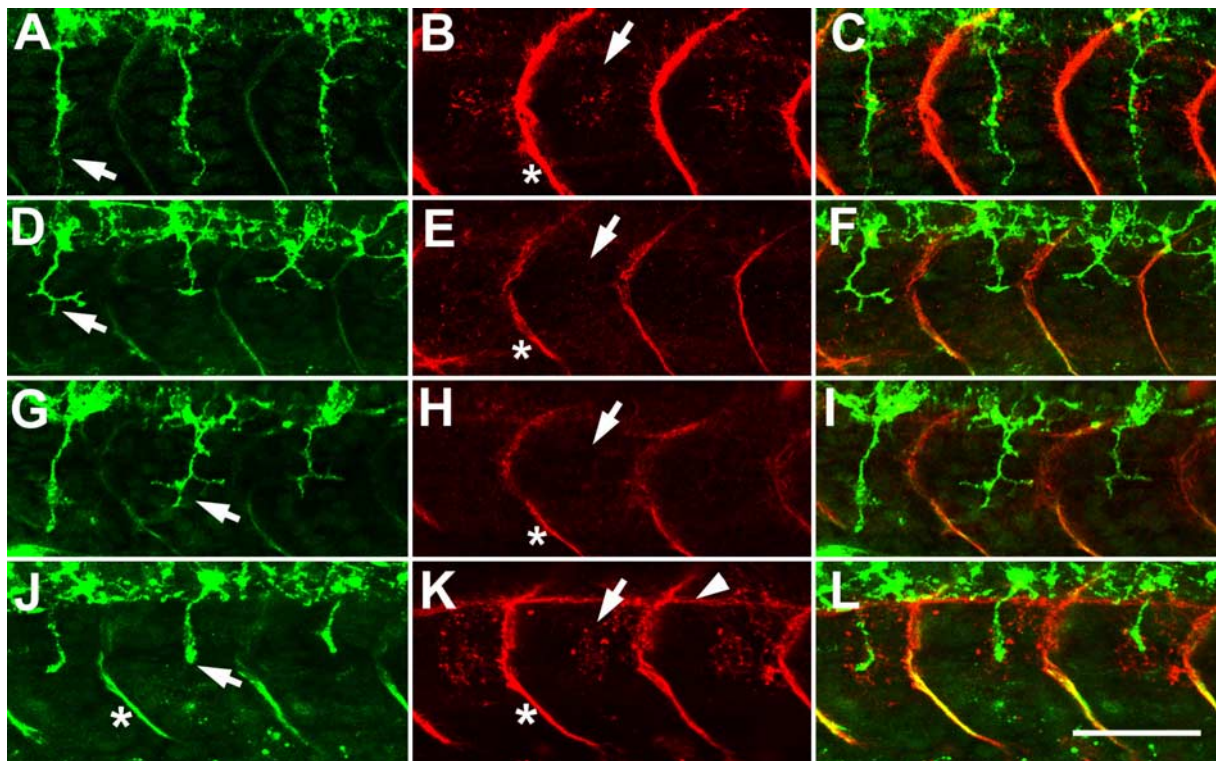


Fig.24. TN-C immunoreactivity is absent at the horizontal myoseptum in zebrafish *unplugged* mutants but not in *stumpy* mutants. Lateral views of confocal image stacks of whole mounted zebrafish embryos are shown at mid-trunk levels. Rostral is to the left and dorsal is up. Axons in the developing zebrafish are labeled in green. TN-C immunoreactivity is shown in red. **A-C:** A non-homozygous *unplugged* clutch mate identified by the unbranched appearance of ventral motor axons (arrow in A) at 22.5 hpf is shown. TN-C immunoreactivity in this embryo is present at the level of the horizontal myoseptum around the axons (arrow in B, see also C) and at the vertical myosepta (asterisk in B). **D-I:** 22.5 hpf old homozygous *unplugged* zebrafish mutants, identified by abnormal branches of motor axons (arrows in D and G) at the level of the horizontal myoseptum are shown. There is no detectable TN-C immunoreactivity at the level of the horizontal myoseptum around the axons in these embryos (arrows in E and H, see also F and I), although low levels of TN-C immunoreactivity were detected in the vertical myosepta (asterisks in E and H). **J-L:** A 22.5 hpf old *stumpy* mutant is shown. In this mutant, the motor axons stop their growth at the horizontal myoseptum (arrow in J). TN-C immunoreactivity is shown to be located at the horizontal myoseptum around the stalled axons (arrow in K, see also L) and at the vertical myosepta (asterisk in K). The notochord, which is positive for TN-C immunoreactivity in all preparations is included only in the confocal image stacks shown in J-K (arrowhead in K points to the dorsal edge of the notochord). Scale bar in L = 50 μ m for A-L.

4.3.8 TN-C mRNA is expressed by adaxial cells during outgrowth of ventral motor axons in the trunk

To analyze if TN-C mRNA is expressed by adaxial cells which have been shown to be responsible for the *unplugged* phenotype we performed whole mount situ hybridization using 24 hpf old embryos with a cRNA probe specific for TN-C combined with immunohistochemistry using the F59 antibody (Stockdale, 1992). This antibody has been shown to label adaxial cells in the zebrafish (Devoto et al., 1996). This cell type has not been addressed in previous localization studies of TN-C mRNA (Tongiorgi, 1999; Tongiorgi et al., 1995b). During later stages of development, the F59 antibody also labels deep cells of the myotome which have been shown to develop into fast muscle fibers (Devoto et al., 1996). We analyzed only 24 hpf old embryos taking advantage of the developmental rostro-caudal gradient of trunk differentiation. Segmentation starts at 10.5 hpf, additional somites are produced at intervals of 30 min. At 24 hpf, segmentation is complete, but somites in the most caudal part are the least mature ones. (Stickney et al., 2000). Cross sections through the caudal part of a 24 hpf embryo revealed TN-C mRNA expression in a single row of cells adjacent to the notochord (Fig. 25A). Double labeling with the F59 antibody (Fig. 25B) demonstrates that the row of cells expressing TN-C mRNA were F59 immunopositive adaxial cells (Fig. 25C). In more rostral parts of 24 hpf embryos, cross sections also revealed TN-C mRNA expressing cells around the notochord (Fig. 25D). The adaxial cells, which had migrated to more lateral positions of the trunk (Fig. 25E), were no longer positive for TN-C mRNA (Fig. 25F). A subset of adaxial cells, the muscle pioneer cells, remained apposed to the notochord generating an hourglass shape to the layer of superficial muscle cells (Fig. 25E). These cells were shown to express TN-C mRNA also in more differentiated somites (Fig. 25F). The other cells expressing TN-C mRNA adjacent to the notochord were also weakly labeled with the F59 antibody. These cells are not derived from adaxial cells instead belong to myotomal cells giving rise to fast muscle fibers (Devoto et al., 1996). TN-C mRNA in the trunk was also expressed by the notochord (Fig. 25A, D) and migrating neural crest cells (Fig. 25D) as previously described (Tongiorgi, 1999; Tongiorgi et al., 1995b). Hybridization with a sense probe for TN-C served as a control for specificity revealed no signals. Thus, adaxial cells, which are responsible for the *unplugged* but not *stumpy* phenotype, transiently express TN-C mRNA.

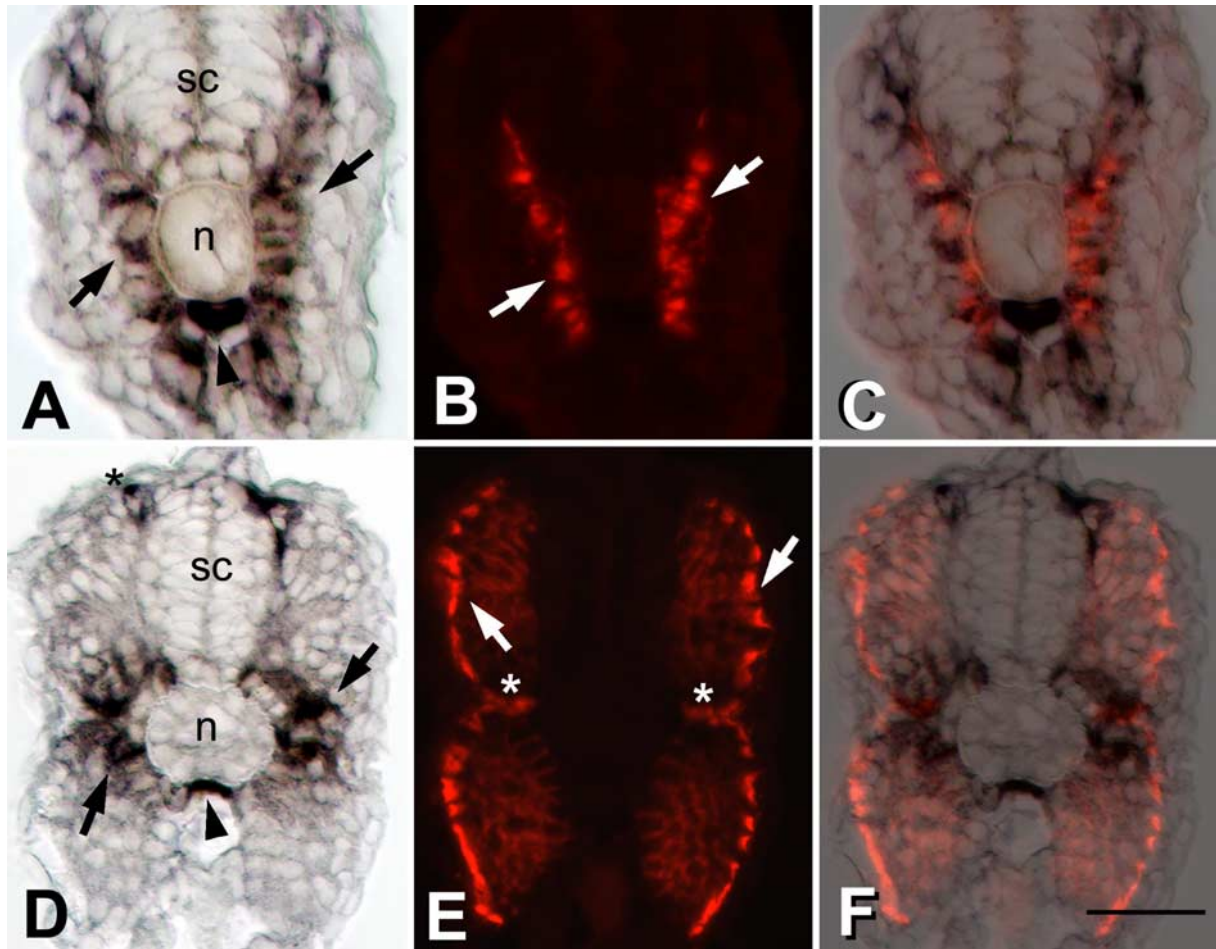


Fig.25. TN-C mRNA is expressed in adaxial cells in the trunk during development of the zebrafish. Cross-sections of a zebrafish embryo (24 hpf) are shown. Dorsal is up. **A-C:** Double labeling of TN-C mRNA (arrows in A) and immunofluorescence for adaxial cells (arrows in B) in a cross-section through the developmentally early, caudal part of the trunk of a 24-hpf-old embryo (see Results) reveals overlapping signals located in single dorso-ventral rows of cells directly left and right of the notochord (n) and spinal cord (sc) (C). **D-F:** Double labeling of TN-C mRNA (arrows in D) and immunofluorescence for adaxial cells (arrows in F) in a cross-section through more mature, rostral parts of the same embryo revealed no overlap of adaxial cells and TN-C mRNA, except for muscle putative muscle pioneer cells (asterisks in E). The arrowheads in A and B indicate high expression levels of TN-C mRNA expression in the hypochord. Migrating neural crest cells expressing TN-C mRNA are indicated by an asterisk in D. Scale bars in F = 25 μ m for A-F.

5. Discussion

Part 1

5.1 Expression of protein zero is increased in lesioned axon pathways in the central nervous system of adult zebrafish

5.1.2 Identification of a homolog of P0 in zebrafish.

The complete sequence of P0 in zebrafish is approximately 40% identical at the amino acid level to human, mouse, chicken and shark P0 and 76% to IP1, the trout homolog of P0. The zebrafish molecule is most similar to that of trout, which is also a teleost species. The similarities between zebrafish and shark P0 are not higher than between zebrafish P0 and P0 in amniotes. This is in agreement with phylogenetic analyses suggesting that cartilaginous fish (e.g. sharks) have separated from the line leading to ray-finned fish (e.g. teleostei) and tetrapods early during evolution (Venkatesh et al., 2001). The observed degrees of amino acid identities are in the expected range for related Ig superfamily molecules in phylogenetically distinct species. For example, the zebrafish L1-related molecules L1.1 and L1.2 share approximately 40% amino acid identity with human L1 (Tongiorgi et al., 1995a). Similar results are obtained for the chicken DM-GRASP and its homolog in fish (39% amino acid identity; Kanki et al., 1994). Furthermore, the structure of zebrafish P0, with a single Ig-like domain, followed by a transmembrane region and a short cytoplasmic region, is identical to that of other P0 molecules. Finally, expression of zebrafish P0 in glial cells of the CNS and PNS (see below) appears to be typical of fish, since P0 homologs in trout (Stratmann and Jeserich, 1995) and shark (Yoshida and Colman, 1996) are also expressed in both of these structures. The amino acid sequence of the molecule we cloned differs in 2 interstitial amino acids and at the C-terminus from the sequence published by Brösamle and Halpern (2002). The C-terminus of their sequence is three amino acids longer than the one we describe here and the terminal two amino acids of our sequence do not align with that of Brösamle and Halpern (2002). These differences may be due to the different EST clones being used in the two studies. To confirm that our sequence represents zebrafish P0, we amplified the entire ORF of the molecule from zebrafish brain cDNA using PCR. Furthermore, the 3' end of the molecule was confirmed by RACE (see Materials and Methods). Thus our sequence was at least three times independently verified.

5.1.3 P0 mRNA is probably expressed by oligodendrocytes during CNS development.

The developmental sequence of appearance of P0 mRNA expressing cells in the CNS coincides with myelination. From studies in trout, myelination in fish is expected to start in the hindbrain (Jeserich et al., 1990). In the optic system, myelination begins in the chiasm (Jeserich and Jacque, 1985). In the hindbrain of zebrafish, the first loose myelin sheaths are detected by electron microscopy in 4-day-old fish and compact myelin by 7 days (Brösamle and Halpern, 2002). Our own immunohistochemical labeling of myelin at 6 days of development using the O1 and O4 antibodies, shown to cross react with fish myelin in tissue sections (Gould et al., 1995), confirm the onset of myelination in the hindbrain of zebrafish. Similar sequences of CNS myelination have also been described for other vertebrates (Bartsch et al., 1994; Woodruff et al., 2001). The appearance of P0 mRNA expressing cells follows this scheme of CNS myelination. We first detected P0 mRNA expressing cells in the hindbrain in 3 days-old larvae and in the optic pathway in 5-day-old larvae in tissue sections. In whole mount preparations, Brösamle and Halpern (2002) found the onset of P0 expression in the same areas, but in both structures one day earlier than in this study. Since the first P0 mRNA expressing cells are very few in number, they might have been lost inadvertently during sectioning of early larvae. In the adult CNS, P0 mRNA expressing cells are accumulated in locations that are heavily myelinated, such as the medulla, and in myelinated tracts, such as the lateral longitudinal fascicle. P0 mRNA positive cells are also present in the optic nerve which is devoid of neuronal cell bodies, indicating glial expression of P0 mRNA. While there are immunohistochemical markers for myelin, such as O1 and O4, there were no markers labeling the somata of fish oligodendrocytes available to us. Nevertheless, we were mostly able to exclude P0 mRNA expression by the other major glial cell types in the adult CNS. Double labeling with an antibody to GFAP revealed that in most brain regions virtually all astrocytes are of the radial type with their somata at the ventricles, which is typical of fish astrocytes (Kalman, 1998; Tomizawa et al., 2000). There was essentially no overlap of GFAP labeled astrocyte somata with P0 mRNA expression at the ventricles. Likewise, a microglial cell/macrophage marker did not show double labeling with P0 mRNA following optic nerve lesion. However, expression of P0 mRNA in astrocytes in the optic nerve, which do not express GFAP (Nona et al., 1989), cannot be excluded. Since single P0 mRNA expressing cells were also present in cell dense regions of the brain, P0 expression in a small subset of neurons can also not be excluded.

5.1.4 P0 mRNA is expressed in the PNS of zebrafish

In agreement with an *in situ* hybridization study in trout (Stratmann and Jeserich, 1995), we found P0 mRNA in the PNS of zebrafish. In sections of adult cranial nerves, the message was clearly detectable. It is noteworthy that during development no PNS-related signal was detected in 1 to 5-day-old zebrafish outside the CNS and in 4-week-old animals only the posterior lateral line nerve contained detectable levels of P0 mRNA. Compact myelin in the PNS of developing zebrafish is first observed at 7 days of development (Brösamle and Halpern, 2002), which is in agreement with the absence of P0 mRNA from the PNS of 5-day-old animals. However, we were unable to detect P0 mRNA in other peripheral nerves than the posterior lateral line nerve in 4-week-old animals, when myelination of the PNS is expected to be well developed. Brösamle and Halpern (2002) did not detect P0 mRNA expression in any peripheral nerves of zebrafish up to 10 days of development. Although only quantification of P0 protein levels could allow inferences as to the functional importance of P0 in the PNS, the present data suggest that P0 is less prominent in PNS than in CNS myelination. Myelination in the PNS could be accomplished by another possible P0 homolog that may have arisen by gene duplication in zebrafish (Amores et al., 1998). However, our search of EST databases for additional P0 homologs has so far only yielded a putative homolog of the epithelial V-like antigen (EVA; Guttinger et al., 1998). Although structurally similar to P0, this gene shares only 17% amino acid identity with human P0, but 31% with human EVA. Moreover, the gene is not expressed in the nervous system, but in fin and intestinal epithelia (own unpublished observations; Genbank Accession No. AJ491253).

5.1.5 Zebrafish P0 may have functions in axon regeneration

We observed increased expression of P0 mRNA within 2 days after an optic nerve lesion in adult animals. Since axons do not show significant regrowth before 1 week post-lesion (Becker et al., 2000a; Bernhardt, 1989), the newly synthesized protein is probably exposed on the cell surface before axons regrow, such that regrowing axons likely encounter P0. Studies on P0 in mammals indicate growth-promoting properties of the molecule for postnatal dorsal root ganglion neurites (Schneider-Schaulies et al., 1990) and embryonic cortical neurites *in vitro*, as well as for adult spinal axons after implantation of P0 expressing cells *in vivo* (Yazaki et al., 1994). If zebrafish P0 has similar functions, its increased expression after a lesion of the CNS may enhance regeneration. Glial cells, probably oligodendrocytes in the

optic nerve of zebrafish also upregulate mRNAs for the L1-related molecules L1.1 and L1.2, as well as for NCAM and beta3 (Bernhardt et al., 1996). Goldfish oligodendrocyte-like cells upregulate the expression of the L1-related E587 molecule (Ankerhold et al., 1998). All of these molecules belong to the Ig-superfamily of recognition molecules, with the exception of beta3, which is a subunit of the Na,K-ATPase (Bernhardt et al., 1996). Mammalian homologs of these molecules exhibit axon growth-promoting properties (Appel et al., 1995; Haspel et al., 2000; Müller-Husmann et al., 1993; Saffell et al., 1995). Thus, fish oligodendrocytes may not only be permissive to axon growth by expressing reduced levels of growth inhibitors (Sivron et al., 1994; Wanner et al., 1995), but may actively promote regeneration by expression or even enhanced expression of conducive molecules. This idea is supported by the observation that growth of goldfish optic axons on goldfish oligodendrocyte-like cells can be perturbed by antibodies to the L1-related E587 molecule *in vitro* (Ankerhold et al., 1998).

5.1.6 The initial upregulation, but not the late peak of P0 mRNA expression after an optic nerve lesion is independent of the presence of regenerating axons

Upregulation is initiated rapidly and simultaneously throughout the optic system at 2 days post-lesion, thus in the absence of contact with viable axons. Moreover, enucleation, instead of optic nerve crush did not alter the increased expression of P0 mRNA for up to 11 days post-lesion. Therefore, axons are not needed to induce increased expression of P0 mRNA. However, the strongest upregulation of P0 mRNA was observed between 4 and 8 weeks after lesion of the optic nerve, which was confirmed by a significantly increased density of P0 mRNA positive cell profiles at these post-lesion intervals. This late increase was not observed in enucleated animals. In fact, labeling intensity of P0 mRNA was declining again at 28 days after enucleation. Thus suggests that the presence of regenerating axons is not necessary to induce an increase in P0 mRNA expression in glial cells after a lesion, but that axons are necessary for the further increase at later time points. These observations are in marked contrast to the regenerating PNS of mammals. Here, basal levels of P0 mRNA expression are reduced after a crush and expression is upregulated in a “wave” beginning at the lesion site (Mitchell et al., 1990) only when cells are in contact with regrowing axons (Gillen et al., 1995; Gupta et al., 1988; LeBlanc and Poduslo, 1990). Removal of axons after initial regeneration induces a second decrease in expression of P0 mRNA, indicating that prolonged contact with axons is necessary to sustain expression of P0 in the PNS of mammals (Gupta et

al., 1993). Underlying these reactions of peripheral nerves are probably myelinating Schwann cells, which initially strongly reduce their high P0 mRNA expression levels in unlesioned nerves to low levels upon a lesion. In contrast, non-myelinating Schwann cells, which normally do not express detectable levels of P0 mRNA, show an increase to low levels of expression after a lesion (Lee et al., 1997). The regulation of P0 mRNA in glial cells of the CNS of zebrafish appears to be different from both these regulation patterns in mammalian Schwann cells, since readily detectable levels of mRNA in unlesioned tracts are strongly increased after a lesion of the optic nerve in zebrafish.

5.1.7 The peak of P0 mRNA expression after optic nerve lesion correlates with remyelination

The relatively late peak in P0 mRNA expression at 4 to 8 weeks post-lesion may be related to remyelination of regenerated axons. This is suggested by studies from goldfish, in which remyelination of the optic nerve has been reported to commence by 3 to 6 weeks post-lesion (Ankerhold and Stuermer, 1999). The observation that expression of P0 mRNA was still elevated at 4 and 6 months post-lesion is also consistent with a role of P0 in remyelination, which proceeds slowly in the goldfish tectum and is still not complete at 5 months post-lesion (Murray, 1976). The absence of the late peak of P0 mRNA expression after enucleation, which prevents remyelination due to a lack of axons, strongly supports the conclusion that the late peak of P0 mRNA expression is related to remyelination.

The significantly increased counts of P0 mRNA positive cell profiles 1 and 2 months post-lesion may be due to detectably increased P0 mRNA expression levels in a constant number of cells, or due to a true increase in the number of cells expressing the message. Proliferation of oligodendrocytes in the lesioned optic nerve of goldfish is low (Ankerhold and Stuermer, 1999), favoring the idea that resident cells show a further increase in expression of P0 mRNA at these late post-lesion intervals. Invasion of Schwann cells from the lesion site, which has been reported for the optic pathway of goldfish (Nona et al., 1994; Nona et al., 2000), is probably not the cause for the rapid initial upregulation of P0 mRNA, because this happens simultaneously throughout the optic pathway, even in locations that are remote from the lesion site, such as the tectum. However, a contribution of Schwann cells to increased numbers of P0 mRNA positive cell profiles at later post-lesion intervals cannot be excluded, even though basal expression of P0 mRNA may be generally lower in Schwann cells than in oligodendrocytes in zebrafish (see above).

5.1.8 There are similarities and differences in the regulation of glial recognition molecules between the lesioned optic nerve and spinal cord

In the spinal cord, glial cells located primarily in the peripheral white matter are also more intensely labeled and numbers of cell profiles are increased following a lesion, showing that spinal and optic pathway glia are similar with respect to regulation of P0 mRNA. The only difference is that a significant increase in P0 mRNA containing cells was observed already at 2 weeks post-lesion in the spinal cord, whereas in the optic nerve it was observed only at 4 weeks post-lesion. The time course of axon regrowth and remyelination in the spinal cord of zebrafish is not known in sufficient detail (Becker et al., 1997), such that this difference cannot easily be explained at present. While putative oligodendrocytes in the spinal cord are similar to those in the optic nerve with regard to the upregulation of P0 and L1.2 mRNA (Becker et al., 1998; Bernhardt et al., 1996), there are also differences between these cell types. In the lesioned optic nerve, there is also an upregulation of L1.1 and NCAM mRNA (Bernhardt et al., 1996), which has not been observed in the lesioned spinal cord (Becker et al., 1998). Interestingly, in the spinal cord the majority of supraspinal descending axons regenerate through the gray matter rather than through the white matter (Becker and Becker, 2001). This suggests that a possibly lower expression level of growth-promoting molecules in the white matter of the spinal cord, compared to the optic nerve, may not be sufficient to fully overcome possible growth-inhibiting molecules in the spinal white matter.

5.1.9 Early expression of P0 mRNA in rhombomeres is not related to myelination

At the early stage of development when P0 mRNA was detected in rhombomeres (16- 18 hpf) the first axons are just beginning to grow out (Metcalf et al., 1990; Ross et al., 1992; Wilson et al., 1990), such that myelin cannot be present. This expression pattern has not previously been reported in the study of P0 mRNA expression in developing zebrafish by Brösamle and Halpern (2002). Non-myelin related expression of P0 has also been described for example in a subset of neural crest cells in chicks and rats (Bhattacharyya et al., 1991) and in the otic vesicle, notochord, enteric nervous system and olfactory ensheathing cells of developing rat (Lee et al., 2001), but never before in rhombomeres. We observed P0 mRNA expression transiently in all cells of some, but not all rhombomeres. Expression is then down-regulated and gives way to an upregulation in a cell-type specific manner discussed above. Given that P0 mRNA expression is detectable in alternating rhombomeres and that P0 is a homophilic

adhesion molecule (D'Urso et al., 1990; Filbin et al., 1990; Griffith et al., 1992; Schneider-Schaulies et al., 1990; Shapiro et al., 1996), it is conceivable that P0 may sustain the integrity of individual rhombomeres. Transient expression in all cells of particular rhombomeres and/or discrete more anterior CNS domains is typical also for other recognition molecules, e.g. tenascin-C (Tongiorgi et al., 1995b), beta3 (Appel et al., 1996), semaphorin 3Ab (Roos et al., 1999) or ephrins (Cooke and Moens, 2002).

Part two

5.2 Evidence for a role of tenascin-R as a repellent guidance molecule for regenerating optic axons in adult fish

Previously results have shown that tenascin-R is inhibitory for regenerating optic axons of mice (Becker et al., 2000b) and salamanders (Becker et al., 1999) *in vitro* and that the disappearance of tenascin-R immunoreactivity from the optic nerve of salamanders, but not of mice, correlates with axonal regeneration in salamanders. Here tenascin-R function in fish was analyzed and two fundamental differences to mice and salamanders were found. Both differences may be related to the unique growth of the optic projection in adult fish (Marcus et al., 1999; Meyer, 1978). (1) A homogeneous tenascin-R substrate promotes growth of fish optic axons while it inhibits it in both mice and salamanders. This may be related to the fact that in fish, but not in tetrapods, newly generated axons need to grow through the tenascin-R positive retina. (2) In zebrafish and goldfish, tenascin-R immunoreactivity in the optic nerve and tract is low both in the unlesioned and lesioned situation. This creates a probably instructive border-like distribution of tenascin-R in the brain of fish that may be recognized by continuously growing optic axons in unlesioned animals as well as by regenerating axons after a lesion. Thus the optic projection in adult fish, but not in salamanders, may be “preadapted” to regeneration due to its continued growth.

5.2.1 Tenascin-R is expressed in the CNS of adult fish

We cloned tenascin-R in zebrafish. The gene shares the identical domain structure and a 60% amino acid identity with human tenascin-R, which is well in the range of other recognition molecule orthologs in zebrafish (e.g. Tongiorgi et al., 1995a; Tongiorgi et al., 1995b; Yeo et al., 2001). Its expression in the adult brain is confirmed here by Northern and Western blot analyses. The presence of tenascin-R in the regeneration competent CNS of adult fish is remarkable, given the evidence that tenascin-R is a potential inhibitor of axonal regeneration in the optic nerve (Becker et al., 2000b), in the dorsal root entry zone (Zhang et al., 2001b) as well as in the olivocerebellar system (Wintergerst et al., 1997) in mammals. Chondroitin sulfates (CSs) of the extracellular matrix, which are inhibitors of axon regeneration in the glial lesion scar of mammals (Moon et al., 2001), are not expressed in a CNS lesion site in zebrafish (Becker and Becker, 2002). Nogo-1 (Chen et al., 2000; GrandPre et al., 2000; Prinjha et al., 2000), another inhibitor of axonal regeneration, may not be expressed in

significant amounts in the CNS of fish (Sivron et al., 1994; Wanner et al., 1995). Tenascin-C (Laywell et al., 1992) may not be present in the optic pathway of fish (but see Battisti et al., 1995; this study and Bernhardt et al., 1996). The unique tissue distribution and reactions of regenerating optic axons to tenascin-R in fish indicate that tenascin-R may actually facilitate growth of optic axons in fish rather than inhibiting it.

5.2.2 The axonal reactions to tenascin-R in fish depend on the way the molecule is encountered

Tenascin-R functions both as a repellent guidance molecule for zebrafish and goldfish optic axons and as a growth-promoting molecule for goldfish optic axons *in vitro*. This is possible because the axonal reaction to tenascin-R critically depends on the way the molecule is presented to growing neurites and on the neuronal cell type analyzed (Schachner et al., 1994). Precedence for the behavior of fish optic axons is given by chick dorsal root neurites, which are promoted on a homogeneous tenascin-R substrate and repelled at a substrate border (Taylor et al., 1993). Dependency of the axonal reactions on the neuronal cell type analyzed and the way the molecules are encountered (soluble, as a homogeneous substrate or as a substrate border) has also been reported for the ECM constituents tenascin-C (Faissner and Kruse, 1990; Lochter and Schachner, 1993a; Lochter et al., 1991; Taylor et al., 1993; Wehrle-Haller and Chiquet, 1993) and CS proteoglycans (Snow et al., 1996; Verna et al., 1989).

5.2.3 The distribution of tenascin-R in the optic pathway in the brain suggests a boundary function of the molecule for regenerating axons

There was no increased immunoreactivity at the crush site in the optic nerve and immunoreactivity in the pathway distal to the lesion was always restricted to putative nodes of Ranvier. However, intense tenascin-R immunoreactivity bordering the optic pathway may restrict axons to their pathway. This is consistent with the *in vitro* border function of tenascin-R for regenerating adult optic axons of fish.

In the pretectum, tenascin-R could act in concert with CSs and semaphorins in repelling axons from the borders of non-retinorecipient nuclei (Fig. 10). We have previously shown that removal of CSs from the accessory pretectal nucleus and the magnocellular superficial/posterior pretectal nucleus increases growth of regenerating optic fibers into the magnocellular superficial/posterior pretectal nucleus, but surprisingly not into the accessory pretectal nucleus (Becker and Becker, 2002). It is therefore noteworthy that both nuclei are

tenascin-R immunopositive, with the accessory pretectal nucleus showing much higher levels of immunoreactivity than the posterior pretectal nucleus. This may explain why a number of fibers could invade the magnocellular superficial/posterior pretectal nucleus, but not the accessory pretectal nucleus after removal of CSs *in vivo*. Additionally, tenascin-R immunoreactivity forms a boundary towards optic fibers in the lateral part of the dorsal accessory optic nucleus. Two axon repellent semaphorins are also strongly expressed in the large neurons at the medial border of the magnocellular superficial/posterior pretectal nucleus (Becker and Becker, 2002), suggesting a complex interplay of repellent guidance molecules in the pretectum.

In the adult tectum, tenascin-R always borders layers that receive optic fibers and the molecule could therefore repel regenerating optic axons from inappropriate layers (Becker et al., 2000a). Similarly, the optic neuropil of the tectum is selectively immunonegative in developing zebrafish (5-day and 4-week-old animals; this report), mice (Becker et al., 2000b), and salamanders (Becker et al., 1999), such that a border is created between the optic neuropil and deeper tenascin-R positive fiber layers. Tenascin-C, which has similar *in vitro* functions as tenascin-R, is also expressed as a border for optic axons towards non-retinorecipient layers in the tectum of amphibian species (Becker et al., 1995). In chicks a similar pattern of tenascin-C immunoreactivity has been suggested (Yamagata et al., 1995), but this is controversial (Bartsch et al., 1995; Perez and Halfter, 1993). Thus, tenascin-R and tenascin-C may have partially overlapping functions.

5.2.4 Tenascin-R may have a dual function for newly growing optic axons

The growth of newly generated axons from the retinal periphery, where new retinal ganglion cells are added in adult fish (Marcus et al., 1999), to the center of the retina where axons exit the retina may be promoted by the intraretinal deposition of tenascin-R in the optic fiber layer. This is suggested by the *in vitro* observation that a homogeneous substrate of tenascin-R promotes growth of adult optic axons. Moreover, substrate coated tenascin-R appeared to promote fasciculation in this assay, while soluble tenascin-R defasciculates cerebellar neurites of mammals (Xiao et al., 1998). An influence of tenascin-R on fasciculation may also be relevant for the *in vivo* situation, since fasciculation with preexisting axon bundles is critical for intraretinal pathfinding of optic axons in fish (Stuermer and Bastmeyer, 2000).

In the optic nerve head, tenascin-R immunoreactivity tapers off towards the optic nerve. This creates a downhill gradient for optic axons, but it is unlikely that this distribution pattern

contains guidance information. Developing optic axons of chicks react to an uphill gradient of repellent activities in membrane preparations of the caudal tectum, but ignore a downhill gradient (Baier and Bonhoeffer, 1992).

Since optic axons encounter tenascin-R from the optic nerve head on in a border-like fashion, the molecule could guide newly growing axons by a repellent mechanism in their path through the brain, as discussed for regenerating axons. The *in vitro* experiments indicate that the different way of confronting tenascin-R in the distal optic pathway may be sufficient to induce a repellent reaction in growing axons. However, it is also possible that optic axons switch their response and thus their signal transduction pathways due to contact with localized cues on their way, e.g. netrin-1 in the optic nerve head (Hopker et al., 1999).

No difference in the axonal reactions to tenascin-R has previously been found between developing and adult optic axons of mice *in vitro* (Becker et al., 2000b), such that *in vitro* behaviors of adult fish axons may also pertain to larval development, during which the expression pattern of tenascin-R resembles the adult situation. A notable exception is that in 5-day-old zebrafish, two days after the first retinal ganglion cell axons have reached their targets (Stuermer, 1988), the retinal optic fiber layer is still immunonegative for tenascin-R. This suggests that for the relatively short intraretinal distances axons grow during early development tenascin-R is not needed.

Part three

5.3 Tenascin-C is involved in outgrowth of motor axons in the trunk of zebrafish

Ventral motor nerves of zebrafish grow through an environment rich in ECM components in a straight line on a midsegmental path without forming side branches for at least 33 hours of development. We show here that TN-C immunoreactivity is located at the level of the horizontal myoseptum which is a critical choice point for outgrowing motor axons. Perturbation of TN-C functions using mRNA overexpression and protein injections of the EGF-like domains of TN-C induces truncations, whereas the injection of a morpholino specific for TN-C induces abnormal branching and pathfinding errors of ventral motor nerves in developing zebrafish embryos suggesting an important function of TN-C for motor axon outgrowth.

5.3.1 Identification of a TN-C homolog in zebrafish

Two partial sequences of the zebrafish TN-C cDNA containing the FN-III-like domains 6-8 and the fibrinogen knob at the 3'-end have been described in previous studies (Qiao et al., 1995; Tongiorgi et al., 1995b). We have cloned the full length cDNA by PCR-based techniques. The complete sequence of TN-C in zebrafish is approximately 45% identical at the amino acid level to human, mouse and chicken TN-C. The observed degrees of amino acid identities are in the expected range for related molecules in phylogenetically distinct species. For example, the zebrafish TN-R shares approximately 60% amino acid identity with human TN-R (see 4.2.1). Similar results are obtained for the chicken DM-GRASP and its homolog in fish (39% amino acid identity, Kanki et al., 1994). Zebrafish TN-R and TN-C share approximately 35% amino acid identity. Furthermore, the structure of TN-C, with 14.5 EGF-like domains, followed by 8 FN-III-like domains and a fibrinogen knob, is identical to that of other TN-C molecules. Since approximately 30 % of the zebrafish genes are duplicated due to genome duplication events that involve large chromosome sections in ray finned fish (Postlethwait et al., 1999) the zebrafish genome often contains two copies of the mammalian orthologs. For example, the recognition molecules L1.1 and L1.2 (Tongiorgi et al., 1995a) which are the homologs of human L1. A second TN-C paralog in zebrafish may exist but has not been analyzed in this study. To confirm that our sequence represents zebrafish TN-C, all

amplified PCR products were sequenced twice. Finally, our obtained sequence data confirm the partial sequences obtained by Tongiorgi et al. (1995b) and Qiao et al. (1995).

5.3.2 TN-C immunoreactivity is concentrated at the level of the horizontal myoseptum in the pathway of outgrowing motor axons.

In this study, we analyzed the distribution of TN-C immunoreactivity during early trunk development in the zebrafish using confocal microscopy. We also analyzed the distribution of TN-C mRNA in the trunk by in situ hybridization. We show here for the first time that TN-C immunoreactivity is concentrated in the medial somite at the level of the horizontal myoseptum before, during and after motor axon growth through this region between 22 and 24 hpf. TN-C immunoreactivity at the horizontal myoseptum in the developing zebrafish was detected by an antibody directed against zebrafish TN-C (Tongiorgi, 1999) and also an antibody against chicken TN-C (Bartsch et al., 1995), which is known to cross-react with zebrafish TN-C (Bernhardt et al., 1998). Both antibodies are specific for the cloned TN-C, because labeling intensities of both antibodies are reduced after the injection of a TN-C MO. The distribution of TN-C immunoreactivity and mRNA during early development of the trunk in zebrafish has been described in previous studies (Tongiorgi, 1999, Bernhardt et al., 1998; Tongiorgi et al., 1995b). TN-C immunoreactivity in the trunk has been located to the posterior half of the somite, the notochord and the vertical myosepta (Bernhardt et al., 1998) at 16 hpf, which is in agreement with our findings. At 18-20 hpf, TN-C immunoreactivity is present in the posterior half of the somite at the level of the horizontal myoseptum (Bernhardt et al., 1998). At 24 hpf, TN-C immunoreactivity in the trunk has been shown in the vertical myosepta and around the notochord but not at the level of the horizontal myoseptum (Tongiorgi, 1999). Using confocal microscopy, which allows a detailed spatial resolution of whole mounted embryos, we detect TN-C immunoreactivity in the trunk of 22-24 hpf embryos around the notochord and in the vertical myosepta, which is in agreement with the previous studies. Surprisingly, we additionally detected TN-C immunoreactivity in the pathway of outgrowing motor axons at the level of the horizontal myoseptum. This TN-C immunoreactivity was shown to be specific, since TN-C levels at the horizontal myoseptum were reduced after injection of a TN-C MO. We have used the same antibodies which had been used in the previous studies. Therefore, the concentrated TN-C immunoreactivity at the medial surface in the pathway of outgrowing motor axons in 22-24 hpf embryos might have been overlooked using conventional microscopy.

To analyze the possible source of TN-C protein at the horizontal myoseptum, we analyzed TN-C mRNA expression by in situ hybridization. Here we show that TN-C mRNA is initially expressed by adaxial cells in the trunk of the developing zebrafish by double labeling with an antibody recognizing adaxial cells in the zebrafish (Devoto et al., 1996). At later stages, TN-C mRNA is only expressed by muscle pioneer cells, which are a subpopulation of adaxial cells and other myotomal cells in the somite in addition to TN-C mRNA expression in migrating neural crest cells and in the hypochord (Tongiorgi, 1999). Our data confirm these results and we furthermore colocalize the expression of TN-C mRNA in the trunk of early zebrafish embryos in adaxial cells, which may be the source of TN-C protein at the horizontal myoseptum..

5.3.3 Perturbations of TN-C specifically affect motor nerves.

Several observations suggest that the overexpression of TNCEGFmyc and the injection of the recombinantly expressed protein fragment containing the EGF domains of TN-C specifically perturbed growth and pathfinding of the ventral motor nerves. The lateral line nerve which is susceptible to perturbation experiments by RNA overexpression and protein injections (Becker et al., 2001b; Shoji et al., 1998) develops normally in embryos injected with the TNCEGFmyc mRNA or the protein fragment containing the EGF-like domains of TN-C. The posterior commissure and the dorso-ventral diencephalic tract also develop normally in embryos injected with the TNCEGFmyc mRNA or the protein fragment containing the EGF-like domains of TN-C. This indicates that axonal pathfinding was not generally compromised by overexpressing TNCEGFmyc mRNA or injecting the protein fragment containing the EGF domains of TN-C.

The vertical myosepta, and the notochord (labeled by antibodies to chondroitin sulfates) and the muscle pioneer cells (labeled by antibodies to engrailed) at the level of the horizontal myoseptum, where trunk motor axons have to make critical pathway choices are indistinguishable from those in uninjected controls. The finding, that the structure of axon pathways is unaffected also indicates that early developmental deficits leading to an abnormal outgrowth of ventral motor nerves are unlikely. These deficits, which may influence the onset of somitogenesis for example, may occur due to the early expression of the TNCEGFmyc mRNA after injection into the one-to-four cell stage eggs.

The observed phenotypes and their frequencies after overexpression of the TNCEGFmyc mRNA or injecting the protein fragment containing the EGF-like domains of TN-C are comparable, suggesting a specific similar mechanism of perturbation by the *in vivo* treatment. The injection of a MO specific for TN-C also specifically perturbs the growth of motor axons. Embryos injected with the TN-C MO or the control MO were indistinguishable from uninjected controls at 24 hpf, so that early developmental defects are unlikely to be responsible for the observed effects at 33 hpf. Furthermore, the different treatments lead to different specific phenotypes. The observed phenotypes after TNCEGFmyc mRNA overexpression and the injection of the protein fragment containing the EGF domains of TN-C are mainly truncations of motor axons, whereas the injection of the TN-C MOs induces additional growth of motor axons. This suggests specificity of both treatments. Thus, the observed motor nerve phenotypes are probably a consequence of perturbing TN-C functions in the pathway of growing motor axons.

5.3.4 TN-C is involved in growth and pathfinding of ventral motor nerves

Increased presence of TN-C fragments containing the EGF-like domains in the pathway of motor axons as achieved by overexpression of TNCEGFmyc mRNA and injection of the protein fragment containing the EGF-like domains mainly led to truncation of primary motor axons in 24 hpf embryos. After TNCEGFmyc mRNA overexpression, 3.3% of all axons analyzed were truncated and after injection of the EGF-L fragment, 5.2% of all nerves analyzed were truncated in 24 hpf embryos. In all groups of control embryos truncations rarely occurred (0.2-1.2% of all nerves analyzed). We therefore conclude that the truncations of motor nerves observed in embryos injected with the TNCEGFmyc mRNA or the protein fragment containing the EGF-like domains of TN-C are induced by the presence of additional complete EGF-like domains of TN-C. This also indicates that the growth cones of primary motor axons respond to TN-C. These findings are in good agreement with previous *in vitro* studies. TN-C promotes neurite outgrowth when presented as a homogeneous substrate, but repels axons, when presented as a substrate border *in vitro* (Götz et al., 1996; Lochter and Schachner, 1993b; Lochter et al., 1991; Powell and Geller, 1999; Taylor et al., 1993). Furthermore, the recombinantly expressed EGF-like repeats of TN-C used in this study inhibit neurite outgrowth from freshly dissociated cerebellar neurons *in vitro* when presented in a border-like situation (Dorries et al., 1996). After the injection of TNCEGFmyc mRNA but not after injection of the protein fragment containing the EGF-like domains of TN-C, we also

observed a 2% increase of abnormal branched motor axons compared to control groups. The high number of abnormal branches after injection of TNCEGFmyc may be due to complex interactions and is presently difficult to explain. The overexpression of the complete open reading frame (ORF) of TN-C was not possible due to its large size. It is still possible that this could increase the number of truncated motor axons although this is not very likely, since the EGF-like domains are the only domains of TN-C described to show neurite repulsion (reviewed in Jones and Jones, 2000). Indeed injection of the protein fragment containing the FN 6-8 domains of TN-C did not impede growth of motor axons.

The injection of a MO specific for TN-C did not show any effect at 24 hpf, whereas at 33 hpf we observed abnormal branches but not truncations of the ventral motor nerves. Although we could clearly show that levels of TN-C immunoreactivity were reduced at 24 hpf, residual TN-C immunoreactivity was still detectable at the vertical myosepta. TN-C immunoreactivity was not detectable at the horizontal myoseptum in embryos injected with the TN-C MO at 24 hpf, but levels of TN-C, which were below the detection level might still have been present and accounted for proper primary motor axon outgrowth. At 24 hpf only the three primary axons are present in almost all trunk segments and at 33hpf secondary axons have grown out (Ott et al., 2001; Pike et al., 1992). Therefore, when we observed abnormal branching of the ventral motor nerves at 33 hpf, the number of motor axons which can be influenced by the lack of TN-C is increased and this may contribute to the observed phenotypes. It is also possible, that primary motor axons respond to other guidance systems than secondary axons. For example, Semaphorin 3ab is expressed in the caudal somites, (Roos et al., 1999) at 24 hpf during growth of motor nerves. Neuropilin 1, a putative semaphorin 3ab receptor, is expressed at the same time in primary neurons (Julia Feldner, pers. communication see also Lee et al., 2002). Both molecules are downregulated at later stages of development, when secondary motor axons grow out. There may be also other yet unidentified guidance systems, which are located at the critical choice point at the level of the horizontal myoseptum, which substitute for the lack of TN-C at 24 hpf.

5.3.5 The distribution of TN-C immunoreactivity is altered in *unplugged* but not *stumpy* mutants

The *unplugged* zebrafish mutant (Granato et al., 1996) displays abnormal outgrowth of motor nerves at the horizontal myoseptum (Zhang and Granato, 2000; Zhang et al., 2001a). To explain the aberrant growth of motor axons in the *unplugged* mutant, a disturbed deposition of unidentified ECM molecules, which are necessary for growing motor nerves, by adaxial cells (Devoto et al., 1996) has been assumed [Zhang, 2000 #7808]. Here we identify TN-C as an ECM component, that is absent from the horizontal myoseptum in *unplugged* mutant zebrafish. In *unplugged* mutants, TN-C immunoreactivity is present at the vertical myosepta and around the notochord, but is not detectable at the level of horizontal myoseptum. Furthermore, TN-C immunoreactivity is present at the level of the horizontal myoseptum in addition to the vertical myosepta and the notochord in non-homozygous *unplugged* clutch mates, which are identified by ventral motor axons growing unbranched beyond the horizontal myoseptum. Furthermore, we could clearly show that adaxial cells which are responsible for the observed phenotypes in *unplugged* mutants (Zhang and Granato, 2000) express TN-C mRNA in wild-type embryos. This involves TN-C in the proposed model to explain the *unplugged* phenotype. The penetrance of the *unplugged* phenotype is high (approx. 85% of all segments show defects in motor axon growth at the horizontal myoseptum). In contrast, numbers of phenotypes observed after the perturbation of TN-C function are low (approx. 6-9% of all nerves analyzed were abnormal after perturbation of TN-C functions). Therefore, it is likely, that TN-C is one of a set of guidance molecules, which may be affected at the level of the horizontal myoseptum in the *unplugged* mutant. Thus TN-C may contribute to the observed phenotypes in addition to yet unidentified molecules. Positional cloning approaches in the *unplugged* mutant have revealed, that the *unplugged* gene encodes a putative receptor tyrosin kinase (Zhang et al., 2002). Therefore, the absence of TN-C at the level of the horizontal myoseptum may be explained as a consequence of signaling deficits, for example in adaxial cells, which prevents the deposition of TN-C at the level of the horizontal myoseptum in the *unplugged* mutant. As a control, we also analyzed the distribution of TN-C immunoreactivity in the *stumpy* mutant (Beattie et al., 2000), in which primary motor axons are shown to stall at the level of the horizontal myoseptum. TN-C immunoreactivity is present at the level of the horizontal myoseptum in addition to the vertical myosepta and the notochord in the *stumpy* mutant in a pattern that is indistinguishable from wild-type embryos. Thus, the absence of TN-C immunoreactivity from the horizontal myoseptum is a phenotype specific for *unplugged* mutants.

5.3.6 What is the function of TN-C during outgrowth of ventral motor axons?

The phenotypes observed after the different TN-C perturbations indicate that TN-C plays a role in the precise and stereotypic growth of ventral motor nerves in the trunk. The observed phenotypes after injection of a TN-C MO differ from the phenotypes observed after overexpression of TNCEGFmyc mRNA or injection of a protein fragment containing the EGF-like domains of TN-C. Removal of TN-C induces mainly abnormal branches, whereas additional TN-C achieved by overexpression or injection of the protein fragment containing the complete EGF-like domains of TN-C primarily led to truncations of the motor nerves. The observed phenotypes in the *unplugged* mutant may be explained by a probably complete absence of TN-C at the horizontal myoseptum. Thus, axons form aberrant branches, because they may need TN-C functions to read additional guidance cues in their pathway. An additional loss of other guidance cues at the level of the horizontal myoseptum may explain the high numbers of aberrant motor nerves observed in the mutant. We propose the following model to explain the functions of TN-C during outgrowth of motor axons in the trunk. On the motor axon's way to the horizontal myoseptum, TN-C is present in an ascending gradient and thus may function as an attenuating border to slow down the growth of motor axons at the level of the horizontal myoseptum. This could allow the advancing growth cones to properly read additional guiding cues. In fact, outgrowing primary motor axons were shown to pause at the level of the horizontal myoseptum (Eisen et al., 1986) where we find the highest density of TN-C immunopositive fibrils, before they grow towards their targets. Previous studies described a similar effect of TN-C on migrating oligodendrocyte progenitors in mice. During development of the optic nerve, TN-C expression regresses towards the retina forming a receding uphill gradient for migrating oligodendrocyte progenitors. Concomitantly with the reduction of TN-C expression, oligodendrocyte precursors migrate towards the retina. TN-C is a repellent substrate for oligodendrocytes and their progenitors in vitro (Bartsch et al., 1994). Furthermore, in the optic nerve of TN-C deficient mice, oligodendrocyte progenitor cells migrate faster towards the retina than in wild-type control animals (Garcion et al., 2001) indicating that TN-C probably forms an attenuating barrier for oligodendrocyte migration in vivo. In contrast to the situation in the optic nerve in mice, where TN-C disappears during development, TN-C immunoreactivity at the horizontal myoseptum in the trunk of zebrafish remains detectable during growth of the motor axons. To exit the region of the horizontal myoseptum, the growth cones of motor axons might undergo a change in the responsiveness

to TN-C which may be induced by a change in the expression patterns of receptors, so that the repelling activity of TN-C is no longer recognized. In a recent study it has been shown, that retinal ganglion cell axons, which are led out of the eye by an attractive gradient of netrin-1 at the optic nerve head are excluded from areas expressing netrin-1 in the optic pathway. This indicates a switch in the responsiveness to netrin-1 when the axons have passed the high levels of netrin-1 expression at the optic nerve head (Shewan et al., 2002). A time-lapse analysis of growing motor axons would definitively show whether TN-C can decelerate the growth of motor axons at the level of the horizontal myoseptum thereby allowing the axons to read additional guidance cues properly.

TN-C is a ligand for integrins (Varnum-Finney et al., 1995; Yokosaki et al., 1998). Zebrafish TN-C also contains an RGD motif, which may be recognized by integrins localized on the growth cones of growing motor axons. Perturbation of integrin functions using integrin antagonists led to similar phenotypes as those observed after perturbation of TN-C functions using TN-C morpholinos (Becker, T. pers. communications). At 24 hpf, blocking integrin functions mainly led to abnormal branching of the motor nerves, but truncations were also observed. At 33 hpf only abnormal branches of the ventral motor nerves were observed. This is in agreement with our observed results, since removal of TN-C, a putative ligand of the integrins or blocking of integrins which may be putative TN-C receptors should result in the same phenotype. One explanation for the occurrence of truncated axons after blocking integrin functions, which is in contrast to the observed abnormal branches after injection of the TN-C MO, could be the inability of these axons to recognize other growth promoting ECM cues. Laminin, for example, which is also a ligand for integrins (Gullberg and Ekblom, 1995) is probably expressed in the pathway of growing motor axons (Parsons et al., 2002; Westerfield, 1987). Thus the function of TN-C could at least in part be mediated by integrin receptors localized on the growth cones of motor neurons. F3/contactin, a cell adhesion molecule of the Ig-superfamily is also a receptor for TN-C (Rigato et al., 2002) and is expressed in primary motor neurons during growth of their axons in zebrafish. However, perturbation of F3/contactin functions using morpholinos did not show any effect on growing motor axons (Gimnopoulos et al., 2003).

Given the low incidence of aberrant nerves (approx. 6-9% of all nerves analyzed were abnormal after perturbation of TN-C expression) it is likely that, TN-C is not the only cue in the pathway of ventral motor nerves. In fact, perturbing some other potential guidance molecules present in the somites of zebrafish has been shown to induce aberrant growth of ventral motor axons similar to those observed here for perturbation of TN-C function.

Overexpression of the axon-repellent semaphorin 3A1 (Halloran et al., 2000) and semaphorin 3ab (Roos et al., 1999) and injection of chondroitin sulfates (Bernhardt and Schachner, 2000) also induce truncations of the ventral motor nerve. Conversely, elimination of chondroitin sulfates induces mainly abnormal branching of the nerve (Bernhardt and Schachner, 2000). These additional cues might act in combination with TN-C to guide motor axons on their way to their final targets.

6. Literature

Altschul, S. F., Gish, W., Miller, W., Myers, E. W. and Lipman, D. J. (1990). Basic local alignment search tool. *J Mol Biol* **215**, 403-410.

Amores, A., Force, A., Yan, Y. L., Joly, L., Amemiya, C., Fritz, A., Ho, R. K., Langeland, J., Prince, V., Wang, Y. L. et al. (1998). Zebrafish hox clusters and vertebrate genome evolution. *Science* **282**, 1711-1714.

Ankerhold, R., Leppert, C. A., Bastmeyer, M. and Stuermer, C. A. (1998). E587 antigen is upregulated by goldfish oligodendrocytes after optic nerve lesion and supports retinal axon regeneration. *Glia* **23**, 257-270.

Ankerhold, R. and Stuermer, C. A. (1999). Fate of oligodendrocytes during retinal axon degeneration and regeneration in the goldfish visual pathway. *J Neurobiol* **41**, 572-584.

Appel, C., Gloor, S., Schmalzing, G., Schachner, M. and Bernhardt, R. R. (1996). Expression of a Na,K-ATPase beta 3 subunit during development of the zebrafish central nervous system. *J Neurosci Res* **46**, 551-564.

Appel, F., Holm, J., Conscience, J. F., Halbach, F. V. U., Faissner, A., James, P. and Schachner, M. (1995). Identification of the border between fibronectin type III homologous repeats 2 and 3 of the neural cell adhesion molecule L1 as a neurite outgrowth promoting and signal transducing domain. *J Neurobiol* **28**, 297-312.

Arora, V., Knapp, D. C., Smith, B. L., Statfield, M. L., Stein, D. A., Reddy, M. T., Weller, D. D. and Iversen, P. L. (2000). c-Myc antisense limits rat liver regeneration and indicates role for c-Myc in regulating cytochrome P-450 3A activity. *J Pharmacol Exp Ther* **292**, 921-928.

Baier, H. and Bonhoeffer, F. (1992). Axon guidance by gradients of a target-derived component. *Science* **255**, 472-475.

Baier, H., Klostermann, S., Trowe, T., Karlstrom, R. O., Nüsslein-Volhard, C. and Bonhoeffer, F. (1996). Genetic dissection of the retinotectal projection. *Development* **123**, 415-425.

Barbu, M. (1990). Molecular cloning of cDNAs that encode the chicken P0 protein: evidence for early expression in avians. *J Neurosci Res* **25**, 143-151.

Bartsch, S., Husmann, K., Schachner, M. and Bartsch, U. (1995). The extracellular matrix molecule tenascin: Expression in the developing chick retinotectal system and substrate properties for retinal ganglion cell neurites *in vitro*. *Eur J Neurosci* **7**, 907-916.

- Bartsch, U.** (1996). The extracellular matrix molecule tenascin-C: Expression in vivo and functional characterization in vitro. *Prog Neurobiol* **49**, 145-161.
- Bartsch, U., Faissner, A., Trotter, J., Dörries, U., Bartsch, S., Mohajeri, H. and Schachner, M.** (1994). Tenascin demarcates the boundary between the myelinated and nonmyelinated part of retinal ganglion cell axons in the developing and adult mouse. *J Neurosci* **14**, 4756-4768.
- Bartsch, U., Pesheva, P., Raff, M. and Schachner, M.** (1993). Expression of janusin (J1-160/180) in the retina and optic nerve of the developing and adult mouse. *Glia* **9**, 57-69.
- Bastmeyer, M., Beckmann, M., Schwab, M. E. and Stuermer, C. A. O.** (1991). Growth of regenerating goldfish axons is inhibited by rat oligodendrocytes and CNS myelin but not by goldfish optic nerve tract oligodendrocyte-like cells and fish CNS myelin. *J Neurosci* **11**, 626-640.
- Bastmeyer, M., Schlosshauer, B. and Stürmer, C. A. O.** (1990). The spatio-temporal distribution of N-CAM in the retinotectal pathway of adult goldfish detected by the monoclonal antibody D3. *Development* **108**, 299-311.
- Bateman, A., Birney, E., Durbin, R., Eddy, S. R., Howe, K. L. and Sonnhammer, E. L.** (2000). The Pfam protein families database. *Nucleic Acids Res* **28**, 263-266.
- Battisti, W. P., Wang, J., Bozek, K. and Murray, M.** (1995). Macrophages, microglia, and astrocytes are rapidly activated after crush injury of the goldfish optic nerve: a light and electron microscopic analysis. *J Comp Neurol* **354**, 306-320.
- Beattie, C. E., Granato, M. and Kuwada, J. Y.** (2002). Cellular, genetic and molecular mechanisms of axonal guidance in the zebrafish. *Results Probl Cell Differ* **40**, 252-269.
- Beattie, C. E., Melancon, E. and Eisen, J. S.** (2000). Mutations in the stumpy gene reveal intermediate targets for zebrafish motor axons. *Development* **127**, 2653-2662.
- Becker, C. G. and Becker, T.** (2002). Repellent guidance of regenerating optic axons by chondroitin sulfate glycosaminoglycans in zebrafish. *J Neurosci* **22**, 854-862.
- Becker, C. G., Becker, T. and Meyer, R. L.** (2001a). Increased NCAM-180 immunoreactivity and maintenance of L1 immunoreactivity in injured optic fibers of adult mice. *Exp Neurol* **169**, 438-448.
- Becker, C. G., Becker, T., Meyer, R. L. and Schachner, M.** (1999). Tenascin-R inhibits the growth of optic fibers in vitro but is rapidly eliminated during optic nerve regeneration in the salamander *Pleurodeles waltl*. *J Neurosci* **19**, 813-827.

- Becker, C. G., Meyer, R. L. and Becker, T.** (2000a). Gradients of ephrin-A2 and ephrin-A5b mRNA during retinotopic regeneration of the optic projection in adult zebrafish. *J Comp Neurol* **427**, 469-483.
- Becker, T., Anliker, B., Becker, C. G., Taylor, J., Schachner, M., Meyer, R. L. and Bartsch, U.** (2000b). Tenascin-R inhibits regrowth of optic fibers in vitro and persists in the optic nerve of mice after injury. *Glia* **29**, 330-346.
- Becker, T. and Becker, C. G.** (2001). Regenerating descending axons preferentially reroute to the gray matter in the presence of a general macrophage/microglial reaction caudal to a spinal transection in adult zebrafish. *J Comp Neurol* **433**, 131-147.
- Becker, T., Becker, C. G., Niemann, U., Naujoks-Manteuffel, C., Bartsch, U., Schachner, M. and Roth, G.** (1995). Immunohistological localization of tenascin-C in the developing and regenerating retinotectal system of two amphibian species. *J Comp Neurol* **360**, 643-657.
- Becker, T., Becker, C. G., Schachner, M. and Bernhardt, R. R.** (2001b). Antibody to the HNK-1 glycoepitope affects fasciculation and axonal pathfinding in the developing posterior lateral line nerve of embryonic zebrafish. *Mech Dev* **109**, 37-49.
- Becker, T., Bernhardt, R. R., Reinhard, E., Wullimann, M. F., Tongiorgi, E. and Schachner, M.** (1998). Readiness of zebrafish brain neurons to regenerate a spinal axon correlates with differential expression of specific cell recognition molecules. *J Neurosci* **18**, 5789-5803.
- Becker, T., Wullimann, M. F., Becker, C. G., Bernhardt, R. R. and Schachner, M.** (1997). Axonal regrowth after spinal cord transection in adult zebrafish. *J Comp Neurol* **377**, 577-595.
- Bernhardt, R.** (1989). Axonal pathfinding during the regeneration of the goldfish optic pathway. *J Comp Neurol* **284**, 119-134.
- Bernhardt, R. R.** (1999). Cellular and molecular bases of axonal regeneration in the fish central nervous system. *Exp Neurol* **157**, 223-240.
- Bernhardt, R. R., Goerlinger, S., Roos, M. and Schachner, M.** (1998). Anterior-posterior subdivision of the somite in embryonic zebrafish: Implications for motor axon guidance. *Dev Dyn* **213**, 334-347.
- Bernhardt, R. R. and Schachner, M.** (2000). Chondroitin sulfates affect the formation of the segmental motor nerves in zebrafish embryos. *Dev Biol* **221**, 206-219.
- Bernhardt, R. R., Tongiorgi, E., Anzini, P. and Schachner, M.** (1996). Increased expression of specific recognition molecules by retinal ganglion cells and by the optic

pathway glia accompanies the successful regeneration of retinal axons in adult zebrafish. *J Comp Neurol* **376**, 253-264.

Bhattacharyya, A., Frank, E., Ratner, N. and Brackenbury, R. (1991). P0 is an early marker of the Schwann cell lineage in chickens. *Neuron* **7**, 831-844.

Bolin, L. M. and Shooter, E. M. (1993). Neurons Regulate Schwann Cell Genes by Diffusible Molecules. *J Cell Biol* **123**, 237-243.

Bradbury, E. J., Moon, L. D., Popat, R. J., King, V. R., Bennett, G. S., Patel, P. N., Fawcett, J. W. and McMahon, S. B. (2002). Chondroitinase ABC promotes functional recovery after spinal cord injury. *Nature* **416**, 636-640.

Bregman, B. S., Kunkelbagden, E., Schnell, L., Dai, H. N., Gao, D. and Schwab, M. E. (1995). Recovery from spinal cord injury mediated by antibodies to neurite growth inhibitors. *Nature* **378**, 498-501.

Bristow, J., Tee, M. K., Gitelman, S. E., Mellon, S. H. and Miller, W. L. (1993). Tenascin-X: a novel extracellular matrix protein encoded by the human XB gene overlapping P450c21B. *J Cell Biol* **122**, 265-278.

Brosamle, C. and Halpern, M. E. (2002). Characterization of myelination in the developing zebrafish. *Glia* **39**, 47-57.

Brösamle, C. and Halpern, M. E. (2002). Characterization of myelination in the developing zebrafish. *Glia* **39**, 47-57.

Brückner, G., Grosche, J., Schmidt, S., Hartig, W., Margolis, R. U., Delpech, B., Seidenbecher, C. I., Czaniera, R. and Schachner, M. (2000). Postnatal development of perineuronal nets in wild-type mice and in a mutant deficient in tenascin-R. *J Comp Neurol* **428**, 616-629.

Brümmendorf, T. and Rathjen, F. G. (1993). Axonal Glycoproteins with Immunoglobulin and Fibronectin Type-III-Related Domains in Vertebrates - Structural Features, Binding Activities, and Signal Transduction. *J Neurochem* **61**, 1207-1219.

Burch, G. H., Gong, Y., Liu, W., Dettman, R. W., Curry, C. J., Smith, L., Miller, W. L. and Bristow, J. (1997). Tenascin-X deficiency is associated with Ehlers-Danlos syndrome. *Nat Genet* **17**, 104-108.

Chen, M. S., Huber, A. B., van der Haar, M. E., Frank, M., Schnell, L., Spillmann, A. A., Christ, F. and Schwab, M. E. (2000). Nogo-A is a myelin-associated neurite outgrowth inhibitor and an antigen for monoclonal antibody IN-1. *Nature* **403**, 434-439.

Chiquet, M. and Fambrough, D. M. (1984). Chick myotendinous antigen. I. A monoclonal antibody as a marker for tendon and muscle morphogenesis. *J Cell Biol* **98**, 1926-1936.

- Chuong, C. M., Crossin, K. L. and Edelman, G. M.** (1987). Sequential expression and differential function of multiple adhesion molecules during the formation of cerebellar cortical layers. *J Cell Biol* **104**, 331-342.
- Cifuentes-Diaz, C., Faille, L., Goudou, D., Schachner, M., Rieger, F. and Angaut-Petit, D.** (2002). Abnormal reinnervation of skeletal muscle in a tenascin-C-deficient mouse. *J Neurosci Res* **67**, 93-99.
- Cifuentes-Diaz, C., Velasco, E., Meunier, F. A., Goudou, D., Belkadi, L., Faille, L., Murawsky, M., Angaut-Petit, D., Molgo, J., Schachner, M. et al.** (1998). The peripheral nerve and the neuromuscular junction are affected in the tenascin-C-deficient mouse. *Cell Mol Biol (Noisy-le-grand)* **44**, 357-379.
- Colavincenzo, J. and Levine, R. L.** (2000). Myelin debris clearance during Wallerian degeneration in the goldfish visual system. *J Neurosci Res* **59**, 47-62.
- Cooke, J. E. and Moens, C. B.** (2002). Boundary formation in the hindbrain: Eph only it were simple. *Trends in Neuroscience* **25**, 260-267.
- Crossin, K. L., Hoffman, S., Grumet, M., Thiery, J. P. and Edelman, G. M.** (1986). Site-restricted expression of cytotactin during development of the chick embryo. *J Cell Biol* **102**, 1917-1930.
- Crossin, K. L. and Krushel, L. A.** (2000). Cellular signaling by neural cell adhesion molecules of the immunoglobulin superfamily. *Dev Dyn* **218**, 260-279.
- D'Urso, D., Brophy, P. J., Staugaitis, S. M., Gillespie, C. S., Frey, A. B., Stempak, J. G. and Colman, D. R.** (1990). Protein zero of peripheral nerve myelin: biosynthesis, membrane insertion, and evidence for homotypic interaction. *Neuron* **4**, 449-460.
- Davies, S. J. A., Fitch, M. T., Memberg, S. P., Hall, A. K., Raisman, G. and Silver, J.** (1997). Regeneration of adult axons in white matter tracts of the central nervous system. *Nature* **390**, 680-683.
- Devoto, S. H., Melancon, E., Eisen, J. S. and Westerfield, M.** (1996). Identification of separate slow and fast muscle precursor cells in vivo, prior to somite formation. *Development* **122**, 3371-3380.
- Dorries, U., Taylor, J., Xiao, Z., Lochter, A., Montag, D. and Schachner, M.** (1996). Distinct effects of recombinant tenascin-C domains on neuronal cell adhesion, growth cone guidance, and neuronal polarity. *J Neurosci Res* **43**, 420-438.
- Dörries, U., Taylor, J., Xiao, Z., Lochter, A., Montag, D. and Schachner, M.** (1996). Distinct effects of recombinant tenascin-C domains on neuronal cell adhesion, growth cone guidance, and neuronal polarity. *J Neurosci Res* **43**, 420-438.

- Eisen, J. S., Myers, P. Z. and Westerfield, M.** (1986). Pathway selection by growth cones of identified motoneurons in live zebra fish embryos. *Nature* **320**, 269-271.
- Ekker, S. C. and Larson, J. D.** (2001). Morphant technology in model developmental systems. *Genesis* **30**, 89-93.
- Erickson, H. P. and Bourdon, M. A.** (1989). Tenascin: an extracellular matrix protein prominent in specialized embryonic tissues and tumors. *Annu Rev Cell Biol* **5**, 71-92.
- Erickson, H. P. and Inglesias, J. L.** (1984). A six-armed oligomer isolated from cell surface fibronectin preparations. *Nature* **311**, 267-269.
- Erter, C. E., Wilm, T. P., Basler, N., Wright, C. V. and Solnica-Krezel, L.** (2001). Wnt8 is required in lateral mesendodermal precursors for neural posteriorization in vivo. *Development* **128**, 3571-3583.
- Evers, M.** Generation and phenotyping of Tenascin-C deficient mice and cloning and characterization of new members of the HNK-1 family of sulfotransferases. Dissertation, Universität Bochum.
- Faissner, A. and Kruse, J.** (1990). J1/tenascin is a repulsive substrate for central nervous system neurons. *Neuron* **5**, 627-637.
- Fawcett, J. W. and Asher, R. A.** (1999). The glial scar and central nervous system repair. *Brain Res Bull* **49**, 377-391.
- Fawcett, J. W. and Geller, H. M.** (1998). Regeneration in the CNS: Optimism mounts. *TINS* **21**, 179-180.
- Ffrench-Constant, C., Miller, R. H., Kruse, J., Schachner, M. and Raff, M. C.** (1986). Molecular specialization of astrocyte processes at nodes of Ranvier in rat optic nerve. *J Cell Biol* **102**, 844-852.
- Fields, R. D. and Itoh, K.** (1996). Neural cell adhesion molecules in activity-dependent development and synaptic plasticity. *Trends in Neuroscience* **19**, 473-480.
- Filbin, M. T., Walsh, F. S., Trapp, B. D., Pizzey, J. A. and Tennekoon, G. I.** (1990). Role of myelin P0 protein as a homophilic adhesion molecule. *Nature* **344**, 871-872.
- Fluck, M., Tunc-Civelek, V. and Chiquet, M.** (2000). Rapid and reciprocal regulation of tenascin-C and tenascin-Y expression by loading of skeletal muscle. *J Cell Sci* **113**, 3583-3591.
- Frei, T., Halbach, F. V., Wille, W. and Schachner, M.** (1992). Different extracellular domains of the neural cell adhesion molecule (N-CAM) are involved in different functions. *J Cell Biol* **118**, 177-194.

- Fu, S. Y. and Gordon, T.** (1997). The cellular and molecular basis of peripheral nerve regeneration. *Mol Neurobiol* **14**, 67-116.
- Fuss, B., Wintergerst, E. S., Bartsch, U. and Schachner, M.** (1993). Molecular characterization and in situ messenger RNA localization of the neural recognition molecule J1-160/180 - a modular structure similar to tenascin. *J Cell Biol* **120**, 1237-1249.
- Garcion, E., Faissner, A. and ffrench-Constant, C.** (2001). Knockout mice reveal a contribution of the extracellular matrix molecule tenascin-C to neural precursor proliferation and migration. *Development* **128**, 2485-2496.
- Gaze, R. M.** (1970). The formation of nerve connections. London: Academic Press.
- Giese, K. P., Martini, R., Lemke, G., Soriano, P. and Schachner, M.** (1992). Mouse P0 gene disruption leads to hypomyelination, abnormal expression of recognition molecules, and degeneration of myelin and axons. *Cell* **71**, 565-576.
- Gillen, C., Gleichmann, M., Spreyer, P. and Müller, H. W.** (1995). Differentially expressed genes after peripheral nerve injury. *J Neurosci Res* **42**, 159-171.
- Gimnopoulos, D., Becker, CG, Ostendorff, HP, Bach, I, Schachner, M, Becker T** (2003) Expression of the zebrafish recognition molecule F3/F11/contactin in a subset of differentiating neurons is regulated by cofactors associated with LIM domains **Mech Dev** **120**,135-141.
- Götz, B., Scholze, A., Clement, A., Joester, A., Schutte, K., Wigger, F., Frank, R., Spiess, E., Ekblom, P. and Faissner, A.** (1996). Tenascin-C contains distinct adhesive, anti adhesive, and neurite outgrowth promoting sites for neurons. *J Cell Biol* **132**, 681-699.
- Gould, R. M., Fannon, A. M. and Moorman, S. J.** (1995). Neural cells from dogfish embryos express the same subtype-specific antigens as mammalian neural cells in vivo and in vitro. *Glia* **15**, 401-418.
- Granato, M., van Eeden, F. J., Schach, U., Trowe, T., Brand, M., Furutani-Seiki, M., Haffter, P., Hammerschmidt, M., Heisenberg, C. P., Jiang, Y. J. et al.** (1996). Genes controlling and mediating locomotion behavior of the zebrafish embryo and larva. *Development* **123**, 399-413.
- GrandPre, T., Nakamura, F., Vartanian, T. and Strittmatter, S. M.** (2000). Identification of the Nogo inhibitor of axon regeneration as a reticulon protein. *Nature* **403**, 439-444.
- Griffith, L. S., Schmitz, B. and Schachner, M.** (1992). L2/HNK-1 carbohydrate and protein-protein interactions mediate the homophilic binding of the neural adhesion molecule P0. *J Neurosci Res* **33**, 639-648.

- Grumet, M., Hoffman, S., Crossin, K. L. and Edelman, G. M.** (1985). Cytotactin, an extracellular matrix protein of neural and non-neural tissues that mediates glia-neuron interaction. *Proc Natl Acad Sci* **82**, 8075-8079.
- Gullberg, D. and Ekblom, P.** (1995). Extracellular matrix and its receptors during development. *Int J Dev Biol* **39**, 845-854.
- Gupta, S. K., Poduslo, J. F. and Mezei, C.** (1988). Temporal changes in PO and MBP gene expression after crush-injury of the adult peripheral nerve. *Brain Res* **464**, 133-141.
- Gupta, S. K., Pringle, J., Poduslo, J. F. and Mezei, C.** (1993). Induction of myelin genes during peripheral nerve remyelination requires a continuous signal from the ingrowing axon. *J Neurosci Res* **34**, 14-23.
- Guttinger, M., Sutti, F., Panigada, M., Porcellini, S., Merati, B., Mariani, M., Teesalu, T., Consalez, G. G. and Grassi, F.** (1998). Epithelial V-like antigen (EVA), a novel member of the immunoglobulin superfamily, expressed in embryonic epithelia with a potential role as homotypic adhesion molecule in thymus histogenesis. *J Cell Biol* **141**, 1061-1071.
- Hagios, C., Brown-Luedi, M. and Chiquet-Ehrismann, R.** (1999). Tenascin-Y, a component of distinctive connective tissues, supports muscle cell growth. *Exp Cell Res* **253**, 607-617.
- Hagios, C., Koch, M., Spring, J., Chiquet, M. and Chiquet-Ehrismann, R.** (1996). Tenascin-Y: A protein of novel domain structure is secreted by differentiated fibroblasts of muscle connective tissue. *J Cell Biol* **134**, 1499-1512.
- Halloran, M. C., Sato-Maeda, M., Warren, J. T., Su, F., Lele, Z., Krone, P. H., Kuwada, J. Y. and Shoji, W.** (2000). Laser-induced gene expression in specific cells of transgenic zebrafish. *Development* **127**, 1953-1960.
- Hasegawa, K., Yoshida, T., Matsumoto, K., Katsuta, K., Waga, S. and Sakakura, T.** (1997). Differential expression of tenascin-C and tenascin-X in human astrocytomas. *Acta Neuropathol (Berl)* **93**, 431-437.
- Haspel, J., Friedlander, D. R., Ivy-May, N., Chickramane, S., Roonprapunt, C., Chen, S., Schachner, M. and Grumet, M.** (2000). Critical and optimal Ig domains for promotion of neurite outgrowth by L1/Ng-CAM. *J Neurobiol* **42**, 287-302.
- Hayasaka, K., Nanao, K., Tahara, M., Sato, W., Takada, G., Miura, M. and Uyemura, K.** (1991). Isolation and sequence determination of cDNA encoding the major structural protein of human peripheral myelin. *Biochem Biophys Res Commun* **180**, 515-518.

- Hirsch, S., Cahill, M. A. and Stuermer, C. A.** (1995). Fibroblasts at the transection site of the injured goldfish optic nerve and their potential role during retinal axonal regeneration. *J Comp Neurol* **360**, 599-611.
- Hopker, V. H., Shewan, D., Tessier-Lavigne, M., Poo, M. and Holt, C.** (1999). Growth-cone attraction to netrin-1 is converted to repulsion by laminin-1. *Nature* **401**, 69-73.
- Husmann, K., Faissner, A. and Schachner, M.** (1992). Tenascin Promotes Cerebellar Granule Cell Migration and Neurite Outgrowth by Different Domains in the Fibronectin Type-III Repeats. *J Cell Biol* **116**, 1475-1486.
- Ikuta, T., Ariga, H. and Matsumoto, K.** (2000). Extracellular matrix tenascin-X in combination with vascular endothelial growth factor B enhances endothelial cell proliferation. *Genes Cells* **5**, 913-927.
- Jeserich, G. and Jacque, C.** (1985). Immunohistochemical localization of myelin basic protein in the developing optic system of trout. *J Neurosci Res* **13**, 529-538.
- Jeserich, G., Muller, A. and Jacque, C.** (1990). Developmental expression of myelin proteins by oligodendrocytes in the CNS of trout. *Brain Res Dev Brain Res* **51**, 27-34.
- Jones, F. S., Hoffman, S., Cunningham, B. A. and Edelman, G. M.** (1989). A detailed structural model of cytotactin: protein homologies, alternative RNA splicing, and binding regions. *Proc Natl Acad Sci U S A* **86**, 1905-1909.
- Jones, F. S. and Jones, P. L.** (2000). The tenascin family of ECM glycoproteins: structure, function, and regulation during embryonic development and tissue remodeling. *Dev Dyn* **218**, 235-259.
- Kalman, M.** (1998). Astroglial architecture of the carp (*Cyprinus carpio*) brain as revealed by immunohistochemical staining against glial fibrillary acidic protein (GFAP). *Anat Embryol (Berl)* **198**, 409-433.
- Kanki, J. P., Chang, S. and Kuwada, J. Y.** (1994). The molecular cloning and characterization of potential chick DM-GRASP homologs in zebrafish and mouse. *J Neurobiol* **25**, 831-845.
- Kawano, H., Ohyama, K., Kawamura, K. and Nagatsu, I.** (1995). Migration of dopaminergic neurons in the embryonic mesencephalon of mice. *Brain Res Dev Brain Res* **86**, 101-113.
- Kimmel, C. B.** (1993). Patterning the brain of the zebrafish embryo. *Annu Rev Neurosci* **16**, 707-732.

- Kruse, J., Keilhauer, G., Faissner, A., Timpl, R. and Schachner, M.** (1985). The J1 glycoprotein: a novel nervous system cell adhesion molecule of the L2/HNK-1 family. *Nature* **316**, 146-148.
- Laywell, E. D., Dorries, U., Bartsch, U., Faissner, A., Schachner, M. and Steindler, D. A.** (1992). Enhanced expression of the developmentally regulated extracellular matrix molecule tenascin following adult brain injury. *Proc Natl Acad Sci U S A* **89**, 2634-2638.
- LeBlanc, A. C. and Poduslo, J. F.** (1990). Axonal modulation of myelin gene expression in the peripheral nerve. *J Neurosci Res* **26**, 317-326.
- Lee, M. J., Calle, E., Brennan, A., Ahmed, S., Sviderskaya, E., Jessen, K. R. and Mirsky, R.** (2001). In early development of the rat mRNA for the major myelin protein P(0) is expressed in nonsensory areas of the embryonic inner ear, notochord, enteric nervous system, and olfactory ensheathing cells. *Dev Dyn* **222**, 40-51.
- Lee, P., Goishi, K., Davidson, A. J., Mannix, R., Zon, L. and Klagsbrun, M.** (2002). Neuropilin-1 is required for vascular development and is a mediator of VEGF-dependent angiogenesis in zebrafish. *Proc Natl Acad Sci U S A* **99**, 10470-10475.
- Lemke, G. and Axel, R.** (1985). Isolation and sequence of a cDNA encoding the major structural protein of peripheral myelin. *Cell* **40**, 501-508.
- Leprini, A., Gherzi, R., Siri, A., Querze, G., Viti, F. and Zardi, L.** (1996). The human tenascin-R gene. *J Biol Chem* **271**, 31251-31254.
- Lethias, C., Elefteriou, F., Parsiegla, G., Exposito, J. Y. and Garrone, R.** (2001). Identification and characterization of a conformational heparin-binding site involving two fibronectin type III modules of bovine tenascin-X. *J Biol Chem* **276**, 16432-16438.
- Lochter, A. and Schachner, M.** (1993a). Tenascin and extracellular matrix glycoproteins - From promotion to polarization of neurite growth in vitro. *J Neurosci* **13**, 3986-4000.
- Lochter, A. and Schachner, M.** (1993b). Tenascin and extracellular matrix glycoproteins: from promotion to polarization of neurite growth in vitro. *J Neurosci* **13**, 3986-4000.
- Lochter, A., Taylor, J., Fuss, B. and Schachner, M.** (1994). The extracellular matrix molecule janusin regulates neuronal morphology in a substrate- and culture time-dependent manner. *Eur J Neurosci* **6**, 597-606.
- Lochter, A., Vaughan, L., Kaplony, A., Prochiantz, A., Schachner, M. and Faissner, A.** (1991). J1/Tenascin in substrate-bound and soluble form displays contrary effects on neurite outgrowth. *J Cell Biol* **113**, 1159-1171.

- Maggs, A. and Scholes, J.** (1990). Reticular astrocytes in the fish optic nerve: macroglia with epithelial characteristics form an axially repeated lacework pattern, to which nodes of Ranvier are apposed. *J Neurosci* **10**, 1600-1614.
- Marcus, R. C., Delaney, C. L. and Easter, S. S., Jr.** (1999). Neurogenesis in the visual system of embryonic and adult zebrafish (*Danio rerio*). *Vis Neurosci* **16**, 417-424.
- Martini, R.** (1994). Expression and functional roles of neural cell surface molecules and extracellular matrix components during development and regeneration of peripheral nerves. *J Neurocytol* **23**, 1-28.
- Martini, R. and Schachner, M.** (1997). Molecular bases of myelin formation as revealed by investigations on mice deficient in glial cell surface molecules. *Glia* **19**, 298-310.
- Melancon, E., Liu, D. W., Westerfield, M. and Eisen, J. S.** (1997). Pathfinding by identified zebrafish motoneurons in the absence of muscle pioneers. *J Neurosci* **17**, 7796-7804.
- Metcalf, W. K., Myers, P. Z., Trevarrow, B., Bass, M. B. and Kimmel, C. B.** (1990). Primary neurons that express the L2/HNK-1 carbohydrate during early development in the zebrafish. *Development* **110**, 491-504.
- Meyer, R. L.** (1978). Evidence from thymidine labeling for continuing growth of retina and tectum in juvenile goldfish. *Exp Neurol* **59**, 99-111.
- Mitchell, L. S., Griffiths, I. R., Morrison, S., Barrie, J. A., Kirkham, D. and McPhilemy, K.** (1990). Expression of myelin protein gene transcripts by Schwann cells of regenerating nerve. *J Neurosci Res* **27**, 125-135.
- Moon, L. D., Asher, R. A., Rhodes, K. E. and Fawcett, J. W.** (2001). Regeneration of CNS axons back to their target following treatment of adult rat brain with chondroitinase ABC. *Nat Neurosci* **4**, 465-466.
- Müller-Husmann, G., Gloor, S. and Schachner, M.** (1993). Functional characterization of beta isoforms of murine Na,K-ATPase. The adhesion molecule on glia (AMOG/beta 2), but not beta 1, promotes neurite outgrowth. *J Biol Chem* **268**, 26260-26267.
- Mullins, M.** (1995). Genetic methods: conventions for naming zebrafish genes. In *The zebrafish book*, (ed. M. Westerfield), pp. 7.1-7.4. Eugene: Oregon University Press.
- Murray, M.** (1976). Regeneration of retinal axons into the goldfish optic tectum. *J Comp Neurol* **168**, 175-195.
- Myers, P. Z., Eisen, J. S. and Westerfield, M.** (1986). Development and axonal outgrowth of identified motoneurons in the zebrafish. *J Neurosci* **6**, 2278-2289.

- Nakai, K. and Horton, P.** (1999). PSORT: a program for detecting sorting signals in proteins and predicting their subcellular localization. *Trends Biochem Sci* **24**, 34-36.
- Nasevicius, A. and Ekker, S. C.** (2000). Effective targeted gene 'knockdown' in zebrafish. *Nat Genet* **26**, 216-220.
- Neidhardt, J.** (2001) Identification, cloning and charakterisation of the novel tenascin family member tenascin-N. Dissertation, Universität Hannover).
- Nona, S. N., Shehab, S. A., Stafford, C. A. and Cronly-Dillon, J. R.** (1989). Glial fibrillary acidic protein (GFAP) from goldfish: Its localisation in visual pathway. *Glia* **2**, 189-200.
- Nona, S. N., Stafford, C. A., Duncan, A., Cronlydillon, J. R. and Scholes, J.** (1994). Myelin repair by Schwann cells in the regenerating goldfish visual pathway: Regional patterns revealed by X-irradiation. *J Neurocytol* **23**, 400-409.
- Nona, S. N., Thomlinson, A. M., Bartlett, C. A. and Scholes, J.** (2000). Schwann cells in the regenerating fish optic nerve: Evidence that CNS axons, not the glia, determine when myelin formation begins. *J Neurocytol* **29**, 285-300.
- Nörenberg, U., Hubert, M., Brümmendorf, T., Tárnok, A. and Rathjen, F. G.** (1995). Characterization of functional domains of the tenascin-R (restrictin) polypeptide: Cell attachment site, binding with F11, and enhancement of F11-mediated neurite outgrowth by tenascin-R. *J Cell Biol* **130**, 473-484.
- Nörenberg, U., Wille, H., Wolff, J. M., Frank, R. and Rathjen, F. G.** (1992). The chicken neural extracellular matrix molecule restrictin - similarity with EGF-like, fibronectin type-III-like, and fibrinogen-like motifs. *Neuron* **8**, 849-863.
- Ott, H., Diekmann, H., Stuermer, C. A. and Bastmeyer, M.** (2001). Function of neurolin (dm-grasp/sc-1) in guidance of motor axons during zebrafish development. *Dev Biol* **235**, 86-97.
- Parsons, M. J., Campos, I., Hirst, E. M. and Stemple, D. L.** (2002). Removal of dystroglycan causes severe muscular dystrophy in zebrafish embryos. *Development* **129**, 3505-3512.
- Perez, R. G. and Halfter, W.** (1993). Tenascin in the developing chick visual system - distribution and potential role as a modulator of retinal axon growth. *Dev Biol* **156**, 278-292.
- Pesheva, P., Gennarini, G., Goridis, C. and Schachner, M.** (1993). The F3/11 cell adhesion molecule mediates the repulsion of neurons by the extracellular matrix glycoprotein J1-160/180. *Neuron* **10**, 69-82.
- Pesheva, P., Spiess, E. and Schachner, M.** (1989). J1-160 and J1-180 are oligodendrocyte-secreted nonpermissive substrates for cell adhesion. *J Cell Biol* **109**, 1765-1778.

- Pike, S. H., Melancon, E. F. and Eisen, J. S.** (1992). Pathfinding by zebrafish motoneurons in the absence of normal pioneer axons. *Development* **114**, 825-831.
- Postlethwait, J., Amores, A., Force, A. and Yan, Y. L.** (1999). The zebrafish genome. *Methods Cell Biol* **60**, 149-163.
- Powell, E. M. and Geller, H. M.** (1999). Dissection of astrocyte-mediated cues in neuronal guidance and process extension. *Glia* **26**, 73-83.
- Prinjha, R., Moore, S. E., Vinson, M., Blake, S., Morrow, R., Christie, G., Michalovich, D., Simmons, D. L. and Walsh, F. S.** (2000). Inhibitor of neurite outgrowth in human. *Nature* **403**, 383-384.
- Probstmeier, R., Stichel, C. C., Müller, H. W., Asou, H. and Pesheva, P.** (2000). Chondroitin sulfates expressed on oligodendrocyte-derived tenascin-R are involved in neural cell recognition. Functional implications during CNS development and regeneration. *J Neurosci Res* **60**, 21-36.
- Qiao, T., Maddox, B. K. and Erickson, H. P.** (1995). A novel alternative splice domain in zebrafish tenascin-C. *Gene* **156**, 307-308.
- Rathjen, F. G., Wolff, J. M. and Chiquet-Ehrismann, R.** (1991). Restrictin - a chick neural extracellular matrix protein involved in cell attachment co-purifies with the cell recognition molecule F11. *Development* **113**, 151-164.
- Rigato, F., Garwood, J., Calco, V., Heck, N., Faivre-Sarrailh, C. and Faissner, A.** (2002). Tenascin-C promotes neurite outgrowth of embryonic hippocampal neurons through the alternatively spliced fibronectin type III BD domains via activation of the cell adhesion molecule F3/contactin. *J Neurosci* **22**, 6596-6609.
- Roos, M., Schachner, M. and Bernhardt, R. R.** (1999). Zebrafish semaphorin Z1b inhibits growing motor axons in vivo. *Mech Dev* **87**, 103-117.
- Rose, T. M., Schultz, E. R., Henikoff, J. G., Pietrokovski, S., McCallum, C. M. and Henikoff, S.** (1998). Consensus-degenerate hybrid oligonucleotide primers for amplification of distantly related sequences. *Nucleic Acids Res* **26**, 1628-1635.
- Ross, L. S., Parrett, T. and Easter, S. S.** (1992). Axonogenesis and morphogenesis in the embryonic zebrafish brain. *J Neurosci* **12**, 467-482.
- Rupp, R. A., Snider, L. and Weintraub, H.** (1994). Xenopus embryos regulate the nuclear localization of XMyoD. *Genes Dev* **8**, 1311-1323.
- Saavedra, R. A., Fors, L., Aebersold, R. H., Arden, B., Horvath, S., Sanders, J. and Hood, L.** (1989). The myelin proteins of the shark brain are similar to the myelin proteins of the mammalian peripheral nervous system. *J Mol Evol* **29**, 149-156.

- Saffell, J. L., Doherty, P., Tiveron, M. C., Morris, R. J. and Walsh, F. S.** (1995). NCAM requires a cytoplasmic domain to function as a neurite outgrowth-promoting neuronal receptor. *Mol Cell Neurosci* **6**, 521-531.
- Saga, Y., Tsukamoto, T., Jing, N., Kusakabe, M. and Sakakura, T.** (1991). Murine tenascin: cDNA cloning, structure and temporal expression of isoforms. *Gene* **104**, 177-185.
- Saga, Y., Yagi, T., Ikawa, Y., Sakakura, T. and Aizawa, S.** (1992). Mice develop normally without tenascin. *Gene Develop* **6**, 1821-1831.
- Sakai, T., Furukawa, Y., Chiquet-Ehrismann, R., Nakamura, M., Kitagawa, S., Ikemura, T. and Matsumoto, K.** (1996). Tenascin-X expression in tumor cells and fibroblasts: glucocorticoids as negative regulators in fibroblasts. *J Cell Sci* **109**, 2069-2077.
- Sambrook, J., Fritsch, E. F. and Maniatis, T.** (1989). Molecular cloning. New York: Cold Spring Harbour Laboratory Press.
- Schachner, M., Antonicek, H., Fahrig, T., Faissner, A., Fischer, G., Künemund, V., Martini, R., Meyer, A., Persohn, E., Pollerberg, E. et al.** (1990). Families of neural recognition molecules. In *Morphoregulatory molecules*, (ed. G. M. Edelman B. A. Cunningham and J. P. Thiery), pp. 443-468. New York: J. Wiley.
- Schachner, M., Taylor, J., Bartsch, U. and Pesheva, P.** (1994). The perplexing multifunctionality of janusin, a tenascin-related molecule. *Perspect. Devel. Neurobiol.* **2**, 33-41.
- Schneider-Schaulies, J., von Brunn, A. and Schachner, M.** (1990). Recombinant peripheral myelin protein P0 confers both adhesion and neurite outgrowth-promoting properties. *J Neurosci Res* **27**, 286-297.
- Schnell, L. and Schwab, M. E.** (1993). Myelin associated neurite growth inhibitors. *Restor. Neurol. Neurosci.* **5**, 32-33.
- Schultemerker, S., Vaneeden, F. J. M., Halpern, M. E., Kimmel, C. B. and Nussleinvolhard, C.** (1994). No Tail (Ntl) Is the Zebrafish Homologue of the Mouse T (Brachyury) Gene. *Development* **120**, 1009-1015.
- Shapiro, L., Doyle, J. P., Hensley, P., Colman, D. R. and Hendrickson, W. A.** (1996). Crystal structure of the extracellular domain from P0, the major structural protein of peripheral nerve myelin. *Neuron* **17**, 435-449.
- Shewan, D., Dwivedy, A., Anderson, R. and Holt, C. E.** (2002). Age-related changes underlie switch in netrin-1 responsiveness as growth cones advance along visual pathway. *Nat Neurosci* **5**, 955-962.

- Shoji, W., Yee, C. S. and Kuwada, J. Y.** (1998). Zebrafish semaphorin Z1a collapses specific growth cones and alters their pathway in vivo. *Development* **125**, 1275-1283.
- Sivron, T., Schwab, M. E. and Schwartz, M.** (1994). Presence of growth inhibitors in fish optic nerve myelin - postinjury changes. *J Comp Neurol* **343**, 237-246.
- Snow, D. M., Brown, E. M. and Letourneau, P. C.** (1996). Growth cone behavior in the presence of soluble chondroitin sulfate proteoglycan (cspg), compared to behavior on cspg bound to laminin or fibronectin. *International Journal Of Developmental Neuroscience* **14**, 331-349.
- Solomon, K. S. and Fritz, A.** (2002). Concerted action of two dlx paralogs in sensory placode formation. *Development* **129**, 3127-3136.
- Sommer, I. and Schachner, M.** (1981). Monoclonal antibodies (O1 to O4) to oligodendrocyte cell surfaces: An immunocytological study in the central nervous system. *Dev Biol* **83**, 311-327.
- Sommer, L. and Suter, U.** (1998). The glycoprotein P0 in peripheral gliogenesis. *Cell Tissue Res* **292**, 11-16.
- Sonnhammer, E. L., Eddy, S. R., Birney, E., Bateman, A. and Durbin, R.** (1998). Pfam: multiple sequence alignments and HMM-profiles of protein domains. *Nucleic Acids Res* **26**, 320-322.
- Spiryda, L. B.** (1998). Myelin protein zero and membrane adhesion. *J Neurosci Res* **54**, 137-146.
- Steen, P., Kalghatgi, L. and Constantine-Paton, M.** (1989). Monoclonal antibody markers for amphibian oligodendrocytes and neurons. *J Comp Neurol* **289**, 467-480.
- Stickney, H. L., Barresi, M. J. and Devoto, S. H.** (2000). Somite development in zebrafish. *Dev Dyn* **219**, 287-303.
- Stockdale, F. E.** (1992). Myogenic cell lineages. *Dev Biol* **154**, 284-298.
- Stratmann, A. and Jeserich, G.** (1995). Molecular cloning and tissue expression of a cDNA encoding IP1--a P0- like glycoprotein of trout CNS myelin. *J Neurochem* **64**, 2427-2436.
- Stuermer, C. A.** (1988). Retinotopic organization of the developing retinotectal projection in the zebrafish embryo. *J Neurosci* **8**, 4513-4530.
- Stuermer, C. A. and Bastmeyer, M.** (2000). The retinal axon's pathfinding to the optic disk. *Prog Neurobiol* **62**, 197-214.
- Stuermer, C. A., Bastmeyer, M., Bähr, M., Strobel, G. and Paschke, K.** (1992). Trying to understand axonal regeneration in the CNS of fish. *J Neurobiol* **23**, 537-550.

- Summerton, J.** (1999). Morpholino antisense oligomers: the case for an RNase H-independent structural type. *Biochim Biophys Acta* **1489**, 141-158.
- Summerton, J., Stein, D., Huang, S. B., Matthews, P., Weller, D. and Partridge, M.** (1997). Morpholino and phosphorothioate antisense oligomers compared in cell-free and in-cell systems. *Antisense Nucleic Acid Drug Dev* **7**, 63-70.
- Tan, S. S., Crossin, K. L., Hoffman, S. and Edelman, G. M.** (1987). Asymmetric expression in somites of cytotactin and its proteoglycan ligand is correlated with neural crest cell distribution. *Proc Natl Acad Sci U S A* **84**, 7977-7981.
- Taylor, J., Pesheva, P. and Schachner, M.** (1993). Influence of janusin and tenascin on growth cone behavior in vitro. *J Neurosci Res* **35**, 347-362.
- Taylor, J. S., Van de Peer, Y., Braasch, I. and Meyer, A.** (2001). Comparative genomics provides evidence for an ancient genome duplication event in fish. *Philos Trans R Soc Lond B Biol Sci* **356**, 1661-1679.
- Tessier-Lavigne, M. and Goodman, C. S.** (1996). The molecular biology of axon guidance. *Science* **274**, 1123-1133.
- Tomizawa, K., Inoue, Y., Doi, S. and Nakayasu, H.** (2000). Monoclonal antibody stains oligodendrocytes and Schwann cells in zebrafish (*Danio rerio*). *Anat. Embryol. (Berl.)* **201**, 399-406.
- Tongiorgi, E.** (1999). Tenascin-C expression in the trunk of wild-type, cyclops and floating head zebrafish embryos. *Brain Res Bull* **48**, 79-88.
- Tongiorgi, E., Bernhardt, R. R. and Schachner, M.** (1995a). Zebrafish neurons express two L1-related molecules during early axonogenesis. *J Neurosci Res* **42**, 547-561.
- Tongiorgi, E., Bernhardt, R. R., Zinn, K. and Schachner, M.** (1995b). Tenascin-C mRNA is expressed in cranial neural crest cells, in some placodal derivatives, and in discrete domains of the embryonic zebrafish brain. *J Neurobiol* **28**, 391-407.
- Tucker, R. P., Hagios, C. and Chiquet-Ehrismann, R.** (1999). Tenascin-Y in the Developing and Adult Avian Nervous System. *Dev Neurosci* **21**, 126-133.
- Van de Peer, Y., Taylor, J. S., Joseph, J. and Meyer, A.** (2002). Wanda: a database of duplicated fish genes. *Nucleic Acids Res* **30**, 109-112.
- Varnum-Finney, B., Venstrom, K., Muller, U., Kypta, R., Backus, C., Chiquet, M. and Reichardt, L. F.** (1995). The integrin receptor alpha 8 beta 1 mediates interactions of embryonic chick motor and sensory neurons with tenascin-C. *Neuron* **14**, 1213-1222.

- Venkatesh, B., Erdmann, M. V. and Brenner, S.** (2001). Molecular synapomorphies resolve evolutionary relationships of extant jawed vertebrates. *Proc Natl Acad Sci U S A* **98**, 11382-11387.
- Verna, J. M., Fichard, A. and Saxod, R.** (1989). Influence of glycosaminoglycans on neurite morphology and outgrowth patterns in vitro. *Int J Dev Neurosci* **7**, 389-399.
- Walsh, F. S. and Doherty, P.** (1997). Neural cell adhesion molecules of the immunoglobulin superfamily: Role in axon growth and guidance. *Annu Rev Cell Dev Biol* **13**, 425-456.
- Wanner, M., Lang, D. M., Bandtlow, C. E., Schwab, M. E., Bastmeyer, M. and Stuermer, C. A. O.** (1995). Reevaluation of the growth-permissive substrate properties of goldfish optic nerve myelin and myelin proteins. *J Neurosci* **15**, 7500-7508.
- Weber, P., Bartsch, U., Rasband, M. N., Czaniera, R., Lang, Y., Bluethmann, H., Margolis, R. U., Levinson, S. R., Shrager, P., Montag, D. et al.** (1999). Mice deficient for tenascin-R display alterations of the extracellular matrix and decreased axonal conduction velocities in the CNS. *J Neurosci* **19**, 4245-4262.
- Weber, P., Montag, D., Schachner, M. and Bernhardt, R. R.** (1998). Zebrafish tenascin-W, a new member of the tenascin family. *J Neurobiol* **35**, 1-16.
- Wehrle-Haller, B. and Chiquet, M.** (1993). Dual function of tenascin - Simultaneous promotion of neurite growth and inhibition of glial migration. *J Cell Sci* **106**, 597-610.
- Weller, A., Beck, S. and Ekblom, P.** (1991). Amino Acid Sequence of Mouse Tenascin and Differential Expression of Two Tenascin Isoforms During Embryogenesis. *J Cell Biol* **112**, 355-362.
- Westerfield, M.** (1987). Substrate interactions affecting motor growth cone guidance during development and regeneration. *J Exp Biol* **132**, 161-175.
- Westerfield, M.** (1989). The zebrafish book: a guide for the laboratory use of zebrafish (*Brachydanio rerio*). Eugene: University of Oregon Press.
- Westerfield, M. and Eisen, J. S.** (1988). Neuromuscular specificity: Pathfinding by identified motor growth cones in a vertebrate embryo. *TINS* **11**, 18-22.
- Westerfield, M., McMurray, J. V. and Eisen, J. S.** (1986). Identified motoneurons and their innervation of axial muscles in the zebrafish. *J Neurosci* **6**, 2267-2277.
- Wilson, S. W., Ross, L. S., Parrett, T. and Easter, S. S., Jr.** (1990). The development of a simple scaffold of axon tracts in the brain of the embryonic zebrafish, *Brachydanio rerio*. *Development* **108**, 121-145.
- Wintergerst, E. S., Bartsch, U., Batini, C. and Schachner, M.** (1997). Changes in the expression of the extracellular matrix molecules tenascin-C and tenascin-R after 3-

acetylpyridine-induced lesion of the olivocerebellar system of the adult rat. *Eur J Neurosci* **9**, 424-434.

Wolburg, H. and Bouzheouane, U. (1986). Comparison of the glial investment of normal and regenerating fiber bundles in the optic nerve and optic tectum of the goldfish and the Crucian carp. *Cell Tissue Res* **244**, 187-192.

Woodruff, R. H., Tekki-Kessarlis, N., Stiles, C. D., Rowitch, D. H. and Richardson, W. D. (2001). Oligodendrocyte development in the spinal cord and telencephalon: common themes and new perspectives. *Int J Dev Neurosci* **19**, 379-385.

Xiao, Z. C., Bartsch, U., Margolis, R. K., Rougon, G., Montag, D. and Schachner, M. (1997). Isolation of a tenascin-R binding protein from mouse brain membranes. A phosphacan-related chondroitin sulfate proteoglycan. *J Biol Chem* **272**, 32092-32101.

Xiao, Z. C., Revest, J. M., Laeng, P., Rougon, G., Schachner, M. and Montag, D. (1998). Defasciculation of neurites is mediated by tenascin-R and its neuronal receptor F3/11. *J Neurosci Res* **52**, 390-404.

Xiao, Z. C., Taylor, J., Montag, D., Rougon, G. and Schachner, M. (1996). Distinct effects of recombinant tenascin-R domains in neuronal cell functions and identification of the domain interacting with the neuronal recognition molecule F3/11. *Eur J Neurosci* **8**, 766-782.

Yamagata, M., Herman, J. P. and Sanes, J. R. (1995). Lamina-specific expression of adhesion molecules in developing chick optic tectum. *J Neurosci* **15**, 4556-4571.

Yazaki, T., Miura, M., Asou, H., Toya, S. and Uyemura, K. (1994). Peripheral myelin P0 protein mediates neurite outgrowth of cortical neurons in vitro and axonal regeneration in vivo. *Neurosci Lett* **176**, 13-16.

Yeo, S. Y., Little, M. H., Yamada, T., Miyashita, T., Halloran, M. C., Kuwada, J. Y., Huh, T. L. and Okamoto, H. (2001). Overexpression of a slit homologue impairs convergent extension of the mesoderm and causes cyclopia in embryonic zebrafish. *Dev Biol* **230**, 1-17.

Yokosaki, Y., Matsuura, N., Higashiyama, S., Murakami, I., Obara, M., Yamakido, M., Shigeto, N., Chen, J. and Sheppard, D. (1998). Identification of the ligand binding site for the integrin alpha9 beta1 in the third fibronectin type III repeat of tenascin-C. *J Biol Chem* **273**, 11423-11428.

Yoshida, M. and Colman, D. R. (1996). Parallel evolution and coexpression of the proteolipid proteins and protein zero in vertebrate myelin. *Neuron* **16**, 1115-1126.

You, K. H., Hsieh, C. L., Hayes, C., Stahl, N., Francke, U. and Popko, B. (1991). DNA sequence, genomic organization, and chromosomal localization of the mouse peripheral myelin protein zero gene: Identification of polymorphic alleles. *Genomics* **9**, 751-757.

Zhang, J. and Granato, M. (2000). The zebrafish unplugged gene controls motor axon pathway selection. *Development* **127**, 2099-2111.

Zhang, J., Malayaman, S., Davis, C. and Granato, M. (2001a). A dual role for the zebrafish unplugged gene in motor axon pathfinding and pharyngeal development. *Dev Biol* **240**, 560-573.

Zhang, Y., Tohyama, K., Winterbottom, J. K., Haque, N. S., Schachner, M., Lieberman, A. R. and Anderson, P. N. (2001b). Correlation between putative inhibitory molecules at the dorsal root entry zone and failure of dorsal root axonal regeneration. *Mol Cell Neurosci* **17**, 444-459.

Zhang, J., Shuxia Z., and Granato, M. (2002). Positional cloning of the unplugged gene. 5th International conference on zebrafish development and genetics, Wisconsin-Madison.

7. Zusammenfassung

Das zentrale Nervensystem (ZNS) der Fische wächst während ihres gesamten Lebens und ist in der Lage verletzte Axone zu regenerieren. Diese Eigenschaft unterscheidet es von dem der Säuger, die nicht in der Lage sind, verletzte Axone im ZNS zu regenerieren. Vielmehr ähnelt das ZNS der Fische dem peripheren Nervensystem (PNS) der Säuger, mit seiner Fähigkeit zur Regeneration. Während der Entwicklung des Nervensystems und auch während der Regeneration des adulten Nervensystems werden Moleküle exprimiert, die den Zell-Zell-Kontakt, oder auch den Kontakt einer Zelle mit der extrazellulären Matrix vermitteln. Zu diesen Molekülen gehören die neuronalen Zellerkennungsmoleküle Protein Zero (P0), Tenascin-R (TN-R) und Tenascin-C (TN-C). In dieser Arbeit wurde die Expression und Funktion der neuronalen Zellerkennungsmoleküls P0 und TN-R während der Entwicklung und Regeneration des Nervensystems des Zebrafisches untersucht. Weiterhin wurde die Funktion von TN-C während des Auswuchses von Motoraxonen im Rumpfbereich des Zebrafisches analysiert.

P0 gehört zur Immunglobulin-Superfamilie der neuronalen Zelladhäsionsmoleküle, und ist im PNS von Säugern an der Kompaktierung des Myelins beteiligt. Die Durchsuchung einer EST-(expressed sequence tag)-Datenbank führte zur Identifizierung des P0 Gens im Zebrafisch. Ein Vergleich der Proteinsequenz zeigte, daß das Zebrafisch P0 zu 45% identisch mit anderen P0 Homologen aus Wirbeltieren ist. Untersuchungen des zeitlichen und räumlichen Expressionsmusters mittels in-situ Hybridisierung während der frühen Entwicklung des Zebrafisches zeigten eine Expression von P0 mRNA im Nachhirn. Zu späteren Zeitpunkten konnte die Expression von P0 mRNA hauptsächlich in Gliazellen in myelinisierten Bereichen des ZNS und im PNS nachgewiesen werden. Dies läßt auf eine Rolle von P0 bei der Myelinisierung von Axonen schließen. Nach einer Läsion des optischen Nervs wird die mRNA für P0 im gesamten optischen Trakt von adulten Zebrafischen transient hochreguliert. Dabei ist die verstärkte Expression von P0 mRNA im optischen Trakt abhängig von der Anwesenheit regenerierender Axone. Nach einer Läsion des Rückenmarks konnte ebenfalls eine erhöhte Expression der P0 mRNA, die sich hauptsächlich auf die weiße Substanz beschränkte, beschrieben werden. Die Hochregulation von P0 mRNA in Gliazellen nach einer Läsion des ZNS läßt auf einen positiven Einfluß dieses Moleküles während der Regeneration und Remyelinisierung von Axonen im adulten Zebrafisch schließen.

TN-R, ein Molekül der extrazellulären Matrix, wurde im Gegensatz zu P0 als ein inhibitorisches Molekül für regenerierende Axone von Säugern beschrieben. Um den Einfluß von TN-R während der Regeneration im Zebrafisch zu untersuchen, wurde das Gen im Zebrafisch kloniert. Eine Analyse der abgeleiteten Proteinsequenz ergab eine hohe Identität

(60%) zu anderen TN-R Homologen in Wirbeltieren. Die Expression von TN-R wurde im sich entwickelnden und adulten optischen System sowie nach einer Läsion des adulten optischen Nerven mit Hilfe von in-situ Hybridisierung und Immunhistochemie untersucht. Diese Analysen zeigten, daß TN-R vor und nach einer Läsion des optischen Nerven mit Retinaganglienzellaxonen innerhalb der Retina assoziiert ist. Außerhalb der Retina begrenzt TN-R den Pfad der Retinaganglienzellaxone bis hin zu ihren Zielorten im Tektum. Um die Funktion von TN-R während des Wachstums von Retinaganglienzellaxonen zu untersuchen, wurden Retinaexplantate *in vitro* mit einem homogenen TN-R Substrat (Situation in der Retina) oder mit TN-R in einer Grenzsituation konfrontiert (Situation im Gehirn). Während sich das homogene TN-R Substrat als wachstumsfördernd erwies, wurden auswachsende Neuriten von einer TN-R Grenze aufgehalten. Diese Ergebnisse lassen auf eine duale Rolle von TN-R während des Wachstums von Retinaganglienzellaxonen schließen. In der Retina fördert TN-R den Auswuchs von neuen Axonen, im Gehirn hingegen fungiert TN-R als Wegfindungsmolekül, indem es dazu beiträgt, daß die Retinaganglienzellaxone zu ihren Zielorten im Tektum gelangen. Es ist vorstellbar, daß TN-R auch für regenerierende Axone ein Wegfindungsmolekül darstellt und so im Gegensatz zu Säugern, bei denen es inhibierend auf regenerierende Axone wirkt, zu einer erfolgreichen Regeneration von Axonen im ZNS von Zebrafischen beiträgt.

TN-C, ebenfalls ein Molekül der extrazellulären Matrix, wird während der frühen Entwicklung des Zebrafisches in Myotomzellen des Somiten, in Neuralleistenzellen und im Hypochord exprimiert. Das TN-C Gen welches zuvor nur in Teilen bekannt war, wurde vollständig kloniert. Eine Analyse der abgeleiteten Proteinsequenz zeigte eine 45% Identität zu anderen TN-C Homologen in Wirbeltieren. Die genaue Verteilung von TN-C im Rumpfbereich des sich entwickelnden Embryos wurde durch in situ Hybridisierung und immunhistochemische Färbungen untersucht. Dabei konnte das Protein in einer Region am horizontalen Myoseptum, die wichtig für die Wegfindung von Motoraxonen ist, nachgewiesen werden. Um den Einfluß von TN-C auf das Wachstum von Motoraxonen zu untersuchen, wurde die Funktion von TN-C *in vivo* perturbiert. Die Translation der TN-C mRNA wurde durch Injektion von *antisense* Oligonukleotiden (Morpholinos) inhibiert. In einem alternativen Experiment wurde die Menge an vorhandenem TN-C durch die Injektion von *in vitro* transkribierter mRNA oder Proteinfragmenten erhöht. Der Phänotyp der behandelten Embryonen wurde 24 und 33 Stunden nach der Befruchtung durch immunhistochemische Färbungen analysiert. Diese Experimente zeigten einen eindeutigen Einfluß von TN-C auf die embryonale Wegfindung von Motoraxonen im Rumpfbereich. Eine

Reduktion von TN-C führte dabei zu abnormalen Verzweigungen von Motoraxonen, während eine Erhöhung von TN-C zu einer Verkürzung dieser Axone führte. In der Zebrafisch *unplugged* Mutante, die ähnliche Phänotypen aufweist wie sie nach der Injektion von Morpholinos beobachtet wurden, ist TN-C in der Entscheidungsregion der Motoraxone am horizontalen Myoseptum nicht vorhanden. Weiterhin konnte die Expression von TN-C mRNA in adaxialen Zellen, die an der Entstehung des *unplugged* Phänotyps beteiligt sind, nachgewiesen werden. Zusammengefasst deuten diese Resultate auf eine wichtige Funktion von TN-C während der Wegfindung von Motoraxonen im Rumpfbereich des Zebrafisches hin.

In dieser Arbeit wurden drei Gene im Zebrafisch kloniert und ihre Expression charakterisiert. Weiterhin konnten neue Funktionen dieser Gene während des axonalen Wachstums und der Regeneration im Zebrafisch beschrieben werden.

7. Summary

The central nervous system (CNS) of fish is growing throughout its lifetime, it also retains the capacity to regrow severed axons after a lesion. In this capacity, the fish CNS differs from the adult mammalian CNS which generally does not support axon regeneration but resembles the adult mammalian peripheral nervous system (PNS) in which axon regeneration occurs. During development of the CNS and also during regeneration of the adult CNS, neural cell recognition molecules are expressed which mediate the contact between cells or the contact between cells and the extracellular matrix. Protein zero (P0), tenascin-R (TN-R) and tenascin-C (TN-C) belong to this family of neural cell recognition molecules. In this work, we analyzed the expression and function of P0 and TN-R during development and regeneration of the CNS. Furthermore, we analyzed a potential role of TN-C during the growth of motor axons in the trunk at early developmental stages in the zebrafish.

P0 belongs to the immunoglobulin superfamily of neural cell adhesion molecules and mediates the compaction of myelin in the PNS of mammals. Furthermore, P0 supports axon regeneration in the mammalian PNS. We identified a P0 homolog in zebrafish, which is 45% identical to other P0 homologs in vertebrates on the amino acid level. The expression of P0 mRNA was analyzed by *in situ* hybridisation. At early stages, the expression of P0 mRNA could be detected in the hindbrain of the zebrafish embryo. Later, the expression of P0 mRNA was detected in glial cells in the CNS and PNS in areas known to be myelinated. This is consistent with a role for P0 in myelination. After an optic nerve crush, a transient upregulation of P0 mRNA in the optic pathway was observed. Furthermore, it could be shown that the upregulation of P0 mRNA is dependent on the presence of regenerating axons. Spinal cord transection also leads to an increased expression of P0 mRNA in the white matter tracts of the spinal cord. The upregulation of P0 mRNA expression in glial cells after a lesion of the adult zebrafish CNS suggests a role for P0 in promoting axon regeneration and remyelination after injury.

In contrast to P0, which has been described to promote axon regeneration, TN-R, a molecule of the extracellular matrix, has been described to inhibit axon regeneration in mammals. To analyze the function of TN-R during regeneration of the CNS in fish, the gene was cloned in the zebrafish. Sequence analysis revealed a high degree of homology (60%) to other TN-R homologs in vertebrates. In the developing and adult optic pathway before and after optic nerve crush, TN-R co-localizes with optic fibers in the retina, but closely borders the pathway of optic axons on their way to the tectum, as determined by *in situ* hybridization and immunohistochemistry. We mimicked the distribution of TN-R in the optic pathway *in vitro*

by confronting zebrafish optic axons with a homogeneous TN-R substrate (retinal situation) or with a border of TN-R (brain situation). While the homogeneous substrate enhanced growth of optic axons, the substrate border repelled these axons. Thus, TN-R may play a dual role for optic axons by promoting growth of newly added axons in the retina and guiding these axons by a repellent mechanism in the brain. TN-R bordering the optic pathway in the brain is also available to potentially guide regenerating optic axons after injury and thus, in contrast to mammals, may contribute to successful regeneration of axons in the zebrafish.

TN-C, which is also a molecule of the extracellular matrix, is expressed in myotomal cells of the somites, in neural crest cells and in the hypochord during early development. The cloning of TN-C gene in the zebrafish, which was only partially known was . Analysis of the protein sequence revealed an identity of 45% of zebrafish TN-C to other TN-C homologs in vertebrates. The distribution of TN-C in the trunk of the developing zebrafish embryo was analyzed using immunohistochemistry and in situ hybridization. TN-C immunoreactivity was detected in the middle of the somites at the level of the horizontal myoseptum, which is an important choice point for growing motor axons. To analyze a potential role of TN-C during growth of motor axons in the trunk, the function of this molecule was perturbed. The translation of TN-C mRNA was inhibited by injection of antisense oligonucleotides (morpholinos). In another experiment, the amount of TN-C was increased by mRNA overexpression and protein injections. The phenotypes of the injected embryos were analyzed by immunohistochemistry at 24 and 33 hours post fertilization. These experiments revealed an explicit role of TN-C on motor axon guidance in the trunk of the developing embryo. A reduction of TN-C induces abnormal branches of motor axons, whereas increased amounts of TN-C led to truncations of these axons. In the zebrafish *unplugged* mutant, which displays a phenotype similar to what was observed after injection of the TN-C morpholino, TN-C immunoreactivity was found to be absent from the choice point of motor axons at the level of the horizontal myoseptum. Furthermore, the expression of TN-C mRNA was detected in adaxial cells, which have been described to play a role in the formation of the *unplugged* phenotype. These results indicate an important function of TN-C during motor axon pathfinding in the trunk of the developing zebrafish embryo.

In this work, three genes in the zebrafish have been cloned and the corresponding expression patterns were described. Furthermore, new functions of these genes during axon growth and regeneration could be elucidated.

8. APPENDIX

8.1 Abbreviations

∅	“without”, diameter
μ	micro (10 ⁻⁶)
× g	g-force
°C	grad celsius
aa	amino acid
A	adenine
Acc.	accession number
Amp	ampicillin
ATP	adenosine triphosphate
bp	base pairs
BSA	bovine serum albumine
C	Cytosine
cDNA	complementary deoxyribonucleic acid
CTP	cytosine triphosphate
Da	dalton
dATP	2'-desoxyadenosinetriphosphate
dCTP	2'-desoxycytidinetriphosphate
DEPC	diethylpyrocarbonate
dGTP	2'-desoxyguanosinetriphosphate
DMSO	dimethylsulfoxide
DNA	deoxyribonucleic acid
DNase	desoxyribonuclease
dNTP	2'-desoxyribonucleotide-5'-triphosphate
DTT	dithiothreitol
<i>E. coli</i>	escherichia coli
EDTA	ethylendiamintetraacetic acid
f.c.	final concentration
g	gramm
G	guanosine
h	human, hour
HEPES	2-(4-(2-Hydroxyethyl)-piperzino)-ethansulfonic acid
hpf	hours post fertilization
IPTG	isopropyl-β-D-thiogalactoside
Kana	kanamycin
kb	kilo base pairs
l	litre
LB	Luria Bertani
m	milli (10 ⁻³)
min	minute
MOPS	(4-(N-morpholino)-propan)-sulfonic acid
mRNA	messenger ribonucleic acid
n	nano (10 ⁻⁹)
Nt	nucleotide(e)
OD _x	optic density

ORF	open reading frame
p	pico (10^{-12})
PAGE	polyacrylamide gel electrophoresis
PBS	phosphat-buffered saline
PCR	polymerase chain reaction
rpm	rounds per minute
psi	pounds per square inch
RNA	ribonucleic acid
RNase	ribonuclease
RT	room temperature
s	second
SDS	sodium dodecyl sulfate
T	thymine
TABS	(N-tris(Hydroxymethyl)methyl-3-aminopropane-sufonic acid
Tab.	table
TE	tris-EDTA
TEMED	N,N,N',N'-tetraethylenamine
Tet	tetracycline
T_m	melting temperature
TM	transmembrane segment
Tris	tris(-hydroxymethyl)-aminomethane
U	unit (enzymatic)
V	volt
v/v	volume per volume
Vol.	volume
w/v	weight per volume
ZMNH	Zentrum für Molekulare Neurobiologie Hamburg

8.2 Morpholino sequences

Nr.	Morpholino	Sequence (5` - 3`)	remarks
1	TNC 1	GAGAGGATCTCACAGGACACTCC	Strong inhibition of TNC expression
2	Control	CCTCTTACCTCAGTTACAATTTATA	Standard control morpholino

8.3 Full length cDNA sequences of myelin protein zero, tenascin-R and tenascin-C

Myelin protein zero:

CAGGCCCGGTCCGGAATTCCTGGTTCGACCCACGCGYCCGGTCTCATTCTCTTTTCTCCCTCCATCTCTTCTCC
 TTTCTCCATCCCTTGCTCTCTCGGGACCCCTCACGTATACTGACCTGCGGGGAGATCGGAGAGAGATCATGCTGT
 CCGTACTGGCACTGACCTCCGTGGTGTCTTTGGGCATAGCCTCTCAGAGCACGGCTCTAGTGGTGAACACAGACT
 CGGAGAAACATGCATTGGTGGGCTCAGATGTCAGACTCTCCTGCTCTTTCTTCTCCTGGCAGTGGACTTCTCCAG
 AAGTGTCTTTTACATGGCATTACCGTCCAGATGGGGCTAAGGACGCAATCTCAATTTTCCACTATGGAGGTGGAG
 AAGCTTATCCAGCTAATAAAGGCCATTCCTAAAACCGCTGGAGTTTGTGGGCAACCCTAGTCGCCGTGACGGTT
 CTATCCTGATCAAGAACCTTGATTTTCGGAGACAATGGAACCTTCACCTGTGATGCCAAGAACCACCTGACATCG
 GCGGCCACCCCTCAACCATTCGGCTGCTGGTGTGTTGAGAAGGTTCCAGTGCAGGCTGGTGTGATAACGGGCTCCA
 TTATTGGTGTAGTGTGGGACTGCTGATCCTCGTTGTGGCAATTTACTATCTGATGCGCTTCTCTGGTGGCCAGAA
 GGGTGTTCAGCTTGAGCATGAGCAAACATGGCAAGAAAGGCAAGGAAAAGGATCACAGCAAAAAACAGCGTA
 TCTGACACCCCTTTTTCTGGTCAATTTTTCTACTTTTACATGTATAAAATTCATCTCATCATCTGATACACTGGTGCT
 ATTACTTCCCTGTAGGCCGGCCCCAAAAGTAGCCTCCCATCCCCACCCCTTCATTTACTGAGAGCTAAATATATAG
 CACTAGTATTTTTAGTACACACACTTTTTTAGTCTCACTTTTTTAAAATTCATTACAGTCAAAGAGAATTCCTTC
 TTTCGGAAACACACACTCACTAACACTCATCTCATGTATCCCATCACGCAGTTTTAAGTGCCTTCCCAAAGTA
 CATTTACAGCGAATCTGGCTTAGTTTTGCTCTGACAGCGTCGACTGAAATACCCGAAATGACGTTGATACTGTT
 GGCAGCGAAACTCAAACATGCTGTGAGAGTTACTTGACACTCTAAGCCAGATTCTCACGCTCTGTTGTCTGACAAG
 CAGCTGATTATTTTAAAGCACACTTGTAAATGGCAGAACGACCTCTGTCTCCATTCGCCCCATTATTTTTTTAAGC
 CAATGAGGGCCGGCTCCTATGGAGGCACTGTCCCTCGACCTTCATATATCATTAGTAAAGCTCCATCGCTCCATC
 CCGAATCATAGTTTTACTTCACCTCTCTCTAATTCCTCTAACTATCATAAACGCTCATCCACCAGCTCCTCTT
 CTCATTCCCTGTTTTCTGCTGGTATGGTGTCTCTCTCTGCCCCCTGTGCCCACAGGAGAAACATTTACATTCCG
 CCAGTCAAAAGACGTCAATGCAAAAACAAAAAGTTAATTTAACTAGCTCTCTGCAGACTATGAGGCGCATGTGT
 ATGTTTTTATCTGATGAGATGTAACCTGTCAACATTAGGGGAACAAAACAACATAAAGACGCCATGTCAATTGTA
 AGTAATGAAAATCCTATGACTGTTTTGTGTGTGCGGAAGCAGAAATGTAATAGAGTTTTAATGATGTTTAATAATGT
 TTCTGCACTTTTCACTGACTGACGTGGCGGTGTTTATGTGGCTGCTGCTTCAACAGTGTTTACCATCAGCTTG
 TTGGCTTGCTAAGTCCACAGGAAGTGATGCAACGAGGGCAGAGAGGTTTTTCGAGAGAGATATAAAATGATGAAATA
 CCGGGTCGGAGACTTGACTGAATACATATTGAGGGGAAAAGTCCAGGCCAAAGTCCAGTAAACATTTCTCACTGGA
 TGTGTTTTTGTGTCTTCAAGTCTTCGTGTCAACCCTGAGACCGAGAGGGGCTCTCATCGGGAAAAGTTTTAGAATA
 GTGAGGGCTTGTGGGAAATATGTTTTGTACTAGAGACAGATGTTTTTATGCATCTCAGAGTTGAGGTGCGAGC
 AGCCACATGGCTTCTGCCATTAACCTGTGTTTTAAATATTGGGGAATCGCCATGTTGTATGTATTGTGTGCCCTG

TATTGGTAAAGGTC TAGGTAACCGTTC TCTCTCTTTAAACTCCATTTAAAACGGCTAATAATTTTTTACTTTTATTT
 TGACTTTAACCTCGCTAACATTGGTTTTCTGTAAAATGTCTTGTAAAATGTAAATGCTCAAGTTCAAATAATTTTC
 AGAAAAATGTCAATAAAAAAATCAGATCCCTAAAAAAGGGCGCCGCTCTAGAGGATCCA
 AGCTTACGTACG

Tenascin-R

AGCCTCCTCATTGCAGCCNGACAGGCAGCCAGAGAGGAGCTCCAGTTCGAACCCGTGGCAACAATAGACTACAGA
 AAACACAGCTTGACCAATCAATAGACCTCTGCCAGAAACATTTGTGAGCCGAGAGAGCTGCTCAAGGACCACGGA
 GGAGCAGATAAGGTGAAGGTC TGAGGCAATTACAGCGCCGCTTTCCAAACTAGAAACTACTGGGGAAATTTCCA
 GAGCAGCAGACGGCACTAGTTATCCTTCTTTGTGGTGAGACAGGAGGAACATCAGCACTGGCACTTAAGTGCCAA
 TCAGAGGTCTATTTGTGGAGTTGATGATCTCACCCTAGTGCCGAGTTGTGATGTGGGGGTGCaCCATGGCAATA
 CAAGGTT CAGTAGTGAGCCTGGCTCTACTGTTCTTCGGGATTC AAGCTGTTC CAGCCCCACCAGCAA ACTAGTG
 AGGACCACAAGGGTGAGGCGACAGGTTCCAGAGGGGGCGATCCTGCTGACAACCAGATGCAGCCTATGGTCTTC
 AATCACGTATAACAATCAACGTACCTGTAGAGTCCCTCTGTT CAGTGGACCTAGATGCGGTGACAGGTCCAGAG
 ACGAACAAAACAGCATCTGGGAGTGATAAGATGCCGACGGAGTACACAGAGGAAA CAGTGGACTCGGACAGCCAG
 GTGACCTTCACCCATCGCATCAATATCCCAAAGCAGGCTGTGCTTGTCTTCGGCTACCACCATAGAGCAGCTG
 GCAAGCCGCATAGAGATGCTGGAGAGAGAGGTGTCGCTGCTTCGAACGCAGTGTAGCTCCAGCTGCTGCGGAGAG
 AGCTCTGT CATGGGTCGCC TAGACTTCGTCCCTCAGTGC GGCCATGGCACATTCAGTATGGAGGTTTTCGGGGTGT
 GTTTGTGAAGAAGGCTGGATTGGCAAGA ACTGC ACTGAGCCACGCTGCC CAGACGACTGCTCGGGCCAGGGCATT
 TGCATCGAAGGCGATTGTGTTTGC GACCGTAATTTCCGGTGGTGAAA ACTGCTCCGAGCCACGATGTCCAAGTGAC
 TGCTCTGACAGGGGCTTGTGTATTGACGGGGAGTGTGTTTGTGAGGAGGCTTCGCGGGGGAGGACTGCTCACTG
 GGCAGATGTCTAAACGACTGCTCGGATCAAGGGCCCTGTGTGAACGGGAGCTGCCAGTGCCGATCCGGCTTCCTG
 GGGGAAGACTGCTCTCTCATCTTCTGCGCTAATAACTGCAGCCAGAGAGGGGTGTGCAAGGAGGGCTTCTGCGTC
 TGTC AAGAGGGATACACAGGAGATGACTGC ACTTCAGTTTTACCTCCAATGAATCTGCGAGTTTCGGGAGTGTCA
 GAAAACACCATTGATCTACAGTGGGAAGGCCAGCGATCCTGACAGACTATCTCATCACTTATGAACCAACA ACT
 CCAGGCGGAGTCCAGCTAGAAATGAGAGTCCCGGGAAATGTTACCAACATCACCATCAAAGGTTTAAATCCGGGT
 CTGGAGTACAATGTCAATGTGTATGCAGTGATTGACAACATCATCAGCTCCCCAATGAACACCTTAGTCTCCACC
 TATCTCTCAAATCCAGACGGTTTACTCTTCAAATCCATCATGGAGACATCCGTGGAGGTTCAATGGCAACCCTTA
 GACTACTTGT TTTGATGGTTGGGAAATAAGCTTCATTC CCAAGGACAATGATGGAGGGATGACAGCACAGCTACCC
 AGTACCATCACATCTTTCCACCAAACGGGACTGAAGCCTGGAGAAGAATACACTGTCAACCTGGTGGCCCTGAAA
 GACCAAGGCAGGAGCCTGCCTGTTACCGCAACTGTTACCACACTGATTGATGGGCCAATACAGCTTATTGTGCGA
 GACATCTCAGACACGGTTGCGTTTGTGGAGTGGAGCCACCCAAGGCTAAAGTGGACCAGATTATACTGCGTTAC
 GGGCTGGTAGGGGTAGAAGGGCCAAAACACCCTTTCGCCTTCAGCCTACTCTGAGCCAGTACTCACTCCAAGTC
 CTGAGGCCGGGATCTACATATGAAGTATCAGTCAGTGGAGTCCGCAATGGCACTGAGAGTGGAGTTATTTCAACA
 GAATTCACAACAGAAATCGATGCGCCAAAGAACCTGAGAGTGTCTGCAAAA ACTTCTATTAGCCTGGAGCTGGAA
 TGGGACAATAGTGAAGCTGATGTTGAGGGTTACAGTGTGGTCTATAGCACACTTGCCGGTGATCAGTATGACAAA
 GTCATTGTCCCACGCAAYGATGGTCCAAGCACTAAA ACTACTCTCAATGA ACTAATGCCAGGCACAGAGTATGGA
 ATAGGAATTT CAGCTGTACTTGGTGCCAACCAGAGCACCC CAGCAACGATGAATGCCAGAACGGGTCTGGACGTC
 CCATTAGATTTGACTGTCACAGCCTCCACCGACAACACCATCACCCTTTTATGGGGCACAGTGCAGGGGGCTATT
 GATCACTATAGGGTGACTTACACATCATCCAGTGGAGTCACTGAGCTCACTGTGCCTAAAGACGTCACCACC
 ACCACACTGACAAGCCTACAGCCGGGCACCGAGTACACAATCACTGTGGCAGCGCAACGAGGCAGGCAGCAGAGC

ACGGCGGCCACTATCGATGCC TTCACAGGGTCCGCCCAATCACACAGCTCTTCTTCTCTGAGGTCTCCTCTGAT
 TCATTGACTGTGGCGTGGAGTTCACCGGCTCCACCTGCTGACGCATTTCATCTTGAAC TACAGCGCTCAGGACTCC
 AGTGAGGATTCTGAGATTGCGCTTGATGGGTCGAAAACCAGAATCACCC TACTGGTCTAATGCCATCCAGGCGC
 TACACTGCTACATTGGTCACCATGCATGGCAATGTGACTTCAAAGCCAGTTGTAGGCTCAGTCAACACAGGAATG
 GATCCTCCTAGAGACATCACTGTGCTGTATGTCACTGAAGAATCTGTAACCATAACATGGATTCAACCCCTCGCT
 CTCCTTGATTACTACAGAATGTCTTACCAATCATCTAAAGGAAGGATGGACAGTGTGGTGATTGACAGCGACATT
 AATAACTATACCCTAACCAGCCTCCATCCAGCAACAGAGTATGAAATCAAGCTGAACGCAGTGAGAGGAAGCCAA
 GAGAGCAAGGTCATCACCCTACCGTATTCACAGCTATAGACATGCCAGCGGAGCTCACTGCACTGAACGTTACA
 CCCAAGGGGCTCTGCTGCGCTGGAACCCCCCAGCTTCCAGTGTGATAACTACGTGCTCACTGTCAACCCGGAAC
 CAAGTTACAGCAGACACCTTCTTAGTGGAGGGTAACAAGCAGGAGTATCAGCTGAGTCAGCTCATCCCCAGCACC
 ACCTACTCAGTGGCCCTTTATGCCACCAAAGGTCTCTCACCAGCGGCACGGTCATCTCCAACCTTTGTACACCC
 ATGGATGCTCCCCAGAACCTGACAGCTAGTGAGATTAACCATCGAAGTGCCCTCATATCCTGGCAGCCACCATC
 GCAGACATCGACAATTACATGCTGACCTACAAAGCAGCGGATGGCAGTCGAAAGGAGCTGATCTTAGATGCGGAA
 GACACATGGATTCTGCTCGAGGGGCTGGCGGAGACCACCGAATATACTGTGAGACTGCAAGTCGCCAGAGGATTA
 GAAACCAGTGTATTGTCTTCTACATCTTTCACAACAGGAAACCGATTGTTTCCAACGCCACAGAACTGTGCGCAA
 CACCTCCTAAACGGCGAGACTCTAGGTGGGATCTACACTATCTACGTCAACCGAGACCTCAGTCAAGGCGTGCAG
 GTTTACTGTGACATGACCCTGATGGAGGCGGCTGGATAGTGTTCAGAGACGTCAAAACGGTTTGACGGATTTC
 TCCAGAAAGTGGACTGACTACAAGATCGTTCGGCAGCCTGGAGGACGAATCTGGCTCGGTTTGACAAACATT
 CATAAGATTGCAGCTCAAGGTCTGTTACGAGCTTCGTATTGACATGAAGGATGGCCAGGAGTCTGTATACGCCAAC
 TATGACAGGTTTTCCATTGGGGACTCCAAGAGCCTTTACAAACTGAGGATAGGAGAGTACAGTGGCACCCGAGGT
 GATCTTTGAGCTACCACCAGAGCCGCCCTTTCTCTACCAAGGACAAAGACAATGACATGCTGTACCAACTGT
 GCACTGTCTTACAAGGGAGCCTGGTGGTACAAAACTGTTCATCGGGCAAACCTTAACGGCAAATACGGAGAGTCT
 AGACATAGTCAGGGTATAAACTGGTATCACTGGAAAGGCCATGAGTTTTCCATCCCTTTTGTGGAGATGAAGATG
 AGACCGTTCAACTACCGCAGCATCAGTGGCAAACGGAGGAGATCCGCTCATTAATCTACCGTCTTCTAGCGCTT
 TCTATTTTTAAACAGGGTGGAGGAGACACAAGGAGCGATGTAATTTATTTGAATCTTTTGAATGACAAAACCCCT
 CTGACGAATGTCTGATGTAAATTGTAAACCTCAAGGTTCCGGTGACTTTCTTATATGTAATGCTGTTTGTTCAGTT
 CTGGGAGATTGAAGACTGGGTAGAGTTTGGGTCACACTTTATTTTAAATGGTCCGTTTGTGAAATTTAGGTTACAT
 TGCATCTACATGCCGTTAATCTCTTTAGATTATCAGTAGACTGTTAGCTTGGGGGAGGGGTTACGGTTAGTTT
 AAGTTGACATGTACTTGAAAAGTTCTTATAGTGAGTTAAATGTTTGTGTAAGGAGCAGTATCAGTAGATATTAA
 GCAGACAGCCTACTAATACTCAAAGGACCATCAAACAAAGTGTACCAAAGTTTGAGATTGTTCCGCACGTTT
 ACAGTGTTAGGCTGCAGAAAGAAACCTGATTAATAAGTGAAGAAAAGATCATTCCTCCCTTTGAGACAAAAAAA
 AAAAAGAGCTCGAATTCAGCTTTGGATCCAATCACTAGTGAAT

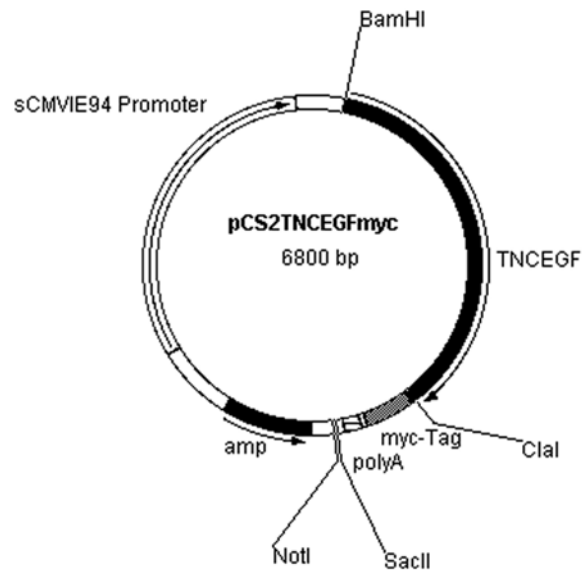
Tenascin-C

TTTACAGCTATGGCCTGCTGAAGACCTTTTCTTCTTTCTGAGAAAGTGAACATTTCTGCCATAGGATCCAGTGCC
 AACTGAAGAGCATCGGCGCCAGCTCCTTTTTCATCTTTCACAACAACCGACGGCATTATTTAGTCTGCTGTGTTGC
 TAAAAACAGGCTCATCGATGCTCAATGACACTCGGGCGCACCAGATTCTATGGGACCACGCATAAGAATTTCTGA
 CATCATACTCTCTCAGACACTCTTGAGTAGCAGATGACCATTCTGTCACTTCAGACGAAGGAGCTTCTGCTGAAG
 ATGAGAGCCTTCCATGGGAAACAGGATGAATCCTATACATTCAGTATCTTATCCACACCCGTGAGGAGTGTCTCTG
 TGAGATCCTCTCATCATGGGGATGCGAGGCCCTGCTGCTGGCCTCTATGGCAGTGGCTGTTTTAGTTTCATCTGTCT
 AGTGCTGGCCTGGTGAAGAGTAATCAGACACAGAAGAGAATCCCTCTACCAACCACTGAGAACTTGACCCTG

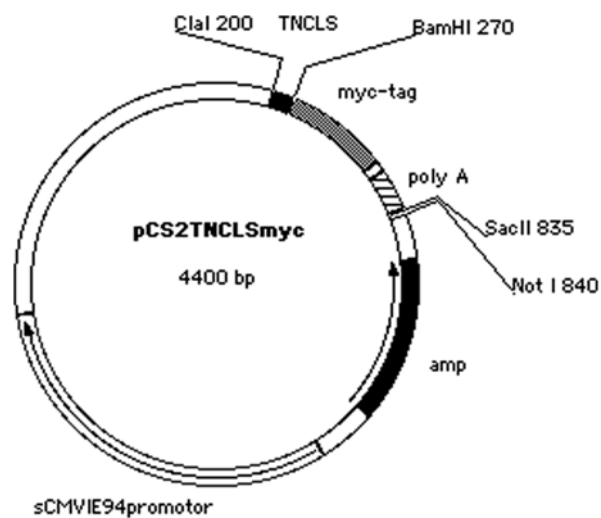
CCGAGCCCTGATCAGCCTGTGGTCTTCAACCATGTGTACAACATCAACGTCCCCTCCGGGTCCCTGTGCTCTGTG
GACATGGATTACCCCGAACAACAGAAATTAAGTCCAAGTCGGAGCAATCTGACCAGCACATAGAACACACCACA
GACGGAGAGAATCAGATTGTTTTTACTCATAGGATTAATATTTCCCAAGCAAGCTTGCGGTGTGATAACCACATG
CCGGATATGAAGGAGCTTCTGAATAGGCTGGAAATGCTGGAGGCAGAGGTTTCCAGTTTAAGAGAGCAGTGCACC
AGTGGGGCCGGCTGCTGTTCTGCTCAGGTTACAGGTGAAGTACAACCAAACCTACTGCAGTGGCCGGGGCAAC
TACAGCACTGACACCTGCAGCTGTGTTTGTGAACCCGGGTGGAAGGGAGTCAACTGCTCTGAGCCAGAATGCCCA
AACTACTGCCAGGATCAAGGGCGTTGTGAGGATGGCAAGTGTGCTGCTTCGAGGGCTTCGGTGGTGAGGATTGT
GGCATCGAGCTGTGCCCTGTGGATTGCGGTGAGAATGGAGAGTGTATCGACGGGGCTTGTATCTGCGCTGAAGGC
TTCATTGGTGAGGATTGTAGTTTAAGCAACTGCCAAGCAACTGCCTCGGCAGGGGGCGCTGTGTGGATGACGAA
TGTGTATGCGACGAGCCTTGGACAGGGTTTACTGCTCCGAGCTTATATGTCCCAACGACTGCTTCGACCGAGGC
CGCTGCGAGAATGGAACCTGCTATTGCGATGAGGGCTTTACTGGGGAAGACTGCGGGGAGCTTACCTGCCCCAA
AACTGCAACCACCATGGAAGGTGCGTCAATGGCCAGTGCATCTGCAATATTGGCTACAGTGGGGAAGACTGCTCC
AAGCTAACATGTCTCAATGACTGCAGTGAGAGAGGTCACTGCTTTAATGGCAAGTGTATATGTGACCCTGGATT
GAGGGCGAGGACTGTAGCCTTCTCTCCCTGCCAGACAACCTGCAATGGCCGAGGACATTTGTGTCAACGGTGAGTGT
ATTTGTGGTCTTGGATATGAAGGTGATGACTGCTCGGAGCTTTCTGTCTCAATAACTGCCACGATCGTGGTCTGA
TGTGTCAACGGGAAGTGCATATGCAAAGCAGGTTTTGCTGGAGAAGATTGCAGCATCAAGACCTGTCTCATGAC
TGCCATGGACGTGGAGAGTGTGTAGATGGCAAGTGTGTTTGCATGATGGATTGCTGGAGAACACTGTGGCATC
AAGACCTGCCCCATCACTGCCATGGACATGGACAATGTGTGGACGGCAAGTGCATTTGCCACAAAGGCTTTGCT
GGAGAAGACTGCAGTATCAAAACCTGCCCTAATCACTGCCATGGACAGGGACAGTGTATAGATGGTAAATGCATT
TGTATGACGGCTTTGCTGGAGAAGATTGCAGCATCAAAACCTGCCCTAATCACTGCCATGGACGTGGACGTTGC
CATGCTGGCTTACAGGCCACGACTGCAGTGAGTTGACTTGCCCCAATGACTGCCATAACCGAGGACGTTGTGTA
AATGGGCAATGTGTGTGTAACATCGGGTTCACTGGGGAGGACTGTGGTACAAGACATGTCCCAACAACCTGTCTG
GACCGTGGCTTCTGCGAAGATGGAAAGTGTGCTGCTTTGAGGGCTACACCGGTGAGGATTGCTCTGTACTGACC
TGCCCTGCAGACTGCAATGACCAAGGCCAGTGTCTGAATGGAATGTGCATATGTGATCTGGGCTTTACTGGCGAT
GACTGCTCTGAGATCTCCCCACCCAGAGACCTTACTGTGACTGAGGTCGACCTCGAGGGGGGGCCGAGGTGAC
CCAGAAACAGTGGACGTGCGCTGGGTTAATGAGATGCTTGTGACAGAGTATCTTATCACCTATGTACCTACGGCT
CCTGGAGGTTTGGAGATGGAAATGAGAGTATCTGGTGAAGAAGACAGCTACTATTAGGGAGCTAGAGCCTGGC
ATAGAGTACCTAATCAGTGTCTTTGCAGTCTCAACAGCAAGATGAGCGTCCCTGTCAGTGCCAGAATAGCCACA
CATCTTCTGAACCTGAGGGCTGAAATTCAAATCCGTGAAAGAGACTTCAGTGGAGGTTGAGTGGGACCCCTTG
AACATCCCCTTTGATGGCTGGAATCTGATCTTCAGAAACACAAAAGAAGAAGATGGAGAGATTTTGAACCTCTCTC
GCTCCTCTGAGACCACCTTTGAGCAGTCTGGACTTGGACCTGGACAAGAGTATGAAGTTAAGCTTGAAGTCTGTA
AAGAACAACACCCGTGGACCCCCAGCCAGCAAGAACGTTGTACAATGATTTGATGCTCCTAGCCAGGTGGATGTG
CGTGACGTGACGGACACTACAGCCCTGGTACGTTGCTCAGCTGCTCAGGTGGACGGCATCTCTGTTTCC
TATGGCCCAAACACAGACTCCTCCGACAGGAACACAATTGAGCTTTCTCCATAGAAACCCAGTACCATCTGGCT
GAGCTGTCTCCTGACACTGAGTATGAGGTCTCTTTATGGCCCCGGGGGAGAGATGAGCAGCTTCCCCATCTAT
GAGACCTTACAACAGATCTGGATTCCCCAAAGCACCTCAAGGCAATTGAGCAGACAGATGAGAGCATAACTCTG
GAGTGGAGAAACAGCAGAGCCAACGTCTCAATTACCGTGTCAAATACGGCCACTTCTGAGGGGAGCATGGA
GAGCTGGTCTTCCCCAGCGGCCGTGCAAGACACCCTCAGGCTAAGATCACTGGCCTCAGGCCTGGGACTGAATAT
GGAATGGGAGTGACTTCAATCAAGGAAGAGCGTGAGAGTTTGCCTGCTACGACCAACGCTGTGACTGATCTTGAT
CCTCCCAAAGACCTTCAAGTAAGTGAGACCACAGAGACCACCCTGGCACTGGTTTTGGAGAAGGCCGGTTGCTAAA
ATCGACACCTATAGTCTAGTGTATACCTGCGGATGGAGATAGAACGGAACCTGAAGATACCTGGTGCTGCAAAAT
ACCTACATCCTGACTGGCCTGAACCTGGCATGCTGCACACGATACCTGGTGCTGCAAAATACCTACATCCTGACT
GGCCTGAACCTGGCATGCTGCACACCATTACCCTGACCGCTGAGAGAGGAAGAAAGATGAGTGCACCAGCCACT

CTGTCAGCATCCACAGATGAGGAGAAGCCTCAGGTGGGCAACATCACCATCTCTGATGTGTCTTGGGACAGCTTC
AGTATGTCTGGGATCTGGACAGAGGAGAGGTTGAGGGATTTCTGATTGAAGTGTCTGACCCAGATGGCTTATCT
GATGGCCAGAACCACACACTGTCTGGCCAGGAGTTCAGCCTGGCTGTCACTGACCTCTCTCCTAGTACTTTCTAC
AGGGTCACACTGTACGGGCTGTACAAGGGAGAGCTCTTAGACCCTGTCTTTGCCGAAGCCATCACAGGGCTTGGT
GCACCGAAGGGAATACGCTTTTCTGATGTGACCGATAACATCAGCTACTGTTCACTGGACTATGCCACATAACCCGT
GTAGACAACACTACAGGGTCATCTATGTGCCATTTCAGGGTGGCAGTCTCTGACACTGAGAGTGGATGGAGGAGAG
TCTCAAGCCATGCTCTCCAATCTGACCCCTGGTGTACCTACCAGGTCACGGTCATCGCTGTTAAGGGCTTGGAG
GAGAGTGAACCCGGATCTGAAAGGGTCACCACAGCTCTGGATAAACCTCGAGGCCTGACAGCAGTGAACATCAGC
GACACTGAAGCCCTGCTGTTGTGGCAGCCGTCCATCGCCACTGTAGACGGATATGTGATCACATACAGCGCAGAC
AGTGTGGCTCCGGTGTATGGAAAGGGTGTCTGGGAACACGGTGGAGTTTGGAGATGAGCTCCCTCACTCCTGCTACT
TTATACACTGTTAAAGTCTATGCATTCAGGACACAGCCAAGAGTGCAGGCAACCAGCACTGACTTCACTACAGAT
GTTGATGCCCCCTCAGAATCTGGCCGCCAGTAACATTCAAACAGAGACCGCCATGTTGACGTGGAAGCCGCCAAGA
GCAGACATCAGTGGGTACATCCTTAGCTTTGAGTCCGCTGATGGTGTAGTCAAGGAGGTGGTCTCAGCCCCACA
GCAACATTTTACAGCATGTCCAGCTCACCGCCTCCACTGAGTACACAGTAAAACGACAGGCCATCGCTGGACCA
AAGAGAAGCAGAGTCATCTCTACAGTCTTCCTCACAATTTGGAGTGTGTATAAGCATCTAAAAGACTGCTCGCAG
GCTCTGCTGAATGGAGACACCACCTCAGGCTTGTACACCATTTACCTGCGTGGAGATGAGAGTCAACCCCTGCAG
GTCTATTGTGATATGACCACCGATGGAGGCGGTTGGATCGTGTGTTGTGAGGCGGCAGAGTGGCAAAGTGGAGTTT
TTCAGAAACTGGAAGAACACACGGCAGGCTTCGGTGTACCTGAATGATGAATTCGGCTTGGTCTATCTAACCTC
CATAAAATCACCTCCTTTGGGCAGTATGAGCTGCGTGTGGACCTCAGAGATAAGGGGAGAGTCTGCATACGCGCAA
TATGACAAGTTTTCAATCTCTGAACCACGTGCTCGCTACAAAGTCCATGTTGGAGGATACAGTGGCACAGCAGGT
GATTCAATGACGTATCATCACGGCCGTCCATTCCTCAACTTACGATAATGACAATGATATAGCGGTCACCAACTGT
GCTCTGTATATAAGGGAGCTTTCTGGTATAAAAACCTGTCATCGAGTAAATATAATGGGCAGATATGGAGACAAC
AGCCACAGCAAGGGTGTAAACTGGTTCCTGGAAGGGTACAGGACTCTGTGGAGTTTGCAGAGATGAAGATC
AGACCTGCCAACTTCAGGAACCTTGGAGGGAAGAAAAAGCGATCATAAACCACTATACTTACAGCTGGATTCAACC
AACCCATTTGGCCCCAGTTCCTCCTGCATCATCTCATCCCTTCATCTACCAAAGACTGCCAGGAGCCCGGCC
TGCTCTCTACACTCGCCTGTTTCATGGAGAACAAATTCACAACAAAAGTTTTTACCCCAACCCCATTCAAAGCT
AAAGTCTTAACACGGTCTGTATGTGTATACACTTCTGTCCACATCAATCTGACAGTAAACCAATAGACTCATAG
TGAAGTGGTAAACACTACACACTGTGCCTGTTTCATCATAAGCACACCAAAGACAGACCTCCGATAACATAAAAC
ACAATGCAGACAGAGAGGAGATTTGAGTGTGGCTTGGCGTTTTCAAGTTTTTAAAAAATACTGATATTTATCTTT
GTATCGCATAACAGTTACTGTGGAGAGAGTTGAATGTTTGTGTGTGGTGTTTTTTTTTTTTTTGTGTCATTAGAGCCT
CATCCTGAATATGTTATTTTCTCAGTTAGGTTGAGAAGTTTAAAAGCACATGATTAAAAAATCTAGTGGGGAGG
CTCTCGGATATTTATTTGTTTTTACCTCTTTCTTGGCTGTCTGTAATAAATCGAAGTACCCATCCTCTCTGTCT
TCTCTCTCCGACAAAATCCTGCATTCCTGCTGATCAGTTTCCAGAACCGAACCTTTACAGTACTGCGAAGTGTTC
ATTTATATGCACCTTTTGTCTGTTTCTGTACCTTATACCTCTATTGGCATTTCAGTCACAGAGCATAAGAACAT
TTGTTGCTTGTATTTAAAAGAAAGATTTAAAAGAAATAAAAGTTAAGGCAGGACCTATGTTTCAGTTTTTTGGTTTT
TAAGCGATGCTGTGTTCCGAGTTATGAGCTTGTGTAATGTTCAAGATTCAGAAAAGAAAAAGTAAACAGCCGGGTT
TTTGGAAATGTTGTAACATAGCCTTATATGAAAGTTCTGTTTGAAGAAAAAAGAAATTAATATACAGGATA
AGTCTTCGTGTTTGGCCCTACCTGCTATTGACTAAACCACTGACCTATACAAAACCTGTGTAATTTATGTCTC
GTTTTGGTATTTGAATATTTTTGTTTTGTTTCGATTGTTTTGTTTTGTTTATTAATGGGTGTACAACAGGTGTTTCTT
TGTAACCCCTCTTACAATAAAACAGATTTTTGTTTTAAAAAAGAAAAAAAAAAAAAAAAAAAAAAAAAAGA

8.4 Vector maps



pCS2TNCEGFmyc (overexpression vector): The EGF-like domains of TN-C were PCR-amplified introducing ClaI and BamHI sites and inserted into pCS2MT (Rupp et al., 1994). To generate mRNA, cut with SacII or NotI and transcribe with SP6.



pCS2TNCLSmyc (overexpression vector): The secretion signal of TN-C was PCR amplified introducing ClaI and BamHI sites and inserted into pCS2MT (Rupp et al., 1994). To generate mRNA, cut with SacII or NotI and transcribe with SP6.

8.5 Publications and Poster presentations

Poster presentations:

Schweitzer J.; Becker T.; Becker C. and Schachner M. Increased expression of a P0-like molecule in the optic pathway during regeneration of optic fibers in adult zebrafish. In: Elsner N, Kreutzberg GW, editors. Proceedings of the fourth meeting of the German neuroscience society. Stuttgart, Germany: Thieme. p 933. 28th Göttingen Neurobiology Conference, 2001.

Publications:

Schweitzer J.; Becker T.; Becker C. and Schachner M. Expression of protein zero (P0) is increased in the lesioned axon pathways in the central nervous system of adult zebrafish (in press, GLIA, John Wiley and Sons, Inc.)

Becker C.; Schweitzer J.; Becker T. and Schachner M. Evidence for a role of tenascin-R as a repellent guidance molecule for regenerating optic axons in adult fish (in revision).

Curriculum vitae

Persönliche Daten

Name: Jörn Schweitzer
Geburtstag: 21.09.1971
Geburtsort: Celle

Schulausbildung

1979 Einschulung an der Grundschule Hohne
1983 Orientierungsstufe Lachendorf
1985 Übergang zum Kaiserin-Auguste-Viktoria Gymnasium in Celle
1992 Abitur

Akademischer Werdegang

November 93 Beginn des Biologiestudiums an der Julius-Maximilians
Universität in Würzburg
März 96 Vordiplom im Studiengang Biologie an der Julius-Maximilians
Universität in Würzburg
August 98 Diplomprüfung im Studiengang Biologie an der Julius-
Maximilians Universität in Würzburg (Gesamtnote: sehr gut)
September 98 Diplomarbeit in der Abteilung für Biochemie des Fachbereichs
bis August 1999 Chemie an der Julius-Maximilians Universität in Würzburg mit
dem Thema "Herstellung einer Enkephalin-überexprimierenden
Zelllinie mit Hilfe eines Hochkopienvektorsystems für die
somatische Gentherapie zur Schmerzbekämpfung"(Note sehr
gut)
November 99 Promotion am Zentrum für Molekulare Neurobiologie Hamburg
bis Januar 03 bei Frau Professor Melitta Schachner

Danksagung

Sehr herzlich bedanken möchte ich mich bei Frau Professor Melitta Schachner, für die Überlassung des Themas und die hervorragenden Bedingungen, die ich in Ihrem Institut vorgefunden habe. Ich bedanke mich für die vielfältigen Möglichkeiten zur Weiterbildung und Ihre stete Diskussionsbereitschaft.

Herrn Prof. L. Renwrantz am Zoologischen Institut der Universität Hamburg danke ich für die Übernahme der Begutachtung meiner Dissertation.

Besonders herzlich bedanken möchte ich mich bei Dr. Catherina Becker und Dr. Thomas Becker, die ganz wesentlich an dem erfolgreichen Abschluß dieser Arbeit beteiligt waren.

Bei meinen Laborkollegen Bettina Lieberoth und Julia Feldner möchte ich mich für die freundliche Zusammenarbeit im Labor bedanken, ohne die manches sicherlich wesentlich schwerer zu ertragen gewesen wäre.

Allen Mitarbeitern des Instituts danke ich für die nette Zusammenarbeit, die stete Diskussionsbereitschaft und die Freundschaft, die uns verbunden hat.

Meinen Eltern und meiner Freundin Saskia danke ich für Ihre Geduld und Unterstützung.